

# 1 Title Page

## Bimodal inference in humans and mice

### Authors:

Veith Weilnhammer<sup>1,2</sup>, Heiner Stuke<sup>1,2</sup>, Kai Standvoss<sup>1,3,5</sup>, Philipp Sterzer<sup>1,3,4,5</sup>

### Affiliations:

<sup>1</sup> Department of Psychiatry, Charité-Universitätsmedizin Berlin, corporate member of Freie Universität Berlin and Humboldt-Universität zu Berlin, 10117 Berlin, Germany

<sup>2</sup> Berlin Institute of Health, Charité-Universitätsmedizin Berlin and Max Delbrück Center, 10178 Berlin, Germany

<sup>3</sup> Bernstein Center for Computational Neuroscience, Charité-Universitätsmedizin Berlin, 10117 Berlin, Germany

<sup>4</sup> Berlin School of Mind and Brain, Humboldt-Universität zu Berlin, 10099 Berlin, Germany

<sup>5</sup> Einstein Center for Neurosciences Berlin, 10117 Berlin, Germany

### Corresponding Author:

Veith Weilnhammer, Department of Psychiatry, Charité Campus Mitte, Charitéplatz 1, 10117 Berlin, phone: 0049 (0)30 450 517 317, email: veith.weilnhammer@gmail.com

## <sup>1</sup> 2 Abstract

<sup>2</sup> Perception is known to cycle through periods of enhanced and reduced sensitivity to external  
<sup>3</sup> information. Here, we asked whether such infra-slow fluctuations arise as a noise-related  
<sup>4</sup> epiphenomenon of limited processing capacity or, alternatively, represent a structured mech-  
<sup>5</sup> anism of perceptual inference. Using two large-scale datasets, we found that humans and  
<sup>6</sup> mice waver between alternating intervals of externally- and internally-oriented modes of  
<sup>7</sup> sensory analysis. During external mode, perception aligned more closely with the external  
<sup>8</sup> sensory information, whereas internal mode was characterized by enhanced biases toward  
<sup>9</sup> perceptual history. Computational modeling indicated that dynamic changes in mode are  
<sup>10</sup> enabled by two interlinked factors: (i), the integration of subsequent inputs over time and,  
<sup>11</sup> (ii), infra-slow anti-phase oscillations in the perceptual impact of external sensory information  
<sup>12</sup> versus internal predictions that are provided by perceptual history. Simulated data suggested  
<sup>13</sup> that between-mode fluctuations may benefit perception by generating unambiguous error  
<sup>14</sup> signals that enable robust learning and metacognition in volatile environments.

## <sup>15</sup> 3 One sentence summary

<sup>16</sup> Humans and mice fluctuate between external and internal modes of sensory processing.

<sup>17</sup>

<sup>18</sup>

<sup>19</sup> **4 Introduction**

<sup>20</sup> The capacity to respond to changes in the environment is a defining feature of life<sup>1–3</sup>.  
<sup>21</sup> Intriguingly, the ability of living things to process their surroundings fluctuates considerably  
<sup>22</sup> over time<sup>4,5</sup>. In humans and mice, perception<sup>6–12</sup>, cognition<sup>13</sup> and memory<sup>14</sup> cycle through  
<sup>23</sup> prolonged periods of enhanced and reduced sensitivity to external information, suggesting  
<sup>24</sup> that the brain detaches from the world in recurring intervals that last from milliseconds  
<sup>25</sup> to seconds and even minutes<sup>4,5</sup>. Yet breaking from external information is risky, as swift  
<sup>26</sup> responses to the environment are often crucial to survival.

<sup>27</sup> What could be the reason for these fluctuations in perceptual performance<sup>11</sup>? First, periodic  
<sup>28</sup> fluctuations in the ability to parse external information<sup>11,15,16</sup> may arise simply due to  
<sup>29</sup> bandwidth limitations and noise. Second, it may be advantageous to actively reduce the  
<sup>30</sup> costs of neural processing by seeking sensory information only in recurring intervals<sup>5,17</sup>,  
<sup>31</sup> otherwise relying on random or stereotypical responses to the external world. Third, spending  
<sup>32</sup> time away from the ongoing stream of sensory inputs may also reflect a functional strategy  
<sup>33</sup> that facilitates flexible behavior and learning<sup>18</sup>: Intermittently relying more strongly on  
<sup>34</sup> information acquired from past experiences may enable agents to build up stable internal  
<sup>35</sup> predictions about the environment despite an ongoing stream of external sensory signals<sup>19</sup>.  
<sup>36</sup> By the same token, recurring intervals of enhanced sensitivity to external information may  
<sup>37</sup> help to detect changes in both the state of the environment and the amount of noise that is  
<sup>38</sup> inherent in sensory encoding<sup>19</sup>.

<sup>39</sup> In this work, we sought to elucidate whether periodicities in the sensitivity to external  
<sup>40</sup> information represent an epiphenomenon of limited processing capacity or, alternatively,  
<sup>41</sup> result from a structured and adaptive mechanism of perceptual inference. To this end, we  
<sup>42</sup> analyzed two large-scale datasets on perceptual decision-making in humans<sup>20</sup> and mice<sup>21</sup>.  
<sup>43</sup> When less sensitive to external stimulus information, humans and mice showed stronger serial  
<sup>44</sup> dependencies<sup>22–33</sup>, which have been conceptualized as internal predictions that reflect the

45 auto-correlation of natural environments<sup>34</sup> and bias perceptual decisions toward preceding  
46 choices<sup>30,31,35</sup>. Computational modeling indicated that ongoing changes in perceptual perfor-  
47 mance may be driven by systematic fluctuations between externally- and internally-oriented  
48 modes of sensory analysis. Model simulations suggested that such bimodal inference may im-  
49 prove, (i), the ability to robustly determine the statistical properties of volatile environments  
50 and, (ii), the ability to calibrate internal beliefs about the degree of noise inherent in the  
51 encoding of sensory information.

## 52 **5 Results**

### 53 **5.1 Human perception fluctuates between epochs of enhanced and** 54 **reduced sensitivity to external information**

55 We began by selecting 66 studies from the Confidence Database<sup>20</sup> that investigated how  
56 human participants ( $N = 4317$ ) perform binary perceptual decisions (Figure 1A; see Methods  
57 section for details on inclusion criteria). As a metric for perceptual performance (i.e., the  
58 sensitivity to external sensory information), we asked whether the participant's response  
59 and the presented stimulus matched (*stimulus-congruent* choices) or differed from each other  
60 (*stimulus-incongruent* choices; Figure 1B and C) in a total of 21.05 million trials.

61 In a first step, we asked whether the ability to accurately perceive sensory stimuli is constant  
62 over time or, alternatively, fluctuates in periods of enhanced and reduced sensitivity to  
63 external information. We found perception to be stimulus-congruent in  $73.46\% \pm 0.15\%$  of  
64 trials (mean  $\pm$  standard error of the mean; Figure 2A), which was highly consistent across the  
65 selected studies (Supplemental Figure S1A). In line with previous work<sup>8</sup>, we found that the  
66 probability of stimulus-congruence was not independent across successive trials: At the group  
67 level, stimulus-congruent perceptual choices were significantly autocorrelated for up to 15  
68 trials. Autocorrelation coefficients decayed exponentially over time (rate  $\gamma = -1.92 \times 10^{-3} \pm$

69  $4.5 \times 10^{-4}$ ,  $T(6.88 \times 10^4) = -4.27$ ,  $p = 1.98 \times 10^{-5}$ ; Figure 2B). Importantly, the autocorrelation  
70 of stimulus-congruent perception was not a trivial consequence of the experimental design,  
71 but remained significant when controlling for the trial-wise autocorrelation of task difficulty  
72 (Supplemental Figure S2A) or the sequence of presented stimuli (Supplemental Figure S2B).

73 In addition, stimulus-congruence was significantly autocorrelated not only at the group-level,  
74 but also in individual participants, where the autocorrelation of stimulus-congruent perception  
75 exceeded the respective autocorrelation of randomly permuted data within an interval of  $3.24 \pm 2.39 \times 10^{-3}$  trials (Figure 2C). In other words, if a participant's experience was congruent  
76 (or incongruent) with the external stimulus information at a given trial, her perception was  
77 more likely to be stimulus-congruent (or incongruent) for approximately 3 trials into the  
78 future.

80 To further corroborate the autocorrelation of stimulus-congruence, we used logistic regression  
81 models that predicted the stimulus-congruence of perception at the index trial  $t = 0$  from the  
82 stimulus-congruence at the preceding trials within a lag of 25 trials. We found that regression  
83 weights were significantly greater than zero for up to 16 trials (Supplemental Figure S3).

84 These results confirm that the ability to process sensory signals is not constant over time, but  
85 unfolds in multi-trial epochs of enhanced and reduced sensitivity to external information<sup>8</sup>.

86 As a consequence of this autocorrelation, the dynamic probability of stimulus-congruent  
87 perception (i.e., computed in sliding windows of  $\pm 5$  trials; Figure 1C) fluctuated considerably  
88 within participants (average minimum:  $35.46\% \pm 0.22\%$ , maximum:  $98.27\% \pm 0.07\%$ ). In  
89 line with previous findings<sup>9</sup>, such fluctuations in the sensitivity to external information had a  
90 power density that was inversely proportional to the frequency in the infra-slow spectrum<sup>11</sup>  
91 ( $\text{power} \sim 1/f^\beta$ ,  $\beta = -1.32 \pm 3.14 \times 10^{-3}$ ,  $T(1.84 \times 10^5) = -419.48$ ,  $p < 2.2 \times 10^{-308}$ ; Figure  
92 2D). This feature, which is also known as *1/f noise*<sup>36,37</sup>, represents a characteristic of ongoing  
93 fluctuations in complex dynamic systems such as the brain<sup>38</sup> and the cognitive processes it  
94 entertains<sup>9,10,13,39,40</sup>.

95     **5.2 Human perception fluctuates between external and internal**  
96                 **modes of sensory processing**

97     In a second step, we sought to explain why perception cycles through periods of enhanced and  
98     reduced sensitivity to external information<sup>4,5</sup>. We reasoned that observers may intermittently  
99     rely more strongly on internal information, i.e., on predictions about the environment that  
100    are constructed from previous experiences<sup>19,31</sup>.

101    In perception, *serial dependencies* represent one of the most basic internal predictions that  
102    cause perceptual decisions to be systematically biased toward preceding choices<sup>22–33</sup>. Such  
103    effects of perceptual history mirror the continuity of the external world, in which the recent  
104    past often predicts the near future<sup>30,31,34,35,41</sup>. Therefore, as a metric for the perceptual  
105    impact of internal information, we computed whether the participant’s response at a given  
106    trial matched or differed from her response at the preceding trial (*history-congruent* and  
107    *history-incongruent perception*, respectively; Figure 1B and C).

108    First, we ensured that perceptual history played a significant role in perception despite  
109    the ongoing stream of external information. With a global average of  $52.7\% \pm 0.12\%$   
110    history-congruent trials, we found a small but highly significant perceptual bias towards  
111    preceding experiences ( $\beta = 16.18 \pm 1.07$ ,  $T(1.09 \times 10^3) = 15.07$ ,  $p = 10^{-46}$ ; Figure 2A) that  
112    was largely consistent across studies (Supplemental Figure 1B) and more pronounced in  
113    participants who were less sensitive to external sensory information (Supplemental Figure 1C).

114    Logistic regression confirmed the internal information provided by perceptual history made a  
115    significant contribution to perception ( $\beta = 0.11 \pm 5.79 \times 10^{-3}$ ,  $z = 18.53$ ,  $p = 1.1 \times 10^{-76}$ )  
116    over and above the ongoing stream of external sensory information ( $\beta = 2.2 \pm 5.87 \times 10^{-3}$ ,  
117     $z = 375.11$ ,  $p < 2.2 \times 10^{-308}$ ) and general response biases toward one of the two potential  
118    outcomes ( $\beta = 15.19 \pm 0.08$ ,  $z = 184.98$ ,  $p < 2.2 \times 10^{-308}$ ; see Supplemental Figure S4A for  
119    model comparisons within individual participants).

120    In addition, we confirmed that history-congruence was not a corollary of the sequence of

<sup>121</sup> presented stimuli: History-congruent perceptual choices were more frequent at trials when  
<sup>122</sup> perception was stimulus-incongruent ( $56.03\% \pm 0.2\%$ ) as opposed to stimulus-congruent  
<sup>123</sup> ( $51.77\% \pm 0.11\%$ ,  $\beta = -4.26 \pm 0.21$ ,  $T(8.57 \times 10^3) = -20.36$ ,  $p = 5.28 \times 10^{-90}$ ; Figure 2A,  
<sup>124</sup> lower panel). Despite being adaptive in auto-correlated real-world environments<sup>19,34,35,42</sup>,  
<sup>125</sup> perceptual history thus represented a source of error in the randomized experimental designs  
<sup>126</sup> studied here<sup>24,28,30,31,43</sup>.

<sup>127</sup> Second, we asked whether perception cycles through multi-trial epochs during which perception  
<sup>128</sup> is characterized by stronger or weaker biases toward preceding experiences. Indeed, in close  
<sup>129</sup> analogy to stimulus-congruence, history-congruence was significantly autocorrelated for up  
<sup>130</sup> to 21 trials (Figure 2B). Following a peak at the first trial, the respective autocorrelation  
<sup>131</sup> coefficients decreased exponentially over time (rate  $\gamma = -6.11 \times 10^{-3} \pm 5.69 \times 10^{-4}$ ,  $T(6.75 \times$   
<sup>132</sup>  $10^4) = -10.74$ ,  $p = 7.18 \times 10^{-27}$ ). History-congruence remained significantly autocorrelated  
<sup>133</sup> when controlling for task difficulty (Supplemental Figure S2A) and the sequence of presented  
<sup>134</sup> stimuli (Supplemental Figure S2B). In individual participants, the autocorrelation of history-  
<sup>135</sup> congruence was elevated above randomly permuted data for a lag of  $4.87 \pm 3.36 \times 10^{-3}$   
<sup>136</sup> trials (Figure 2C), confirming that the autocorrelation of history-congruence was not only  
<sup>137</sup> a group-level phenomenon. The autocorrelation of history-congruence was confirmed by  
<sup>138</sup> logistic regression models that successfully predicted the history-congruence of perception at  
<sup>139</sup> an index trial  $t = 0$  from the history-congruence at the preceding trials within a lag of 17  
<sup>140</sup> trials (Supplemental Figure S3).

<sup>141</sup> Third, we asked whether the impact of internal information fluctuates as 1/f noise (i.e.,  
<sup>142</sup> a noise characteristic classically associated with fluctuations in the sensitivity to external  
<sup>143</sup> information<sup>9,10,13,39,40</sup>). The dynamic probability of history-congruent perception (i.e., com-  
<sup>144</sup> puted in sliding windows of  $\pm 5$  trials; Figure 1C) varied considerably over time, ranging  
<sup>145</sup> between a minimum of  $12.77\% \pm 0.14\%$  and a maximum  $92.23\% \pm 0.14\%$ . In analogy to  
<sup>146</sup> stimulus-congruence, we found that history-congruence fluctuated as 1/f noise, with power

<sup>147</sup> densities that were inversely proportional to the frequency in the infra-slow spectrum<sup>11</sup> (power  
<sup>148</sup>  $\sim 1/f^\beta$ ,  $\beta = -1.34 \pm 3.16 \times 10^{-3}$ ,  $T(1.84 \times 10^5) = -423.91$ ,  $p < 2.2 \times 10^{-308}$ ; Figure 2D).

<sup>149</sup> Finally, we ensured that fluctuations in stimulus- and history-congruence are linked to each  
<sup>150</sup> other. When perceptual choices were less biased toward external information, participants  
<sup>151</sup> relied more strongly on internal information acquired from perceptual history (and vice versa,  
<sup>152</sup>  $\beta = -0.1 \pm 8.59 \times 10^{-4}$ ,  $T(2.1 \times 10^6) = -110.96$ ,  $p < 2.2 \times 10^{-308}$ ). Thus, while sharing  
<sup>153</sup> the characteristic of  $1/f$  noise, fluctuations in stimulus- and history-congruence were shifted  
<sup>154</sup> against each other by approximately half a cycle and showed a squared coherence of  $6.49 \pm$   
<sup>155</sup>  $2.07 \times 10^{-3}\%$  (Figure 2E and F; we report the average phase and coherence for frequencies  
<sup>156</sup> below  $0.1 \text{ } 1/N_{trials}$ ; see Methods for details).

<sup>157</sup> In sum, our analyses indicate that perceptual decisions may result from a competition between  
<sup>158</sup> external sensory signals with internal predictions provided by perceptual history. Crucially,  
<sup>159</sup> we show that the impact of these external and internal sources of information is not stable  
<sup>160</sup> over time, but fluctuates systematically, emitting overlapping autocorrelation curves and  
<sup>161</sup> antiphase  $1/f$  noise profiles.

<sup>162</sup> These links between stimulus- and history-congruence suggest that the fluctuations in the  
<sup>163</sup> impact of external and internal information may be generated by a unifying mechanism that  
<sup>164</sup> causes perception to alternate between two opposing *modes*<sup>18</sup> (Figure 1D): During *external*  
<sup>165</sup> *mode*, perception is more strongly driven by the available external stimulus information.  
<sup>166</sup> Conversely, during *internal mode*, participants rely more heavily on internal predictions that  
<sup>167</sup> are implicitly provided by preceding perceptual experiences. Fluctuations in mode (i.e.,  
<sup>168</sup> the degree of bias toward external versus internal information) may thus provide a novel  
<sup>169</sup> explanation for ongoing fluctuations in the sensitivity to external information<sup>4,5,18</sup>.

170 **5.3 Internal and external modes of processing facilitate response**  
171 **behavior and enhance confidence in human perceptual decision-**  
172 **making**

173 Alternatively, however, fluctuating biases toward externally- and internally-oriented modes  
174 may not represent a perceptual phenomenon, but result from cognitive processes that are  
175 situated up- or downstream of perception. For instance, it may be argued that participants  
176 may be prone to stereotypically repeat the preceding choice when not attending to the  
177 experimental task. Thus, fluctuations in mode may arise due to systematic changes in the  
178 level of tonic arousal<sup>44</sup> or on-task attention<sup>45,46</sup>. Since arousal and attention typically link  
179 closely with response times<sup>45,47</sup> (RTs), this alternative explanation entails that RTs increase  
180 monotonically as one moves away from externally-biased and toward internally-biases modes  
181 of sensory processing.

182 As expected, stimulus-congruent (as opposed to stimulus-incongruent) choices were associated  
183 with faster responses ( $\beta = -0.14 \pm 1.61 \times 10^{-3}$ ,  $T(1.99 \times 10^6) = -85.91$ ,  $p < 2.2 \times 10^{-308}$ ;  
184 Figure 2G). Intriguingly, whilst controlling for the effect of stimulus-congruence, we found  
185 that history-congruent (as opposed to history-incongruent) choices were also characterized  
186 by shorter RTs ( $\beta = -9.73 \times 10^{-3} \pm 1.38 \times 10^{-3}$ ,  $T(1.99 \times 10^6) = -7.06$ ,  $p = 1.66 \times 10^{-12}$ ;  
187 Figure 2G).

188 When analyzing the speed of response against the mode of sensory processing (Figure 2H),  
189 we found that RTs were shorter during externally-oriented perception ( $\beta_1 = -11.07 \pm 0.55$ ,  
190  $T(1.98 \times 10^6) = -20.14$ ,  $p = 3.17 \times 10^{-90}$ ). Crucially, as indicated by a quadratic relationship  
191 between the mode of sensory processing and RTs ( $\beta_2 = -19.86 \pm 0.52$ ,  $T(1.98 \times 10^6) =$   
192  $-38.43$ ,  $p = 5 \times 10^{-323}$ ), participants became faster at indicating their perceptual decision  
193 when biases toward both internal and external mode grew stronger. This argued against  
194 the view that the dynamics of pre-perceptual variables such as arousal or attention provide  
195 a plausible alternative explanation for the fluctuating perceptual impact of internal and

<sup>196</sup> external information.

<sup>197</sup> Second, it may be assumed that participants tend to repeat preceding choices when they are  
<sup>198</sup> not yet familiar with the experimental task, leading to history-congruent choices that are  
<sup>199</sup> caused by insufficient training. In the Confidence database<sup>20</sup>, training effects were visible from  
<sup>200</sup> RTs that were shortened by increasing exposure to the task ( $\beta = -7.53 \times 10^{-5} \pm 6.32 \times 10^{-7}$ ,  
<sup>201</sup>  $T(1.81 \times 10^6) = -119.15$ ,  $p < 2.2 \times 10^{-308}$ ). Intriguingly, however, history-congruent choices  
<sup>202</sup> became more frequent with increased exposure to the task ( $\beta = 3.6 \times 10^{-5} \pm 2.54 \times 10^{-6}$ ,  
<sup>203</sup>  $z = 14.19$ ,  $p = 10^{-45}$ ), speaking against the proposition that insufficient training induces  
<sup>204</sup> seriality in response behavior.

<sup>205</sup> As a third caveat, it could be argued that biases toward internal information reflect a post-  
<sup>206</sup> perceptual strategy that repeats preceding choices when the subjective confidence in the  
<sup>207</sup> perceptual decision is low. According to this view, subjective confidence should increase  
<sup>208</sup> monotonically as biases toward external mode become stronger.

<sup>209</sup> Stimulus-congruent (as opposed to stimulus-incongruent) choices were associated with en-  
<sup>210</sup> hanced confidence ( $\beta = 0.04 \pm 1.18 \times 10^{-3}$ ,  $T(2.06 \times 10^6) = 36.86$ ,  $p = 2.93 \times 10^{-297}$ ; Figure 2I).  
<sup>211</sup> Yet whilst controlling for the effect of stimulus-congruence, we found that history-congruence  
<sup>212</sup> also increased confidence ( $\beta = 0.48 \pm 1.38 \times 10^{-3}$ ,  $T(2.06 \times 10^6) = 351.89$ ,  $p < 2.2 \times 10^{-308}$ ;  
<sup>213</sup> Figure 2I).

<sup>214</sup> When depicted against the mode of sensory processing (Figure 2J), subjective confidence was  
<sup>215</sup> indeed enhanced when perception was more externally-oriented ( $\beta_1 = 92.63 \pm 1$ ,  $T(2.06 \times 10^6)$   
<sup>216</sup>  $= 92.89$ ,  $p < 2.2 \times 10^{-308}$ ). Importantly, however, participants were more confident in their  
<sup>217</sup> perceptual decision for stronger biases toward both internal and external mode ( $\beta_2 = 39.3 \pm$   
<sup>218</sup>  $0.94$ ,  $T(2.06 \times 10^6) = 41.95$ ,  $p < 2.2 \times 10^{-308}$ ). In analogy to RTs, subjective confidence thus  
<sup>219</sup> showed a quadratic relationship to the mode of sensory processing (Figure 2J), contradicting  
<sup>220</sup> the notion that biases toward internal mode may reflect a post-perceptual strategy employed  
<sup>221</sup> in situations of low subjective confidence.

222 The above results indicate that reporting behavior and metacognition do not map linearly  
223 onto the mode of sensory processing, suggesting that slow fluctuations in the respective  
224 impact of external and internal information are most likely to affect perception at an early  
225 level of sensory analysis<sup>48,49</sup>. Such low-level processing may integrate perceptual history with  
226 external inputs into a decision variable<sup>50</sup> that influences not only perceptual choices, but also  
227 downstream functions such as speed of response and subjective confidence. Consequently, our  
228 findings predict that human participants lack full metacognitive insight into how strongly  
229 external signals and internal predictions contribute to perceptual decision-making. Stronger  
230 biases toward perceptual history thus lead to two seemingly contradictory effects: more  
231 frequent errors (Supplemental Figure 1C) and increasing subjective confidence (Figure 2I-J).  
  
232 This observation generates an intriguing prediction regarding the association of between-  
233 mode fluctuations and perceptual metacognition: Metacognitive efficiency should be lower in  
234 individuals who spend more time in internal mode, since their confidence reports are less  
235 predictive of whether the corresponding perceptual decision is correct. We computed each  
236 participant's M-ratio<sup>51</sup> ( $\text{meta-d}'/\text{d}' = 0.85 \pm 0.02$ ) to probe this hypothesis independently of  
237 inter-individual differences in perceptual performance. Indeed, we found that biases toward  
238 internal information (i.e., as defined by the average probability of history-congruence) were  
239 stronger in participants with lower metacognitive efficiency ( $\beta = -2.98 \times 10^{-3} \pm 9.82 \times 10^{-4}$ ,  
240  $T(4.14 \times 10^3) = -3.03$ ,  $p = 2.43 \times 10^{-3}$ ).

241 **5.4 Fluctuations between internal and external mode modulate  
242 perceptual performance beyond the effect of general response  
243 biases**

244 The above sections provide correlative evidence that recurring intervals of stronger perceptual  
245 history temporally reduce the participants' sensitivity to external information. Importantly,  
246 the history-dependent biases that characterize internal mode processing must be differentiated

<sup>247</sup> from general response biases. In binary perceptual decision-making, general response biases  
<sup>248</sup> are defined by a propensity to choose one of the two outcomes more often than the alternative.  
<sup>249</sup> Indeed, in the experiments considered here, participants selected the more frequent of the  
<sup>250</sup> two possible outcomes in  $58.71\% \pm 0.22\%$  of trials.

<sup>251</sup> Two caveats have to be considered to make sure that the effect of history-congruence is  
<sup>252</sup> distinct from the effect of general response biases. First, history-congruent states become  
<sup>253</sup> more likely for larger response biases that cause a increasing imbalance in the likelihood of  
<sup>254</sup> the two outcomes ( $\beta = 0.24 \pm 6.93 \times 10^{-4}$ ,  $T(2.09 \times 10^6) = 342.43$ ,  $p < 2.2 \times 10^{-308}$ ). One  
<sup>255</sup> may thus ask whether the autocorrelation of history-congruence could be entirely driven  
<sup>256</sup> by general response biases. Yet the above analyses account for general response biases  
<sup>257</sup> by computing group-level autocorrelations (see Figure 2C) relative to randomly permuted  
<sup>258</sup> data (i.e., by subtracting the autocorrelation of randomly permuted data from the raw  
<sup>259</sup> autocorrelation curve). This precludes that general response biases contribute to the observed  
<sup>260</sup> autocorrelation of history-congruence (see Supplemental Figure S5 for a visualization of the  
<sup>261</sup> correction procedure for simulated data with general response biases ranging from 60 to 90%).

<sup>262</sup> Second, it may be argued that fluctuations in perceptual performance may be solely driven  
<sup>263</sup> by ongoing changes in the strength of general response biases. To assess the links between  
<sup>264</sup> dynamic fluctuations in stimulus-congruence on the one hand and history-congruence as well  
<sup>265</sup> as general response bias on the other hand, we computed all variables as dynamic probabilities  
<sup>266</sup> in sliding windows of  $\pm 5$  trials (see Figure 1C). Linear mixed effects modeling indicated  
<sup>267</sup> that fluctuations in history-congruent biases were larger in amplitude than the corresponding  
<sup>268</sup> fluctuations in general response biases ( $\beta_0 = 0.03 \pm 7.34 \times 10^{-3}$ ,  $T(64.94) = 4.46$ ,  $p =$   
<sup>269</sup>  $3.28 \times 10^{-5}$ ). Crucially, ongoing fluctuations in history-congruence had a significant effect on  
<sup>270</sup> stimulus-congruence ( $\beta_1 = -0.05 \pm 5.63 \times 10^{-4}$ ,  $T(2.1 \times 10^6) = -84.21$ ,  $p < 2.2 \times 10^{-308}$ )  
<sup>271</sup> beyond the effect of ongoing changes in general response biases ( $\beta_2 = -0.06 \pm 5.82 \times 10^{-4}$ ,  
<sup>272</sup>  $T(2.1 \times 10^6) = -103.51$ ,  $p < 2.2 \times 10^{-308}$ ). In sum, the above control analyses confirm that

273 the observed influence of preceding choices on perceptual decision-making cannot not be  
274 reduced to general response biases.

275 **5.5 Internal mode is characterized by lower thresholds as well as**  
276 **by history-dependent changes in biases and lapses**

277 In a final control analysis, we asked whether history-independent changes in biases and  
278 lapses may provide an alternative explanation of internal mode processing. To this end, we  
279 estimated full and history-conditioned psychometric curves to investigate how internal and  
280 external mode relate to biases (i.e., the horizontal position of the psychometric curve), lapses  
281 (i.e., the asymptotes of the psychometric curve) and thresholds (i.e., 1/sensitivity, estimated  
282 from the slope of the psychometric curve). We used a maximum likelihood procedure to  
283 predict trial-wise choices  $y$  ( $y = 0$  and  $y = 1$  for outcomes A and B respectively) from the  
284 choice probabilities  $y_p$ .  $y_p$  was computed from difficulty-weighted inputs  $s_w$  via a parametric  
285 error function defined by the parameters  $\gamma$  (lower lapse),  $\delta$  (upper lapse),  $\mu$  (bias) and  $t$   
286 (threshold; see Methods for details):

$$y_p = \gamma + (1 - \gamma - \delta) * (\text{erf}(\frac{s_w + \mu}{t}) + 1)/2 \quad (1)$$

287 Across the full dataset (i.e., irrespective of the preceding perceptual choice  $y_{t-1}$ ), biases  $\mu$   
288 were distributed around zero ( $-0.05 \pm 0.03$ ;  $\beta_0 = 7.37 \times 10^{-3} \pm 0.09$ ,  $T(36.8) = 0.08$ ,  $p = 0.94$ ;  
289 see Figure 3A and B, upper panel). When conditioned on perceptual history, biases  $\mu$  varied  
290 according to the preceding perceptual choice, with negative biases for  $y_{t-1} = 0$  ( $-0.22 \pm 0.04$ ;  
291  $\beta_0 = 0.56 \pm 0.12$ ,  $T(43.39) = 4.6$ ,  $p = 3.64 \times 10^{-5}$ ) and positive biases for  $y_{t-1} = 1$  ( $0.29 \pm$   
292  $0.03$ ;  $\beta_0 = 0.56 \pm 0.12$ ,  $T(43.39) = 4.6$ ,  $p = 3.64 \times 10^{-5}$ ). Absolute biases  $|\mu|$  were larger in  
293 internal mode ( $1.84 \pm 0.03$ ) as compared to external mode ( $0.86 \pm 0.02$ ;  $\beta_0 = -0.62 \pm 0.07$ ,  
294  $T(45.62) = -8.38$ ,  $p = 8.59 \times 10^{-11}$ ; controlling for differences in lapses and thresholds).

<sup>295</sup> Lower and upper lapses amounted to  $\gamma = 0.13 \pm 2.83 \times 10^{-3}$  and  $\delta = 0.1 \pm 2.45 \times 10^{-3}$  (see  
<sup>296</sup> Figure 3A, C and D). Lapses were larger in internal mode ( $\gamma = 0.17 \pm 3.52 \times 10^{-3}$ ,  $\delta = 0.14$   
<sup>297</sup>  $\pm 3.18 \times 10^{-3}$ ) as compared to external mode ( $\gamma = 0.1 \pm 2.2 \times 10^{-3}$ ,  $\delta = 0.08 \pm 2 \times 10^{-3}$ ;  $\beta_0$   
<sup>298</sup>  $= -0.05 \pm 5.73 \times 10^{-3}$ ,  $T(47.03) = -9.11$ ,  $p = 5.94 \times 10^{-12}$ ; controlling for differences in  
<sup>299</sup> biases and thresholds).

<sup>300</sup> Conditioning on the previous perceptual choice revealed that the between-mode difference in  
<sup>301</sup> lapse was not general, but depended on perceptual history: For  $y_{t-1} = 0$ , only higher lapses  $\delta$   
<sup>302</sup> differed between internal and external mode ( $\beta_0 = -0.1 \pm 9.58 \times 10^{-3}$ ,  $T(36.87) = -10.16$ ,  $p$   
<sup>303</sup>  $= 3.06 \times 10^{-12}$ ), whereas lower lapses  $\gamma$  did not ( $\beta_0 = 0.01 \pm 7.77 \times 10^{-3}$ ,  $T(33.1) = 1.61$ ,  $p$   
<sup>304</sup>  $= 0.12$ ). Vice versa, for  $y_{t-1} = 1$ , lower lapses  $\gamma$  differed between internal and external mode  
<sup>305</sup> ( $\beta_0 = -0.11 \pm 0.01$ ,  $T(40.11) = -9.59$ ,  $p = 6.14 \times 10^{-12}$ ), whereas higher lapses  $\delta$  did not  
<sup>306</sup> ( $\beta_0 = 0.01 \pm 7.74 \times 10^{-3}$ ,  $T(33.66) = 1.58$ ,  $p = 0.12$ ).

<sup>307</sup> Thresholds  $t$  were estimated at  $3 \pm 0.06$  (see Figure 3A and E). Thresholds  $t$  were larger  
<sup>308</sup> in internal mode ( $3.66 \pm 0.09$ ) as compared to external mode ( $2.02 \pm 0.03$ ;  $\beta_0 = -1.77 \pm$   
<sup>309</sup>  $0.25$ ,  $T(50.45) = -7.14$ ,  $p = 3.48 \times 10^{-9}$ ; controlling for differences in biases and lapses).  
<sup>310</sup> In contrast to the bias  $\mu$  and the lapse rates  $\gamma$  and  $\delta$ , thresholds  $t$  were not modulated by  
<sup>311</sup> perceptual history ( $\beta_0 = 0.04 \pm 0.06$ ,  $T(2.97 \times 10^3) = 0.73$ ,  $p = 0.47$ ).

<sup>312</sup> In sum, the above analyses showed that internal and external mode differ with respect  
<sup>313</sup> to biases, lapses and thresholds. Internally-biased processing was characterized by higher  
<sup>314</sup> thresholds, indicating a reduced sensitivity to sensory information, as well as by larger biases  
<sup>315</sup> and lapses. Importantly, between-mode differences in biases and lapses strongly depended on  
<sup>316</sup> perceptual history. This confirmed that internal mode processing cannot be explained solely  
<sup>317</sup> on the ground of a general (i.e., history-independent) increase in lapses or bias.

318 **5.6 Mice waver between external and internal modes of perceptual**  
319 **decision-making**

320 In a prominent functional explanation for serial dependencies<sup>22–28,32,33,48</sup>, perceptual history is  
321 cast as an internal prediction that leverages the temporal autocorrelation of natural environments  
322 for efficient decision-making<sup>30,31,34,35,41</sup>. We reasoned that, since this autocorrelation

323 is one of the most basic features of our sensory world, fluctuating biases toward preceding  
324 perceptual choices should not be a uniquely human phenomenon.

325 To test whether externally and internally oriented modes of processing exist beyond the  
326 human mind, we analyzed data on perceptual decision-making in mice that were extracted  
327 from the International Brain Laboratory (IBL) dataset<sup>21</sup>. Here, we restricted our analyses  
328 to the *basic task*<sup>21</sup>, in which mice responded to gratings of varying contrast that appeared  
329 either in the left or right hemifield of with equal probability. We excluded sessions in which  
330 mice did not respond correctly to stimuli presented at a contrast above 50% in more than  
331 80% of trials (see Methods), which yielded a final sample of  $N = 165$  adequately trained mice  
332 that went through 1.46 million trials.

333 In line with humans, mice were biased toward perceptual history in  $54.03\% \pm 0.17\%$  of trials  
334 ( $T(164) = 23.65$ ,  $p = 9.98 \times 10^{-55}$ ; Figure 4A and Supplemental Figure S1D). Perceptual  
335 history effects remained significant ( $\beta = 0.51 \pm 4.49 \times 10^{-3}$ ,  $z = 112.84$ ,  $p = 0$ ) when  
336 controlling for external sensory information ( $\beta = 2.96 \pm 4.58 \times 10^{-3}$ ,  $z = 646.1$ ,  $p = 0$ ) and  
337 general response biases toward one of the two potential outcomes ( $\beta = -1.78 \pm 0.02$ ,  $z =$   
338  $-80.64$ ,  $p < 2.2 \times 10^{-308}$ ; see Supplemental Figure S4C-D for model comparisons and  $\beta$   
339 values computed within individual mice).

340 In the *basic task* of the IBL dataset<sup>21</sup>, stimuli were presented at random in either the left or  
341 right hemifield. Stronger biases toward perceptual history should therefore decrease perceptual  
342 performance. Indeed, history-congruent choices were more frequent when perception was  
343 stimulus-incongruent ( $61.59\% \pm 0.07\%$ ) as opposed to stimulus-congruent ( $51.81\% \pm 0.02\%$ ,

<sup>344</sup>  $T(164) = 31.37, p = 3.36 \times 10^{-71}$ ;  $T(164) = 31.37, p = 3.36 \times 10^{-71}$ ; Figure 4A, lower panel),  
<sup>345</sup> confirming that perceptual history was a source of error<sup>24,28,30,31,43</sup> as opposed to a feature of  
<sup>346</sup> the experimental paradigm. Overall, perception was stimulus-congruent in  $81.37\% \pm 0.3\%$  of  
<sup>347</sup> trials (Figure 4A).

<sup>348</sup> At the group level, we found significant autocorrelations in both stimulus-congruence (86  
<sup>349</sup> consecutive trials) and history-congruence (8 consecutive trials), which remained significant  
<sup>350</sup> when taking into account the respective autocorrelation of task difficulty and external  
<sup>351</sup> stimulation (Supplemental Figure 2C-D). In contrast to humans, mice showed a negative  
<sup>352</sup> autocorrelation coefficient of stimulus-congruence at trial 2. This was due to a feature of the  
<sup>353</sup> experimental design: Errors at a contrast above 50% were followed by a high-contrast stimulus  
<sup>354</sup> at the same location. Thus, stimulus-incongruent choices on easy trials were more likely to  
<sup>355</sup> be followed by stimulus-congruent perceptual choices that were facilitated by high-contrast  
<sup>356</sup> visual stimuli<sup>21</sup>.

<sup>357</sup> The autocorrelation of history-congruence closely overlapped with the human data and  
<sup>358</sup> decayed exponentially after a peak at the first trial (rate  $\gamma = -6.7 \times 10^{-3} \pm 5.94 \times 10^{-4}$ ,  
<sup>359</sup>  $T(3.69 \times 10^4) = -11.27, p = 2.07 \times 10^{-29}$ ; Figure 4B). On the level of individual mice,  
<sup>360</sup> autocorrelation coefficients were elevated above randomly permuted data within a lag of  $4.59$   
<sup>361</sup>  $\pm 0.06$  trials for stimulus-congruence and  $2.58 \pm 0.01$  trials for history-congruence (Figure  
<sup>362</sup> 4C).

<sup>363</sup> To further corroborate a significant autocorrelation of stimulus- and history-congruence in  
<sup>364</sup> mice, we used logistic regression models that predicted the stimulus-/history-congruence of  
<sup>365</sup> perception at the index trial  $t = 0$  from the stimulus/history-congruence at the preceding  
<sup>366</sup> trials within a lag of 25 trials. We found that regression weights were significantly greater  
<sup>367</sup> than zero for more than 25 trials for stimulus-congruence. For history-congruence, regression  
<sup>368</sup> weights significantly greater than zero for 8 trials prior to the index trial (Supplemental  
<sup>369</sup> Figure S3). In analogy to humans, mice showed anti-phase 1/f fluctuations in the sensitivity

370 to internal and external information (Figure 4D-F).

371 Next, we asked how external and internal modes relate to the trial duration (TD, a coarse  
372 measure of RT in mice that spans the interval from stimulus onset to feedback<sup>21</sup>). Stimulus-  
373 congruent (as opposed to stimulus-incongruent) choices were associated with shorter TDs ( $\delta$   
374  $= -262.48 \pm 17.1$ ,  $T(164) = -15.35$ ,  $p = 1.55 \times 10^{-33}$ ), while history-congruent choices were  
375 characterized by longer TDs ( $\delta = 30.47 \pm 5.57$ ,  $T(164) = 5.47$ ,  $p = 1.66 \times 10^{-7}$ ; Figure 4G).

376 Across the full spectrum of the available data, TDs showed a linear relationship with the  
377 mode of sensory processing, with shorter TDs during external mode ( $\beta_1 = -4.16 \times 10^4 \pm$   
378  $1.29 \times 10^3$ ,  $T(1.35 \times 10^6) = -32.31$ ,  $p = 6.03 \times 10^{-229}$ , Figure 4H). However, an explorative  
379 post-hoc analysis limited to TDs that differed from the median TD by no more than  $1.5 \times$   
380 MAD (median absolute distance<sup>52</sup>) indicated that, when mice engaged with the task more  
381 swiftly, TDs did indeed show a quadratic relationship with the mode of sensory processing  
382 ( $\beta_2 = -1.97 \times 10^3 \pm 843.74$ ,  $T(1.19 \times 10^6) = -2.34$ ,  $p = 0.02$ , Figure 4I).

383 As in humans, it is an important caveat to consider whether the observed serial dependencies  
384 in murine perception reflect a phenomenon of perceptual inference, or, alternatively, an  
385 unspecific strategy that occurs at the level of reporting behavior. We reasoned that, if mice  
386 indeed tended to repeat previous choices as a general response pattern, history effects should  
387 decrease during training of the perceptual task. We therefore analyzed how stimulus- and  
388 history-congruent perceptual choices evolved across sessions in mice that, by the end of  
389 training, achieved proficiency (i.e., stimulus-congruence  $\geq 80\%$ ) in the *basic* task of the IBL  
390 dataset<sup>21</sup>.

391 As expected, we found that stimulus-congruent perceptual choices became more frequent  
392 ( $\beta = 0.34 \pm 7.13 \times 10^{-3}$ ,  $T(8.51 \times 10^3) = 47.66$ ,  $p < 2.2 \times 10^{-308}$ ; Supplemental Figure  
393 S6) and TDs were progressively shortened ( $\beta = -22.14 \pm 17.06$ ,  $T(1.14 \times 10^3) = -1.3$ ,  $p$   
394  $< 2.2 \times 10^{-308}$ ) across sessions. Crucially, the frequency of history-congruent perceptual  
395 choices also increased during training ( $\beta = 0.13 \pm 4.67 \times 10^{-3}$ ,  $T(8.4 \times 10^3) = 27.04$ ,  $p =$

<sup>396</sup>  $1.96 \times 10^{-154}$ ; Supplemental Figure S6).

<sup>397</sup> As in humans, longer within-session task exposure was associated with an increase in history-  
<sup>398</sup> congruence ( $\beta = 3.6 \times 10^{-5} \pm 2.54 \times 10^{-6}$ ,  $z = 14.19$ ,  $p = 10^{-45}$ ) and a decrease in TDs ( $\beta$   
<sup>399</sup>  $= -0.1 \pm 3.96 \times 10^{-3}$ ,  $T(1.34 \times 10^6) = -24.99$ ,  $p = 9.45 \times 10^{-138}$ ). In sum, these findings  
<sup>400</sup> strongly argue against the proposition that mice show biases toward perceptual history due  
<sup>401</sup> to an unspecific response strategy.

<sup>402</sup> As in humans, fluctuations in the strength of history-congruent biases were, (i), larger in  
<sup>403</sup> amplitude than the corresponding fluctuations in general response biases ( $\beta_0 = -5.26 \times 10^{-3}$   
<sup>404</sup>  $\pm 4.67 \times 10^{-4}$ ,  $T(2.12 \times 10^3) = -11.28$ ,  $p = 1.02 \times 10^{-28}$ ) and, (ii), had a significant effect on  
<sup>405</sup> stimulus-congruence ( $\beta_1 = -0.12 \pm 7.17 \times 10^{-4}$ ,  $T(1.34 \times 10^6) = -168.39$ ,  $p < 2.2 \times 10^{-308}$ )  
<sup>406</sup> beyond the effect of ongoing changes in general response biases ( $\beta_2 = -0.03 \pm 6.94 \times 10^{-4}$ ,  
<sup>407</sup>  $T(1.34 \times 10^6) = -48.14$ ,  $p < 2.2 \times 10^{-308}$ ). This confirmed that, in both humans and mice,  
<sup>408</sup> perceptual performance is modulated by systematic fluctuations between externally- and  
<sup>409</sup> internally-oriented modes of sensory processing.

<sup>410</sup> Finally, we fitted full and history-conditioned psychometric curves to the data from the  
<sup>411</sup> IBL database. When estimated based on the full dataset (i.e., irrespective of the preceding  
<sup>412</sup> perceptual choice  $y_{t-1}$ ), biases  $\mu$  were distributed around zero ( $3.87 \times 10^{-3} \pm 9.81 \times 10^{-3}$ ;  
<sup>413</sup>  $T(164) = 0.39$ ,  $p = 0.69$ ; Figure 5A and B, upper panel). When conditioned on the preceding  
<sup>414</sup> perceptual choice, biases were negative for  $y_{t-1} = 0$  ( $-0.02 \pm 8.7 \times 10^{-3}$ ;  $T(164) = -1.99$ ,  $p =$   
<sup>415</sup> 0.05; Figure 5A and B, middle panel) and positive for  $y_{t-1} = 1$  ( $0.02 \pm 9.63 \times 10^{-3}$ ;  $T(164)$   
<sup>416</sup> = 1.91,  $p = 0.06$ ; Figure 5A and B, lower panel). As in humans, mice showed larger biases  
<sup>417</sup> during internal mode ( $0.14 \pm 7.96 \times 10^{-3}$ ) as compared to external mode ( $0.07 \pm 8.7 \times 10^{-3}$ ;  
<sup>418</sup>  $\beta_0 = -0.18 \pm 0.03$ ,  $T = -6.38$ ,  $p = 1.77 \times 10^{-9}$ ; controlling for differences in lapses and  
<sup>419</sup> thresholds).

<sup>420</sup> Lower and upper lapses amounted to  $\gamma = 0.1 \pm 4.35 \times 10^{-3}$  and  $\delta = 0.11 \pm 4.65 \times 10^{-3}$  (see  
<sup>421</sup> Figure 5A, C and D). Lapse rates were higher in internal mode ( $\gamma = 0.15 \pm 5.14 \times 10^{-3}$ ,

422  $\delta = 0.16 \pm 5.79 \times 10^{-3}$ ) as compared to external mode ( $\gamma = 0.06 \pm 3.11 \times 10^{-3}$ ,  $\delta = 0.07$   
423  $\pm 3.34 \times 10^{-3}$ ;  $\beta_0 = -0.11 \pm 4.39 \times 10^{-3}$ ,  $T = -24.8$ ,  $p = 4.91 \times 10^{-57}$ ; controlling for  
424 differences in biases and thresholds).

425 For  $y_{t-1} = 0$ , the difference between internal and external mode was more pronounced for  
426 higher lapses  $\delta$  ( $T(164) = 21.44$ ,  $p = 1.93 \times 10^{-49}$ ). Conversely, for  $y_{t-1} = 1$ , the difference  
427 between internal and external mode was more pronounced for lower lapses  $\gamma$  ( $T(164) =$   
428  $-18.24$ ,  $p = 2.68 \times 10^{-41}$ ). In contrast to the human data, higher lapses  $\delta$  and lower lapses  
429  $\gamma$  were significantly elevated during internal mode irrespective of the preceding perceptual  
430 choice (higher lapses  $\delta$  for  $y_{t-1} = 1$ :  $T(164) = -2.65$ ,  $p = 8.91 \times 10^{-3}$ ; higher lapses  $\delta$  for  
431  $y_{t-1} = 0$ :  $T(164) = -28.29$ ,  $p = 5.62 \times 10^{-65}$ ; lower lapses  $\gamma$  for  $y_{t-1} = 1$ :  $T(164) = -32.44$ ,  $p$   
432  $= 2.92 \times 10^{-73}$ ; lower lapses  $\gamma$  for  $y_{t-1} = 0$ :  $T(164) = -2.5$ ,  $p = 0.01$ ).

433 In mice, thresholds  $t$  amounted to  $0.15 \pm 6.52 \times 10^{-3}$  (see Figure 5A and E) and were higher  
434 in internal mode ( $0.27 \pm 0.01$ ) as compared to external mode ( $0.09 \pm 4.44 \times 10^{-3}$ ;  $\beta_0 =$   
435  $-0.28 \pm 0.04$ ,  $T = -7.26$ ,  $p = 1.53 \times 10^{-11}$ ; controlling for differences in biases and lapses).  
436 Thresholds  $t$  were not modulated by perceptual history ( $T(164) = 0.94$ ,  $p = 0.35$ ).

437 In sum, the above analyses of the psychometric function in mice corroborated our findings in  
438 humans. Higher thresholds indicated a reduced sensitivity to external information during  
439 internal mode. Additionally, internally-biased processing was characterized history-dependent  
440 modulation of biases and lapses.

## 441 **5.7 Fluctuations in mode result from coordinated changes in the 442 impact of external and internal information on perception**

443 The empirical data presented above indicate that, for both humans and mice, perception  
444 fluctuates between internal and external modes, i.e., multi-trial epochs that are character-  
445 ized by enhanced sensitivity toward either internal or external information. Since natural  
446 environments typically show high temporal redundancy<sup>34</sup>, previous experiences are often

<sup>447</sup> good predictors of new stimuli<sup>30,31,35,41</sup>. Serial dependencies may therefore induce autocorrelations in perception by serving as an internal prediction (or *memory* processes<sup>9,13</sup>) about <sup>448</sup> the environment that actively integrates noisy sensory information over time<sup>53</sup>.

<sup>450</sup> Previous work has shown that such internal predictions are built by dynamically updating the <sup>451</sup> estimated probability of being in a particular perceptual state from the sequence of preceding <sup>452</sup> experiences<sup>35,48,54</sup>. The integration of sequential inputs may lead to accumulating effects <sup>453</sup> of perceptual history that progressively override incoming sensory information, enabling <sup>454</sup> internal mode processing<sup>19</sup>. However, since such a process would lead to internal biases that <sup>455</sup> may eventually become impossible to overcome<sup>55</sup>, we assumed that changes in mode may <sup>456</sup> additionally be driven by ongoing wave-like fluctuations<sup>9,13</sup> in the perceptual impact of external <sup>457</sup> and internal information that occur *irrespective* of the sequence of previous experiences and <sup>458</sup> temporarily de-couple the decision variable from implicit internal representations of the <sup>459</sup> environment<sup>19</sup>.

<sup>460</sup> Following Bayes' theorem, we reasoned that binary perceptual decisions depend on the <sup>461</sup> posterior log ratio  $L$  of the two alternative states of the environment that participants learn <sup>462</sup> about via noisy sensory information<sup>54</sup>. We computed the posterior by combining the sensory <sup>463</sup> evidence available at time-point  $t$  (i.e., the log likelihood ratio  $LLR$ ) with the prior probability <sup>464</sup>  $\psi$ :

$$L_t = LLR_t * \omega_{LLR} + \psi_t(L_{t-1}, H) * \omega_\psi \quad (2)$$

<sup>465</sup> We derived the prior probability  $\psi$  at timepoint  $t$  from the posterior probability of perceptual <sup>466</sup> outcomes at timepoint  $L_{t-1}$ . Since a switch between the two states can occur at any time, <sup>467</sup> the effect of perceptual history varies according to both the sequence of preceding experiences <sup>468</sup> and the estimated stability of the external environment (i.e., the *hazard rate*  $H$ <sup>54</sup>):

$$\psi_t(L_{t-1}, H) = L_{t-1} + \log\left(\frac{1-H}{H} + \exp(-L_{t-1})\right) - \log\left(\frac{1-H}{H} + \exp(L_{t-1})\right) \quad (3)$$

469 The *LLR* was computed from inputs  $s_t$  by applying a sigmoid function defined by parameter  
 470  $\alpha$  that controls the sensitivity of perception to the available sensory information (see Methods  
 471 for detailed equations on humans and mice):

$$u_t = \frac{1}{1 + \exp(-\alpha * s_t)} \quad (4)$$

$$LLR_t = \log\left(\frac{u_t}{1 - u_t}\right) \quad (5)$$

472 To allow for *bimodal inference*, i.e., alternating periods of internally- and externally-biased  
 473 modes of perceptual processing that occur irrespective of the sequence of preceding experiences,  
 474 we assumed that the relative influences of likelihood and prior show coherent anti-phase  
 475 fluctuations governed by  $\omega_{LLR}$  and  $\omega_\psi$  that are determined by amplitude  $a$ , frequency  $f$  and  
 476 phase  $p$ :

$$\omega_{LLR} = a_{LLR} * \sin(f * t + p) + 1 \quad (6)$$

$$\omega_\psi = a_\psi * \sin(f * t + p + \pi) + 1 \quad (7)$$

477 Finally, a sigmoid transform of the posterior  $L_t$  yields the probability of observing the  
 478 perceptual decision  $y_t$  at a temperature determined by  $\zeta^{-1}$ :

$$P(y_t = 1) = 1 - P(y_t = 0) = \frac{1}{1 + \exp(-\zeta * L_t)} \quad (8)$$

479 Fitting the bimodal inference model outlined above to behavioral data (see Methods for  
480 details) characterizes each subject by a sensitivity parameter  $\alpha$  that captures how strongly  
481 perception is driven by the available sensory information, and a hazard rate parameter  $H$   
482 that controls how heavily perception is biased by perceptual history. As a sanity check for  
483 model fit, we tested whether the frequency of stimulus- and history-congruent trials in the  
484 Confidence database<sup>20</sup> and IBL database<sup>21</sup> correlate with the estimated parameters  $\alpha$  and  
485  $H$ , respectively. As expected, the estimated sensitivity toward stimulus information  $\alpha$  was  
486 positively correlated with the frequency of stimulus-congruent perceptual choices (humans:  $\beta$   
487  $= 8.4 \pm 0.26$ ,  $T(4.31 \times 10^3) = 32.87$ ,  $p = 1.3 \times 10^{-211}$ ; mice:  $\beta = 1.93 \pm 0.12$ ,  $T(2.07 \times 10^3)$   
488  $= 16.21$ ,  $p = 9.37 \times 10^{-56}$ ). Likewise,  $H$  was negatively correlated with the frequency of  
489 history-congruent perceptual choices (humans:  $\beta = -11.84 \pm 0.5$ ,  $T(4.29 \times 10^3) = -23.5$ ,  $p$   
490  $= 5.16 \times 10^{-115}$ ; mice:  $\beta = -6.18 \pm 0.66$ ,  $T(2.08 \times 10^3) = -9.37$ ,  $p = 1.85 \times 10^{-20}$ ).

491 Our behavioral analyses have shown that humans and mice showed significant effects of percep-  
492 tual history that impaired performance in randomized psychophysical experiments<sup>24,28,30,31,43</sup>  
493 (Figure 2A and 3A). We therefore expected that humans and mice underestimated the true  
494 hazard rate  $\hat{H}$  of the experimental environments (Confidence database<sup>20</sup>:  $\hat{H}_{Humans} = 0.5 \pm$   
495  $1.58 \times 10^{-5}$ ); IBL database<sup>21</sup>:  $\hat{H}_{Mice} = 0.49 \pm 6.47 \times 10^{-5}$ ). Indeed, when fitting the bimodal  
496 inference model outlined above to the trial-wise perceptual choices (see Methods), we found  
497 that the estimated (i.e., subjective) hazard rate  $H$  was lower than  $\hat{H}$  for both humans ( $H =$   
498  $0.45 \pm 4.8 \times 10^{-5}$ ,  $\beta = -6.87 \pm 0.94$ ,  $T(61.87) = -7.33$ ,  $p = 5.76 \times 10^{-10}$ ) and mice ( $H =$   
499  $0.46 \pm 2.97 \times 10^{-4}$ ,  $\beta = -2.91 \pm 0.34$ ,  $T(112.57) = -8.51$ ,  $p = 8.65 \times 10^{-14}$ ).

500 Simulations from the bimodal inference model (based on the posterior model parameters  
501 obtained in humans; see Methods for details) closely matched the empirical results outlined  
502 above: Simulated perceptual decisions resulted from a competition of perceptual history with  
503 incoming sensory signals (Figure 6A). Stimulus- and history-congruence were significantly  
504 auto-correlated (Figure 6B-C), fluctuating in anti-phase as 1/f noise (Figure 6D-F). Simulated

505 posterior certainty<sup>28,30,50</sup> (i.e., the absolute of the posterior log ratio  $|L_t|$ ) showed a quadratic  
506 relationship to the mode of sensory processing (Figure 6H), mirroring the relation of RTs  
507 and confidence reports to external and internal biases in perception (Figure 2G-H and Figure  
508 4G-H). Crucially, the overlap between empirical and simulated data broke down when we  
509 removed the anti-phase oscillations ( $\omega_{LLR}$  and/or  $\omega_\psi$ ) or the accumulation of evidence over  
510 time (i.e., setting  $H$  to 0.5) from the bimodal inference model (see Supplemental Figure  
511 S7-10).

512 To further probe the validity of the bimodal inference model, we tested whether posterior  
513 model quantities could explain aspects of the behavioral data that the model was not fitted to.  
514 First, we predicted that the posterior decision variable  $L_t$  not only encodes perceptual choices  
515 (i.e., the variable used for model estimation), but should also predict the speed of response  
516 and subjective confidence<sup>30,50</sup>. Indeed, the estimated trial-wise posterior decision certainty  
517  $|L_t|$  correlated negatively with RTs in humans ( $\beta = -4.36 \times 10^{-3} \pm 4.64 \times 10^{-4}$ ,  $T(1.98 \times 10^6)$   
518  $= -9.41$ ,  $p = 5.19 \times 10^{-21}$ ) and TDs mice ( $\beta = -35.45 \pm 0.86$ ,  $T(1.28 \times 10^6) = -41.13$ ,  $p <$   
519  $2.2 \times 10^{-308}$ ). Likewise, subjective confidence was positively correlated with the estimated  
520 posterior decision certainty in humans ( $\beta = 7.63 \times 10^{-3} \pm 8.32 \times 10^{-4}$ ,  $T(2.06 \times 10^6) = 9.18$ ,  
521  $p = 4.48 \times 10^{-20}$ ).

522 Second, the dynamic accumulation of information inherent to our model entails that biases  
523 toward perceptual history are stronger when the posterior decision certainty at the preceding  
524 trial is high<sup>30,31,54</sup>. Due to the link between posterior decision certainty and confidence, we  
525 reasoned that confident perceptual choices should be more likely to induce history-congruent  
526 perception at the subsequent trial<sup>30,31</sup>. Indeed, logistic regression indicated that history-  
527 congruence was predicted by the posterior decision certainty  $|L_{t-1}|$  (humans:  $\beta = 8.22 \times 10^{-3}$   
528  $\pm 1.94 \times 10^{-3}$ ,  $z = 4.25$ ,  $p = 2.17 \times 10^{-5}$ ; mice:  $\beta = -3.72 \times 10^{-3} \pm 1.83 \times 10^{-3}$ ,  $z =$   
529  $-2.03$ ,  $p = 0.04$ ) and subjective confidence (humans:  $\beta = 0.04 \pm 1.62 \times 10^{-3}$ ,  $z = 27.21$ ,  $p =$   
530  $4.56 \times 10^{-163}$ ) at the preceding trial.

531 In sum, computational modeling thus suggested that between-mode fluctuations are best  
532 explained by two interlinked processes (Figure 1E): (i), the dynamic accumulation of infor-  
533 mation across successive trials (i.e., following the estimated hazard rate  $H$ ) and, (ii), ongoing  
534 anti-phase oscillations in the impact of external and internal information (i.e., as determined  
535 by  $\omega_\psi$  and  $\omega_{LLR}$ ).

536 **5.8 Bimodal inference improves learning and perceptual metacog-  
537 nition in the absence of feedback**

538 Is there a computational benefit to be gained from temporarily down-regulating biases  
539 toward preceding choices (Figure 2-3 B and C), instead of combining them with external  
540 sensory information at a constant weight (Supplemental Figure S7)? In their adaptive  
541 function for perceptual decision-making, internal predictions critically depend on error-driven  
542 learning to remain aligned with the current state of the world<sup>56</sup>. Yet when the same network  
543 processes external and internal information in parallel, inferences may become circular and  
544 maladaptive<sup>57</sup>: Ongoing decision-related activity may be distorted by noise in external  
545 sensory signals that are fed forward from the periphery or, alternatively, by aberrant internal  
546 predictions about the environment that are fed back from higher cortical levels<sup>18,57</sup>.

547 Purely parallel processing therefore creates at least two challenges for perception: First,  
548 due to the sequential integration of inputs over time, internal predictions may progressively  
549 override sensory information<sup>55</sup>, leading to false inferences about the presented stimuli<sup>19</sup>. As a  
550 consequence, purely parallel processing may also lead to false inferences about the statistical  
551 regularities of volatile environments, where the underlying hazard rate  $\hat{H} = P(s_t \neq s_{t-1})$  (i.e.,  
552 the probability of a change in the state of the environment between two trials) may change  
553 over time. In the absence of feedback, agents have to update the estimate about  $\hat{H}$  solely  
554 on the grounds of their experience, which is determined by the posterior log ratio  $L_t$ . Yet  
555  $L_t$  depends not only on external information from the environment (the log likelihood ratio

556  $LLR_t$ ), but also on internal predictions, i.e., the log prior ratio  $L_{t-1}$  and the assumed hazard  
557 rate  $H_t$ . This circularity may impair the ability to learn about changes in  $H$  that occur in  
558 volatile environments (Figure 7A).

559 Second, purely parallel processing may also reduce the capacity to calibrate metacognitive  
560 beliefs about ongoing changes in the precision at which sensory signals are encoded. In the  
561 absence of feedback, agents depend on internal confidence signals<sup>58</sup> (i.e., the absolute of  
562 the posterior log ratio  $|L_t|$ ) to update beliefs  $M_t$  about the precision of sensory encoding  
563  $\hat{M} = 1 - |s_t - u_t|$ . While  $\hat{M}$  depends only on the likelihood  $LLR_t$ , the estimate  $M_t$  is informed  
564 by the posterior  $L_t$ , which, in turn, is additionally modulated by the prior  $L_{t-1}$  and  $H_t$ .  
565 Relying on internal predictions may thus distort metacognitive beliefs about the precision of  
566 sensory encoding (Figure 7B). This problem becomes particularly relevant when agents do  
567 not have full insight into the strength at which external and internal sources of information  
568 contribute to perceptual inference (i.e., when confidence is high during both internally- and  
569 externally-biased processing; Figure 2I-J; Figure 6G-H).

570 Here, we propose that bimodal inference may provide potential solutions to these problems  
571 of circular inference. By intermittently decoupling the decision variable  $L_t$  from internal  
572 predictions, between-mode fluctuations may create unambiguous error signals that adaptively  
573 update estimates about the hazard rate  $\hat{H}$  and the precision of sensory encoding  $\hat{M}$ .

574 To illustrate this hypothesis, we simulated data for a total of 1000 participants who performed  
575 binary perceptual decisions for a total of 20 blocks of 100 trials each. Each block differed  
576 with respect to the true hazard rate  $\hat{H}$  (either 0.1, 0.3, 0.5, 0.7 or 0.9) and the sensitivity  
577 parameter  $\alpha$  (either 2, 3, 4, 5 or 6, determining  $\hat{M}$  via the absolute of the log likelihood ratio  
578  $|LLR_t|$ , Figure 7A-B, upper panel). Importantly, the synthetic participants did not receive  
579 feedback on whether their perceptual decisions were correct.

580 We initialized each participant at a random value of  $H'_t$  (ranging from  $-0.25$  to  $0$ ) and  $M'_t$   
581 (ranging from  $0.25$  to  $2$ ), which were transformed into the unit interval to yield trial-wise

582 estimates for  $H_t$  and  $M_t$ :

$$H_t = \frac{1}{1 + \exp(-(H'_t))} \quad (9)$$

$$M_t = \frac{1}{1 + \exp(-(M'_t))} \quad (10)$$

583 For each block, we generated stimuli  $s_t$  using the true hazard rate  $\hat{H}$ . Detected inputs  $u_t$   
584 were computed according to the block-wise sensitivity parameter  $\alpha$ . Perceptual decisions  $y_t$   
585 were generated using the bimodal inference model with ( $a_\psi = a_{LLR} = 1$ ,  $\zeta = 1$  and  $f$  between  
586 0.05 and 0.15) and a unimodal control model ( $a_\psi = a_{LLR} = 0$ ,  $\zeta = 1$ ).

587 Leaning about  $H$  was driven by the error-term  $\epsilon_H$  (Figure 7A, lower panel), reflecting the  
588 difference between  $H_t$  and presence of a perceived change in the environment  $|y_t - y_{t-1}|$ :

$$\epsilon_H = |y_t - y_{t-1}| - H_t \quad (11)$$

589 Trial-wise updates to  $H$  were provided by a Resorla-Wagner-rule with learning rate  $\beta_H$   
590 (ranging from 0.05 to 0.25). Since  $y_t$  is more likely to accurately reflect the state of the  
591 environment during external mode, updates to  $H$  were additionally modulated by  $\omega_{LLR}$ :

$$H'_t = H'_{t-1} + \beta_H * \omega_{LLR} * \epsilon_H \quad (12)$$

592 Learning about  $\hat{M}$  was driven by error-term  $\epsilon_M$  (Figure 7B, lower panel), reflecting the  
593 difference between  $M_t$  and the posterior decision-certainty ( $1 - |y_t - P(y_t = 1)|$ ):

$$\epsilon_M = (1 - |y_t - P(y_t = 1)|) - M_t \quad (13)$$

594 In analogy to  $H$ , we modeled trial-wise updates to  $M$  using a Rescorla-Wagner-rule with  
 595 learning rate  $\beta_M$  (ranging from 0.05 to 0.25). Since  $y_t$  reflects the log likelihood ratio  $LLR_t$   
 596 (and therefore the precision of sensory encoding) more closely during external mode, updates  
 597 to  $P$  were additionally modulated by  $\omega_{LLR}$ :

$$M'_t = M'_{t-1} + \beta_M * \omega_{LLR} * \epsilon_M \quad (14)$$

598 For each participant, we simulated data using both the bimodal inference model described  
 599 above and a unimodal control model, in which the between-mode fluctuations were removed by  
 600 setting the amplitude parameter  $a$  to zero ( $a_\psi = a_{LLR} = 0$ ). We compared the bimodal model  
 601 of perceptual inference to the unimodal control model in terms of three dependent variables:  
 602 the probability of stimulus-congruent perceptual choices, the error in the estimate about  $H$   
 603 (i.e.,  $|H - \hat{H}|$ ) and the error in the estimate about  $M$  (i.e.,  $|M - \hat{M}|$ , with  $\hat{M} = 1 - (|s_t - u_t|)$ ).  
 604 We found that the bimodal inference model achieved lower stimulus-congruence in comparison  
 605 to the unimodal control model ( $\beta_1 = -6.71 \pm 0.03$ ,  $T(8.42 \times 10^3) = -234.31$ ,  $p < 2.2 \times 10^{-308}$ ,  
 606 Figure 7C). At the same time, the bimodal inference model yielded lower errors in the estimated  
 607 hazard rate  $H$  ( $\beta_1 = -2.94 \times 10^{-3} \pm 2.89 \times 10^{-4}$ ,  $T(4.96 \times 10^3) = -10.18$ ,  $p = 4.11 \times 10^{-24}$ )  
 608 and probability of stimulus-congruent choices  $P$  ( $\beta_1 = -0.03 \pm 1.86 \times 10^{-4}$ ,  $T(6.07 \times 10^3)$   
 609 =  $-137.75$ ,  $p < 2.2 \times 10^{-308}$ , Figure 7E). This suggests that between-mode fluctuations  
 610 may play an adaptive role for learning and perceptual metacognition by supporting robust  
 611 inferences about the statistical regularities of volatile environments and ongoing changes in  
 612 the precision of sensory encoding.

613 Finally, we asked whether differences between the bimodal inference model the unimodal  
 614 control model depend on the presence of external feedback. We predicted that the benefits of  
 615 the bimodal inference model over the unimodal control model should be lost when feedback  
 616 is provided: With feedback, the error terms that induce updates in  $H$  and  $P$  can be informed  
 617 by the true state of the environment  $s_t$  instead of posterior stimulus probabilities that are

618 distorted by circular inferences:

$$\epsilon_H = |s_t - s_{t-1}| - H_t \quad (15)$$

$$\epsilon_M = (1 - (|y_t - s_t|)) - M_t \quad (16)$$

619 We repeated the above simulation for each participant while providing feedback on a subset  
620 of trials (10%, 20%, 30%, 40%, 50%, 60%, 70%, 80%, 90% and 100%). With increasing  
621 availability of external feedback, the bimodal inference model lost its advantage over the  
622 unimodal control model in terms of, (i), the estimated hazard rate  $H$  ( $\beta_2 = 1.43 \times 10^{-3} \pm$   
623  $3.71 \times 10^{-5}$ ,  $T(10 \times 10^3) = 38.58$ ,  $p = 9.44 \times 10^{-304}$ ) and, (ii), the estimated probability of  
624 stimulus-congruent choices  $M$  ( $\beta_2 = 3.91 \times 10^{-3} \pm 2.51 \times 10^{-5}$ ,  $T(10 \times 10^3) = 156.18$ ,  $p <$   
625  $2.2 \times 10^{-308}$ , Figure 7F). This indicates that the benefits of bimodal inference are limited to  
626 situations in which external feedback is sparse.

627 **6 Discussion**

628 This work investigates the behavioral and computational characteristics of ongoing fluctuations  
629 in perceptual decision-making using two large-scale datasets in humans<sup>20</sup> and mice<sup>21</sup>. We  
630 found that humans and mice cycle through recurring intervals of reduced sensitivity to external  
631 sensory information, during which they relied more strongly on perceptual history, i.e., an  
632 internal prediction that is provided by the sequence of preceding choices. Computational  
633 modeling indicated that these infra-slow periodicities are governed by two interlinked factors:  
634 (i), the dynamic integration of sensory inputs over time and, (ii), anti-phase oscillations in  
635 the strength at which perception is driven by internal versus external sources of information.  
636 These cross-species results suggest that ongoing fluctuations in perceptual decision-making  
637 arise not merely as a noise-related epiphenomenon of limited processing capacity, but result  
638 from a structured and adaptive mechanism that fluctuates between internally- and externally-  
639 oriented modes of sensory analysis.

640 **6.1 Serial dependencies represent a pervasive and adaptive aspect  
641 of perceptual decision-making in humans and mice**

642 A growing body of literature has highlighted that perception is modulated by preceding  
643 choices<sup>22–28,30,32,33</sup>. Our work provides converging cross-species evidence supporting the  
644 notion that such serial dependencies are a pervasive and general phenomenon of perceptual  
645 decision-making (Figures 2 and 4, Supplemental Figures 1 and 3). While introducing errors in  
646 randomized psychophysical designs<sup>24,28,30,31,43</sup> (Figures 2 and 4A), we found that perceptual  
647 history facilitates post-perceptual processes such as speed of response<sup>42</sup> (Figure 2G) and  
648 subjective confidence in humans (Figure 2I).

649 At the level of individual traits, increased biases toward preceding choices were associated  
650 with reduced sensitivity to external information (Supplemental Figure 1C-D) and lower  
651 metacognitive efficiency. When investigating how serial dependencies evolve over time,

652 we observed dynamic changes in strength of perceptual history (Figures 2 and 4B) that  
653 created wavering biases toward internally- and externally-biased modes of sensory processing.  
654 Between-mode fluctuations may thus provide a new explanation for ongoing changes in  
655 perceptual performance<sup>6-11</sup>.

656 In computational terms, serial dependencies may leverage the temporal autocorrelation of  
657 natural environments<sup>31,48</sup> to increase the efficiency of decision-making<sup>35,43</sup>. Such temporal  
658 smoothing<sup>48</sup> of sensory inputs may be achieved by updating dynamic predictions about the  
659 world based on the sequence of noisy perceptual experiences<sup>22,31</sup>, using algorithms such as  
660 Kalman filtering<sup>35</sup>, Hierarchical Gaussian filtering<sup>59</sup> or sequential Bayes<sup>25,42,54</sup>. At the level of  
661 neural mechanisms, the integration of internal with external information may be realized by  
662 combining feedback from higher levels in the cortical hierarchy with incoming sensory signals  
663 that are fed forward from lower levels<sup>60</sup>.

664 Yet relying too strongly on serial dependencies may come at a cost: When accumulating over  
665 time, internal predictions may eventually override external information, leading to circular and  
666 false inferences about the state of the environment. In this work, we used model simulations  
667 to show that, akin to the wake-sleep-algorithm in machine learning<sup>61</sup>, bimodal inference  
668 may help to determine whether errors result from external input or from internally-stored  
669 predictions (Figure 7): During internal mode, sensory processing is more strongly constrained  
670 by predictive processes that auto-encode the agent’s environment. Conversely, during external  
671 mode, the network is driven predominantly by sensory inputs<sup>18</sup>. Between-mode fluctuations  
672 may thus generate an unambiguous error signal that aligns internal predictions with the current  
673 state of the environment in iterative test-update-cycles<sup>61</sup>. On a broader scale, between-mode  
674 fluctuations may thus regulate the balance between feedforward versus feedback contributions  
675 to perception and thereby play a adaptive role in metacognition and reality monitoring<sup>62</sup>.

676 **6.2 Arousal, attentional lapses, general response biases, insuf-**  
677 **ficient training and metacognitive strategies as alternative**  
678 **explanations for between-mode fluctuations**

679 These functional explanations for external and internal modes share the idea that, in order  
680 to form stable internal predictions about the statistical properties of the world (e.g., tracking  
681 the hazard rate of the environment) or metacognitive beliefs about processes occurring within  
682 the agent (e.g., monitoring ongoing changes in the reliability of feedback and feedforward  
683 processing), perception needs to temporarily disengage from internal predictions. By the  
684 same token, they presuppose that fluctuations in mode occur at the level of perceptual  
685 processing<sup>26,30,48,49</sup>, and are not a passive phenomenon that is primarily driven by factors  
686 situated up- or downstream of sensory analysis.

687 First, it may be argued that agents stereotypically repeat preceding choices when less  
688 alert. Our analyses address this alternative driver of serial dependencies by building on the  
689 association between RTs and arousal<sup>45,47</sup>. We found that RTs do not map linearly onto the  
690 mode of sensory processing, but become shorter for stronger biases toward both externally-  
691 and internally-oriented mode (Figure 2G-H; Figure 4I). These observations argue against  
692 the view that biases toward internal mode can be explained solely on the ground of ongoing  
693 changes in tonic arousal or fatigue<sup>44</sup>.

694 However, internal modes of sensory processing may also be attributed to attentional lapses<sup>63</sup>,  
695 which are caused by mind-wandering or mind-blanking and show a more complex relation to  
696 RTs<sup>63</sup>: While episodes of mind-blanking are characterized by an absence of subjective mental  
697 activity, more frequent misses, a relative increase in slow waves over posterior EEG electrodes  
698 and increased RTs, episodes of mind-wandering come along which rich inner experiences,  
699 more frequent false alarms, a relative increase of slow-wave amplitudes over frontal electrodes  
700 and decreased RTs<sup>63</sup>.

701 Yet in contrast to gradual between-mode fluctuations, engaging in mind-wandering as opposed  
702 to on-task attention seems to be an all-or-nothing phenomenon<sup>63</sup>. In addition, internally-  
703 biased processing did not increase either false alarms or misses, but induced choice errors  
704 through an enhanced impact of perceptual history (Figure 2 and 4A) that unfolded in  
705 alternating *streaks*<sup>9,13</sup> of elevated stimulus- and history-congruence. Finally, the increase in  
706 lapse rates during internal mode was not general, but history-dependent (Figures 3 and 5).  
707 While these observations clearly distinguishes between-mode fluctuations from unspecific  
708 effects of lapses on decision-making, it remains an intriguing question for future research how  
709 mind-wandering and -blanking can be differentiated from internally-oriented modes of sensory  
710 processing in terms of their phenomenology, behavioral characteristics, neural signatures and  
711 noise profiles<sup>10,63</sup>.

712 Second, it may be proposed that humans and mice apply a metacognitive response strategy  
713 that repeats preceding choices when less confident about their responses or when insufficiently  
714 trained on the task. In humans, however, confidence increased for stronger biases toward  
715 both external and internal mode (Figure 2I-J). For humans and mice, history-effects grew  
716 stronger with increasing exposure to (and expertise in) the task (Supplemental Figure S6). In  
717 addition, the existence of external and internal modes in murine perceptual decision-making  
718 (Figure 4) implies that between-mode fluctuations do not depend exclusively on the rich  
719 cognitive functions associated with human prefrontal cortex<sup>64</sup>.

720 Third, our computational modeling results provide further evidence against both of the above  
721 caveats: Simulations based on estimated model parameters closely matched the empirical data  
722 (Figure 6), reproduced aspects of behavior it was not fitted to (such as trial-wise confidence  
723 reports and RTs/TD for human and mice, respectively), and predicted that history-congruent  
724 choices occur more frequently after high-confidence trials<sup>30,31</sup>. These findings suggest that  
725 perceptual choices and post-perceptual processes such as response behavior or metacognition  
726 are jointly driven by a dynamic decision variable<sup>50</sup> that encodes uncertainty<sup>31</sup> and is affected

727 by ongoing changes in the integration of external versus internal information.

728 Of note, a recent computational study<sup>65</sup> has used a Hidden Markov Model (HMM) to  
729 investigate perceptual decision-making in the IBL database<sup>21</sup>. In analogy to our findings,  
730 the authors observed that mice switch between temporally extended *strategies* that last for  
731 more than 100 trials: During *engaged* states, perception was highly sensitive to external  
732 sensory information. During *disengaged* states, in turn, choice behavior was prone to errors  
733 due to enhanced biases toward one of the two perceptual outcomes<sup>65</sup>. Despite the conceptual  
734 differences to our approach (discrete states in a HMM that correspond to switches between  
735 distinct decision-making strategies<sup>65</sup> vs. gradual changes in mode that emerge from sequential  
736 Bayesian inference and ongoing fluctuations in the impact of external relative to internal  
737 information), it is tempting to speculate that engaged/disengaged states and between-mode  
738 fluctuations might tap into the same underlying phenomenon.

### 739 **6.3 Fluctuations in mode as a driver of 1/f dynamics in perception**

740 In light of the above, our results support the idea that, instead of unspecific effects of arousal,  
741 attention, training or metacognitive response strategies, perceptual choices are shaped by  
742 dynamic processes that occur at the level of sensory analysis<sup>26,30,49</sup>: (i), the integration of  
743 incoming signals over time and, (ii), ongoing fluctuations in the impact of external versus  
744 internal sources of decision-related information. It is particularly interesting that these two  
745 model components reproduce the established 1/f characteristic<sup>36,37</sup> of fluctuating performance  
746 in perception (see Figure 2-4D and previous work<sup>9,10,13</sup>), since this feature has been attributed  
747 to both a memory process<sup>13</sup> (corresponding to model component (i): internal predictions that  
748 are dynamically updated in response to new inputs) and wave-like variations in perceptual  
749 resources<sup>9</sup> (corresponding to model component (ii): ongoing fluctuations in the impact of  
750 internal and external information).

751 1/f noise is an ubiquitous attribute of dynamic complex systems that integrate sequences

752 of contingent sub-processes<sup>36</sup> and exhibit self-organized criticality<sup>37</sup>. As most real-world  
753 processes are *critical*, i.e. not completely uniform (or subcritical) nor completely random  
754 (or supercritical)<sup>37,66</sup>, the brain may have evolved to operate at a critical point as well<sup>38</sup>:  
755 Subcritical brains would be impervious to new inputs, whereas supercritical brains would be  
756 driven by noise. The 1/f observed in this study thus provides an intriguing connection between  
757 the notion that the brain's self-organized criticality is crucial for balancing network stability  
758 with information transmission<sup>38</sup> and the adaptive functions of between-mode fluctuations<sup>18</sup>,  
759 which we propose to support the build-up of robust internal predictions despite an ongoing  
760 stream of noisy sensory inputs.

## 761 **6.4 Dopamine-dependent changes in E-I-balance as a neural mech- 762 anism of between-mode fluctuations**

763 The link to self-organized criticality suggests that balanced cortical excitation and inhibition<sup>67</sup>  
764 (E-I), which may enable efficient coding<sup>67</sup> by maintaining neural networks in critical states<sup>68</sup>,  
765 could provide a potential neural mechanism of between-mode fluctuations. Previous work has  
766 proposed that the balance between glutamatergic excitation and GABA-ergic inhibition is  
767 regulated by activity-dependent feedback through NMDA receptors<sup>69</sup>. Such NMDA-mediated  
768 feedback has been related to the integration of external inputs over time<sup>67</sup> (model component  
769 (i), Figure 1E), thereby generating serial dependencies in decision-making<sup>70-73</sup>. Intriguingly,  
770 slow neuromodulation by dopamine enhances NMDA-dependent signaling<sup>70,74,75</sup> and fluctuates  
771 at infra-slow frequencies<sup>76,77</sup> that match the temporal dynamics of between-mode fluctuations  
772 observed in humans (Figure 2) and mice (Figure 4). Ongoing fluctuations in the impact of  
773 external versus internal information (model component (ii)) may thus be caused by phasic  
774 changes in E-I-balance that are induced by dopaminergic neuromodulation.

## **775 6.5 Limitations and open questions**

776 In this study, we show that perception is attracted toward preceding choices in mice<sup>21</sup> (Figure  
777 4A) and humans (Figure 2A; see Supplemental Figure S1 for analyses within individual studies  
778 of the Confidence database<sup>20</sup>). Of note, previous work has shown that perceptual decision-  
779 making is concurrently affected by both attractive and repulsive serial biases that operate on  
780 distinct time-scales and serve complementary functions for sensory processing<sup>27,78,79</sup>: Short-  
781 term attraction may serve the decoding of noisy sensory inputs and increase the stability  
782 of perception, whereas long-term repulsion may enable efficient encoding and sensitivity to  
783 change<sup>27</sup>.

784 Importantly, repulsive biases operate in parallel to attractive biases<sup>27</sup> and are therefore  
785 unlikely to account for the ongoing changes in mode that occur in alternating cycles of  
786 internally- and externally-oriented processing. To elucidate whether attraction and repulsion  
787 both fluctuate in their impact on perceptual decision-making will be an important task for  
788 future research, since this would help to understand whether attractive and repulsive biases  
789 are linked in terms of their computational function and neural implementation<sup>27</sup>.

790 A second open question concerns the neurobiological underpinnings of ongoing changes in  
791 mode. Albeit purely behavioral, our results tentatively suggest dopaminergic neuromodulation  
792 of NMDA-mediated feedback as one potential mechanism of externally- and internally-biased  
793 modes. Since between-mode fluctuations were found in both humans and mice, future  
794 studies can apply both non-invasive and invasive neuro-imaging and electrophysiology to  
795 better understand the neural mechanisms that generate ongoing changes in mode in terms of  
796 neuro-anatomy, -chemistry and -circuitry.

797 Finally, establishing the neural correlates of externally- an internally-biased modes will  
798 enable exiting opportunities to investigate their role for adaptive perception and decision-  
799 making. Causal interventions via pharmacological challenges, optogenetic manipulations or  
800 (non-)invasive brain stimulation will help to understand whether between-mode fluctuations

<sup>801</sup> are implicated in resolving credit-assignment problems<sup>18,80</sup> or in calibrating metacognition  
<sup>802</sup> and reality monitoring<sup>62</sup>. Addressing these questions may therefore provide new insight  
<sup>803</sup> into the pathophysiology of hallucinations and delusions, which have been characterized by  
<sup>804</sup> an imbalance in the impact of external versus internal information<sup>60,81,82</sup> and are typically  
<sup>805</sup> associated with metacognitive failures and a departure from consensual reality<sup>82</sup>.

806 **7 Methods**

807 **7.1 Ressource availability**

808 **7.1.1 Lead contact**

809 Further information and requests for resources should be directed to and will be fulfilled by  
810 the lead contact, Veith Weilnhammer (veith.weilnhammer@gmail.com).

811 **7.1.2 Materials availability**

812 This study did not generate new unique reagents.

813 **7.1.3 Data and code availability**

814 All custom code and behavioral data are available on <https://github.com/veithweilnhammer/>  
815 Modes. This manuscript was created using the *R Markdown* framework, which integrates all  
816 data-related computations and the formatted text within one document. With this, we wish  
817 to make our approach fully transparent and reproducible for reviewers and future readers.

818 **7.2 Experimental model and subject details**

819 **7.2.1 Confidence database**

820 We downloaded the human data from the Confidence database<sup>20</sup> on 21/10/2020, limiting our  
821 analyses to the database category *perception*. Within this category, we selected studies in  
822 which participants made binary perceptual decision between two alternative outcomes (see  
823 Supplemental Table 1). We excluded two studies in which the average perceptual accuracy  
824 fell below 50%. After excluding these studies, our sample consisted of 21.05 million trials  
825 obtained from 4317 human participants and 66 individual studies.

826 **7.2.2 IBL database**

827 We downloaded the murine data from the IBL database<sup>21</sup> on 28/04/2021. We limited our  
828 analyses to the *basic task*, during which mice responded to gratings that appeared with  
829 equal probability in the left or right hemifield. Within each mouse, we excluded sessions in  
830 which perceptual accuracy was below 80% for stimuli presented at a contrast  $\geq 50\%$ . After  
831 exclusion, our sample consisted of 1.46 million trials obtained from  $N = 165$  mice.

832 **7.3 Method details**

833 **7.3.1 Variables of interest**

834 **Primary variables of interest:** We extracted trial-wise data on the presented stimulus and  
835 the associated perceptual decision. Stimulus-congruent choices were defined by perceptual  
836 decisions that matched the presented stimuli. History-congruent choices were defined by  
837 perceptual choices that matched the perceptual choice at the immediately preceding trial.  
838 The dynamic probabilities of stimulus- and history-congruence were computed in sliding  
839 windows of  $\pm 5$  trials.

840 The *mode* of sensory processing was derived by subtracting the dynamic probability of history-  
841 congruence from the dynamic probability of stimulus-congruence, such that positive values  
842 indicate externally-oriented processing, whereas negative values indicate internally-oriented  
843 processing. When visualizing the relation of the mode of sensory processing to confidence,  
844 response times or trial duration (see below), we binned the mode variable in 10% intervals.  
845 We excluded bins than contained less than 0.5% of the total number of available data-points.

846 **Secondary variables of interest:** From the Confidence Database<sup>20</sup>, we furthermore  
847 extracted trial-wise confidence reports and response times (RTs; if RTs were available for  
848 both the perceptual decision and the confidence report, we only extracted the RT associated  
849 with the perceptual decision). To enable comparability between studies, we normalized RTs  
850 and confidence reports within individual studies using the *scale* R function. If not available

851 for a particular study, RTs and confidence reports were treated as missing variables. From the  
852 IBL database<sup>21</sup>, we extracted trial durations (TDs) as defined by interval between stimulus  
853 onset and feedback, which represents a coarse measure of RT<sup>21</sup>.

854 **Exclusion criteria for individual data-points:** For non-normalized data (TDs from  
855 the IBL database<sup>21</sup>; d-prime, meta-dprime and M-ratio from the Confidence database<sup>20</sup> and  
856 simulated confidence reports), we excluded data-points that differed from the median by  
857 more than 3 x MAD (median absolute distance<sup>52</sup>). For normalized data (RTs and confidence  
858 reports from the Confidence database<sup>20</sup>), we excluded data-points that differed from the  
859 mean by more than 3 x SD (standard deviation).

### 860 7.3.2 Control variables

861 Next to the sequence of presented stimuli, we assessed the autocorrelation of task difficulty as  
862 an alternative explanation for any autocorrelation in stimulus- and history-congruence. For the  
863 Confidence Database<sup>20</sup>, task difficulty was indicated by one of the following labels: *Difficulty*,  
864 *Difference*, *Signal-to-Noise*, *Dot-Difference*, *Congruency*, *Coherence(-Level)*, *Dot-Proportion*,  
865 *Contrast(-Difference)*, *Validity*, *Setsize*, *Noise-Level(-Degree)* or *Temporal Distance*. When  
866 none of the above was available for a given study, task difficulty was treated as a missing  
867 variable. In analogy to RTs and confidence, difficulty levels were normalized within individual  
868 studies. For the IBL Database<sup>21</sup>, task difficulty was defined by the contrast of the presented  
869 grating.

### 870 7.3.3 Autocorrelations

871 For each participant, trial-wise autocorrelation coefficients were estimated using the R-  
872 function *acf* with a maximum lag defined by the number of trials available per subject.  
873 Autocorrelation coefficients are displayed against the lag (in numbers of trials, ranging from  
874 1 to 20) relative to the index trial ( $t = 0$ , see Figure 2B-C, 4B-C and 6B-C). To account  
875 for spurious autocorrelations that occur due to imbalances in the analyzed variables, we

estimated autocorrelations for randomly permuted data (100 iterations). For group-level autocorrelations, we computed the differences between the true autocorrelation coefficients and the mean autocorrelation observed for randomly permuted data and averaged across participants.

At a given trial, group-level autocorrelation coefficients were considered significant when linear mixed effects modeling indicated that the difference between real and permuted autocorrelation coefficients was above zero at an alpha level of 0.05%. To test whether the autocorrelation of stimulus- and history-congruence remained significant when controlling for task difficulty and the sequence of presented stimuli, we added the respective autocorrelation as an additional factor to the linear mixed effects model that computed the group-level statistics (see also *Mixed effects modeling*).

To assess autocorrelations at the level of individual participants, we counted the number of subsequent trials (starting at the first trial after the index trial) for which less than 50% of the permuted autocorrelation coefficients exceeded the true autocorrelation coefficient. For example, a count of zero indicates that the true autocorrelation coefficients exceeded *less than 50%* of the autocorrelation coefficients computed for randomly permuted data at the first trial following the index trial. A count of five indicates that, for the first five trials following the index trial, the true autocorrelation coefficients exceeded *more than 50%* of the respective autocorrelation coefficients for the randomly permuted data; at the 6th trial following the index trial, however, *less than 50%* of the autocorrelation coefficients exceeded the respective permuted autocorrelation coefficients.

#### 7.3.4 Spectral analysis

We used the R function *spectrum* to compute the spectral densities for the dynamic probabilities of stimulus- and history-congruence as well as the phase (i.e., frequency-specific shift between the two time-series ranging from 0 to  $2 * \pi$ ) and squared coherence (frequency-specific variable that denotes the degree to which the shift between the two time-series is constant,

902 ranging from 0 to 100%). Periodograms were smoothed using modified Daniell smoothers at  
903 a width of 50.

904 Since the dynamic probabilities of history- and stimulus-congruence were computed using  
905 a sliding windows of  $\pm 5$  trials (i.e., intervals containing a total of 11 trials), we report the  
906 spectral density, coherence and phase for frequencies below  $1/11 \text{ } 1/N_{trials}$ . Spectral densities  
907 have one value per subject and frequency (data shown in Figures 2D and 4D). To assess the  
908 relation between stimulus- and history-congruence in this frequency range, we report average  
909 phase and average squared coherence for all frequencies below  $1/11 \text{ } 1/N_{trials}$  (i.e., one value  
910 per subject; data shown in Figure 2E-F and 4E-F).

911 Since the data extracted from the Confidence Database<sup>20</sup> consist of a large set of individual  
912 studies that differ with respect to inter-trial intervals, we defined the variable *frequency* in  
913 the dimension of cycles per trial  $1/N_{trials}$  rather than cycles per second (Hz). For consistency,  
914 we chose  $1/N_{trials}$  as the unit of frequency for the IBL database<sup>21</sup> as well.

## 915 7.4 Quantification and statistical procedures

916 All aggregate data are reported and displayed with errorbars as mean  $\pm$  standard error of  
917 the mean.

### 918 7.4.1 Mixed effects modeling

919 Unless indicated otherwise, we performed group-level inference using the R-packages *lmer*  
920 and *afex* for linear mixed effects modeling and *glmer* with a binomial link-function for logistic  
921 regression. We compared models based on Akaike Information Criteria (AIC). To account  
922 for variability between the studies available from the Confidence Database<sup>20</sup>, mixed modeling  
923 was conducted using random intercepts defined for each study. To account for variability  
924 across experimental session within the IBL database<sup>21</sup>, mixed modeling was conducted using  
925 random intercepts defined for each individual session. When multiple within-participant

926 datapoints were analyzed, we estimated random intercepts for each participant that were  
927 *nested* within the respective study of the Confidence database<sup>20</sup>. By analogy, for the IBL  
928 database<sup>21</sup>, we estimated random intercepts for each session that were nested within the  
929 respective mouse. We report  $\beta$  values referring to the estimates provided by mixed effects  
930 modeling, followed by the respective T statistic (linear models) or z statistic (logistic models).

931 The effects of stimulus- and history-congruence on RTs and confidence reports (Figure 2, 4  
932 and 6, subpanels G-I) were assessed in linear mixed effects models that tested for main effects  
933 of both stimulus- and history-congruence as well as the between-factor interaction. Thus, the  
934 significance of any effect of history-congruence on RTs and confidence reports was assessed  
935 while controlling for the respective effect of stimulus-congruence (and vice versa).

### 936 7.4.2 Psychometric function

937 We obtained psychometric curves by fitting the following error function to the behavioral  
938 data:

$$y_p = \gamma + (1 - \gamma - \delta) * (\operatorname{erf}(\frac{s_w + \mu}{t}) + 1)/2 \quad (17)$$

939 We used a maximum likelihood procedure to predict individual choices  $y$  (outcome A:  $y = 0$ ;  
940 outcome B:  $y = 1$ ) from the choice probability  $y_p$ . In humans, we computed  $s_w$  multiplying  
941 the inputs  $s$  (stimulus A: 0; outcome B: 1) with the task difficulty  $D_b$  (binarized across 7  
942 levels):

$$s_w = (s - 0.5) * D_b \quad (18)$$

943 In mice,  $s_w$  was defined by the respective stimulus contrast in the two hemifields:

$$s_w = \operatorname{Contrast}_{Right} - \operatorname{Contrast}_{Left} \quad (19)$$

944 Parameters of the psychometric error function were fitted using the R-package *optimx*. The  
945 psychometric error function was defined via the parameters  $\gamma$  (lower lapse; lower bound = 0,  
946 upper bound = 0.5),  $\delta$  (upper lapse; lower bound = 0, upper bound = 0.5),  $\mu$  (bias; lower  
947 bound humans = -5; upper bound humans = 5, lower bound mice = -0.5, upper bound mice  
948 = 0.5) and threshold  $t$  (lower bound humans = 0.5, upper bound humans = 25; lower bound  
949 mice = 0.01, upper bound mice = 1.5).

950 **7.4.3 Computational modeling**

951 **Model definition:** Our modeling analysis is an extension of a model proposed by Glaze et  
952 al.<sup>54</sup>, who defined a normative account of evidence accumulation for decision-making. In this  
953 model, trial-wise choices are explained by applying Bayes theorem to infer moment-by-moment  
954 changes in the state of environment from trial-wise noisy observations across trials.

955 Following Glaze et al.<sup>54</sup>, we applied Bayes rule to compute the posterior evidence for the  
956 two alternative choices (i.e., the log posterior ratio  $L$ ) from the sensory evidence available at  
957 time-point  $t$  (i.e., the log likelihood ratio  $LLR$ ) with the prior probability  $\psi$ :

$$L_t = LLR_t * \omega_{LLR} + \psi_t(L_{t-1}, H) * \omega_\psi \quad (20)$$

958 In the trial-wise design studied here, a transition between the two states of the environment  
959 (i.e., the sources generating the noisy observations available to the participant) can occur  
960 at any time. Despite the random nature of the psychophysical paradigms studied here<sup>20,21</sup>,  
961 humans and mice showed significant biases toward preceding choices (Figure 2A and 4A).  
962 We thus assumed that the prior probability of the two possible outcomes depends on the  
963 posterior choice probability at the preceding trial and the hazard rate  $H$  assumed by the  
964 participant. Following Glaze et al.<sup>54</sup>, the prior  $\psi$  is thus computed as follows:

$$\psi_t(L_{t-1}, H) = L_{t-1} + \log\left(\frac{1-H}{H} + \exp(-L_{t-1})\right) - \log\left(\frac{1-H}{H} + \exp(L_{t-1})\right) \quad (21)$$

965 In this model, humans, mice and simulated agents make perceptual choices based on noisy  
 966 observations  $u$ . These are computed by applying a sensitivity parameter  $\alpha$  to the content of  
 967 external sensory information  $s$ . For humans, we defined the input  $s$  by the two alternative  
 968 states of the environment (stimulus A:  $s = 0$ ; stimulus B:  $s = 1$ ), which generated the  
 969 observations  $u$  through a sigmoid function that applied a sensitivity parameter  $\alpha$ :

$$u_t = \frac{1}{1 + \exp(-\alpha * (s_t - 0.5))} \quad (22)$$

970 In mice, the inputs  $s$  were defined by the respective stimulus contrast in the two hemifields:

$$s_t = \text{Contrast}_{Right} - \text{Contrast}_{Left} \quad (23)$$

971 As in humans, we derived the input  $u$  by applying a sigmoid function with a sensitivity  
 972 parameter  $\alpha$  to input  $s$ :

$$u_t = \frac{1}{1 + \exp(-\alpha * s_t)} \quad (24)$$

973 For humans, mice and in simulations, the log likelihood ratio  $LLR$  was computed from  $u$  as  
 974 follows:

$$LLR_t = \log\left(\frac{u_t}{1 - u_t}\right) \quad (25)$$

975 To allow for long-range autocorrelation in stimulus- and history-congruence (Figure 2B and  
 976 4B), our modeling approach differed from Glaze et al.<sup>54</sup> in that it allowed for systematic  
 977 fluctuation in the impact of sensory information (i.e.,  $LLR$ ) and the prior probability

978 of choices  $\psi$  on the posterior probability  $L$ . This was achieved by multiplying the log  
 979 likelihood ratio and the log prior ratio with coherent anti-phase fluctuations according to  
 980  $\omega_{LLR} = a_{LLR} * \sin(f * t + phase) + 1$  and  $\omega_\psi = a_\psi * \sin(f * t + phase + \pi) + 1$ .

981 **Model fitting:** In model fitting, we predicted the trial-wise choices  $y_t$  (option A: 0; option B:  
 982 1) from inputs  $s$ . To this end, we minimized the log loss between  $y_t$  and the choice probability  
 983  $y_{pt}$  in the unit interval.  $y_{pt}$  was derived from  $L_t$  using a sigmoid function defined by the  
 984 inverse decision temperature  $\zeta$ :

$$y_{pt} = \frac{1}{1 + \exp(-\zeta * L_t)} \quad (26)$$

985 This allowed us to infer the free parameters  $H$  (lower bound = 0, upper bound = 1; human  
 986 posterior =  $0.45 \pm 4.8 \times 10^{-5}$ ; murine posterior =  $0.46 \pm 2.97 \times 10^{-4}$ ),  $\alpha$  (lower bound  
 987 = 0, upper bound = 5; human posterior =  $0.5 \pm 1.12 \times 10^{-4}$ ; murine posterior =  $1.06 \pm$   
 988  $2.88 \times 10^{-3}$ ),  $a_\psi$  (lower bound = 0, upper bound = 10; human posterior =  $1.44 \pm 5.27 \times 10^{-4}$ ;  
 989 murine posterior =  $1.71 \pm 7.15 \times 10^{-3}$ ),  $amp_{LLR}$  (lower bound = 0, upper bound = 10; human  
 990 posterior =  $0.5 \pm 2.02 \times 10^{-4}$ ; murine posterior =  $0.39 \pm 1.08 \times 10^{-3}$ ), frequency  $f$  (lower  
 991 bound = 1/40, upper bound = 1/5; human posterior =  $0.11 \pm 1.68 \times 10^{-5}$ ; murine posterior  
 992 =  $0.11 \pm 1.63 \times 10^{-4}$ ),  $p$  (lower bound = 0, upper bound =  $2 * \pi$ ; human posterior =  $2.72 \pm$   
 993  $4.41 \times 10^{-4}$ ; murine posterior =  $2.83 \pm 3.95 \times 10^{-3}$ ) and inverse decision temperature  $\zeta$  (lower  
 994 bound = 1, upper bound = 10; human posterior =  $4.63 \pm 1.95 \times 10^{-4}$ ; murine posterior =  
 995  $4.82 \pm 3.03 \times 10^{-3}$ ) using the R-function *optimx*.

996 To validate our model, we correlated individual posterior parameter estimates with the  
 997 respective conventional variables. We assumed that, (i), the estimated hazard rate  $H$  should  
 998 correlate negatively with the frequency of history-congruent choices and that, (ii), the  
 999 estimated  $\alpha$  should correlate positively with the frequency of stimulus-congruent choices.  
 1000 In addition, we tested whether the posterior decision certainty (i.e. the absolute of the  
 1001 posterior log ratio) correlated negatively with RTs and positively with subjective confidence.

1002 This allowed us to assess whether our model could explain aspects of the data it was not  
1003 fitted to (i.e., RTs and confidence). Finally, we used simulations (see below) to show that  
1004 all model components, including the anti-phase oscillations governed by  $a_\psi$ ,  $a_{LLR}$ ,  $f$  and  $p$ ,  
1005 were necessary for our model to reproduce the empirical data observed for the Confidence  
1006 database<sup>20</sup> and IBL database<sup>21</sup>.

1007 **Model simulation 1: Data recovery:** We used the posterior model parameters observed  
1008 for humans ( $H$ ,  $\alpha$ ,  $a_\psi$ ,  $a_{LLR}$  and  $f$ ) to define individual parameters for simulation in 4317  
1009 simulated participants (i.e., equivalent to the number of human participants). For each  
1010 participant, the number of simulated choices was drawn from a uniform distribution ranging  
1011 from 300 to 700 trials. Inputs  $s$  were drawn at random for each trial, such that the sequence  
1012 of inputs to the simulation did not contain any systematic seriality. Noisy observations  $u$   
1013 were generated by applying the posterior parameter  $\alpha$  to inputs  $s$ , thus generating stimulus-  
1014 congruent choices in  $71.36 \pm 2.6 \times 10^{-3}\%$  of trials. Choices were simulated based on the  
1015 trial-wise choice probabilities  $y_p$ . Simulated data were analyzed in analogy to the human  
1016 and murine data. As a substitute of subjective confidence, we computed the absolute of the  
1017 trial-wise posterior log ratio  $|L|$  (i.e., the posterior decision certainty).

1018 **Model simulation 2: Testing the adaptive benefits of bimodal inference:** In contrast  
1019 to the model applied to the behavioral data, our second set of simulations considered a  
1020 situation in which agents learn about the properties of the environment from experience.  
1021 We modeled dynamic updates in the trial-wise estimates  $H_t$  about the true hazard rate  
1022  $\hat{H} = P(s_t \neq s_{t-1})$  and trial-wise estimates  $M_t$  about the precision of sensory encoding  
1023  $\hat{M} = 1 - (|s_t - u_t|)$ .

1024 In the absence of feedback, leaning about  $\hat{H}$  was driven by the error-term  $\epsilon_H$ , which reflected  
1025 the difference between the currently assumed hazard rate  $H_t$  and the presence of a *perceived*  
1026 change in the environment  $|y_t - y_{t-1}|$ :

$$\epsilon_H = |y_t - y_{t-1}| - H_t \quad (27)$$

1027 In the presence of feedback,  $\epsilon_H$  reflected the difference between the currently assumed hazard  
1028 rate  $H_t$  and an presence of a *true* change in the environment  $|s_t - s_{t-1}|$ :

$$\epsilon_H = |s_t - s_{t-1}| - H_t \quad (28)$$

1029 In the absence of feedback, learning about  $\hat{M}$  was driven by the error-term  $\epsilon_M$ , reflecting the  
1030 difference between  $M_t$  and the posterior decision-certainty  $(1 - |y_t - P(y_t = 1)|)$ :

$$\epsilon_M = (1 - |y_t - P(y_t = 1)|) - M_t \quad (29)$$

1031 In the presence of feedback,  $\epsilon_M$  reflected the difference between  $M_t$  and the stimulus-  
1032 congruence of the current response  $(1 - (|y_t - s_t|))$ :

$$\epsilon_M = (1 - (|y_t - s_t|)) - M_t \quad (30)$$

1033 Updates to  $H$  and  $M$  were computed in logit-space using a Rescorla-Wagner-rule with learning  
1034 rates defined by the product of  $\beta_{H/M}$  and  $\omega_{LLR}$ .  $H_t$  and  $M_t$  are computed by transforming  
1035  $H'_t$  and  $M'_t$  into the unit interval using a sigmoid function:

$$H'_t = H'_{t-1} + \beta_H * \omega_{LLR} * \epsilon_H \quad (31)$$

$$H_t = \frac{1}{1 + exp(-(H'_t))} \quad (32)$$

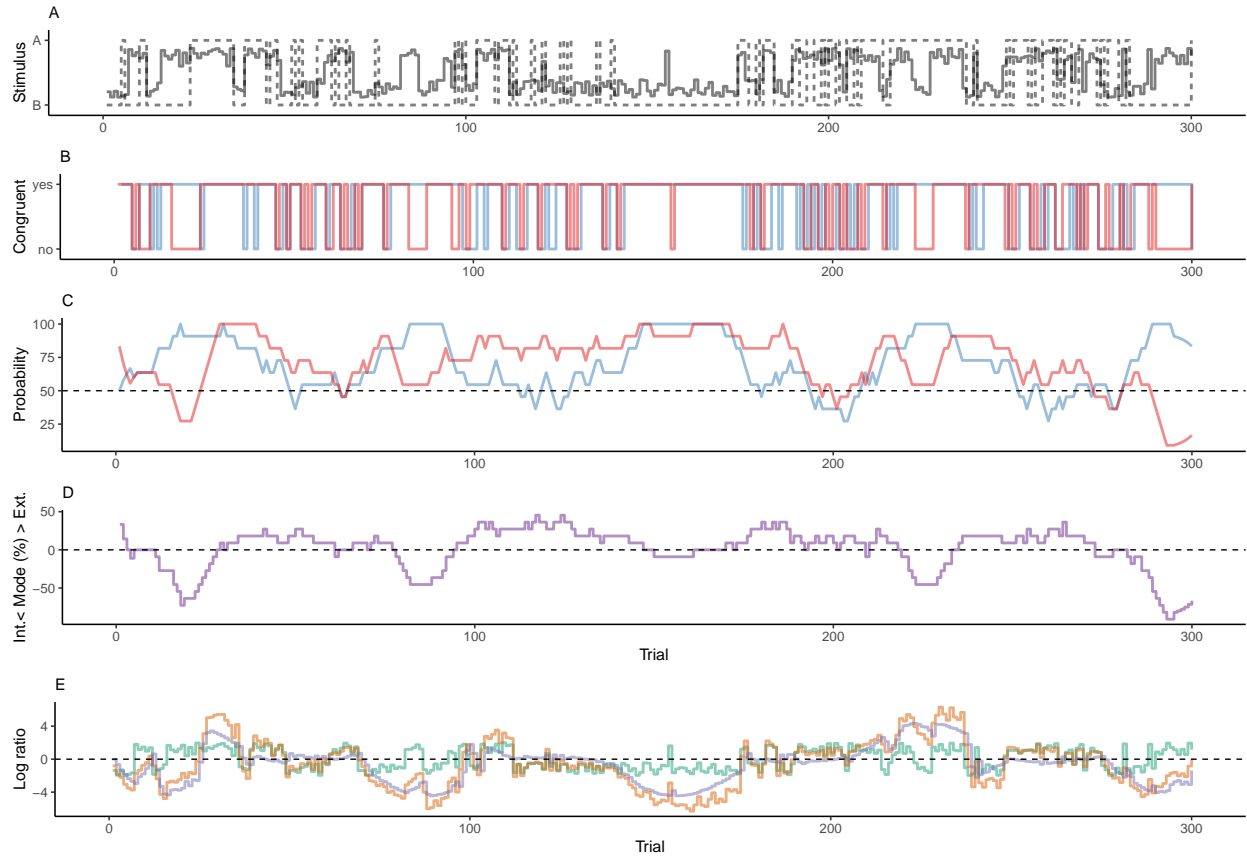
$$M'_t = M'_{t-1} + \beta_M * \omega_{LLR} * \epsilon_M \quad (33)$$

$$M_t = \frac{1}{1 + \exp(-(M'_t))} \quad (34)$$

1036 We simulated data for a total of 1000 participants for a total of 20 blocks of 100 trials each.  
 1037 Each block differed with respect to the true hazard rate  $\hat{H}$  (either 0.1, 0.3, 0.5, 0.7 or 0.9) and  
 1038 the sensitivity parameter  $\alpha$  (either 2, 3, 4, 5 or 6, corresponding to values of  $\hat{M}$  of 0.73, 0.82,  
 1039 0.88, 0.92 or 0.95). Across participants, model parameters were set as follows:  $H'_1$  initialized  
 1040 at random in a unit interval between -0.25 to 0;  $P'_1$  initialized at random in a unit interval  
 1041 between 0.25 to 2;  $a = 1$ ;  $f$  between 0.05 and 0.15 Hz;  $\zeta = 1$ ;  $\beta_H$  and  $\beta_M$  between 0.05 and  
 1042 0.25. For each participant, we ran separate simulations with external feedback provided in  
 1043 0%, 10%, 20%, 30%, 40%, 50%, 60%, 70%, 80%, 90% and 100% of trials.

1044 **8 Figures**

1045 **8.1 Figure 1**



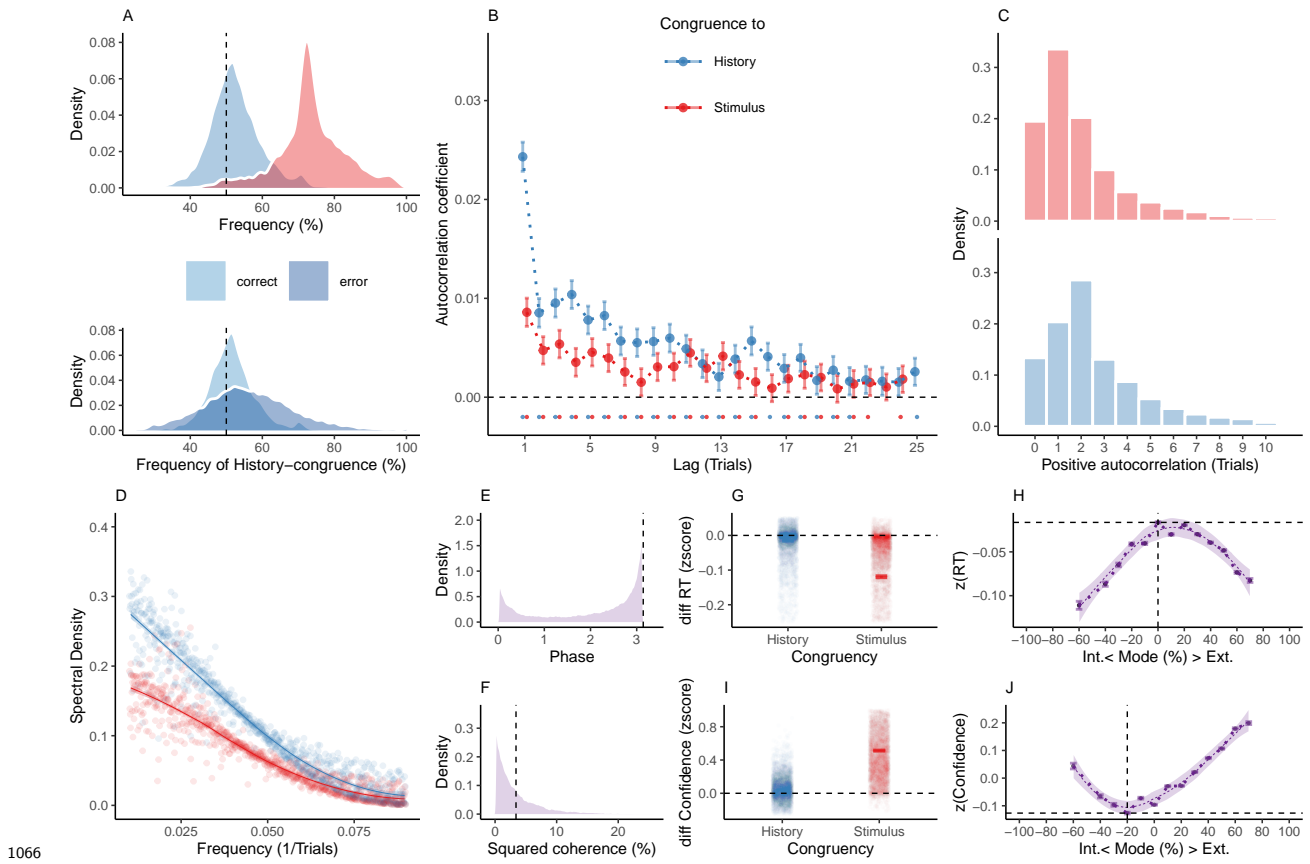
1047 **Figure 1. Concept.**

- 1048 A. In binary perceptual decision-making, a participant is presented with stimuli from two  
1049 categories (A vs. B; dotted line) and reports consecutive perceptual choices via button presses  
1050 (solid line). All panels below refer to this example data.
- 1051 B. When the response matched the external stimulus information (i.e., overlap between dotted  
1052 and solid line in panel A), perceptual choices are *stimulus-congruent* (red line). When the  
1053 response matches the response at the preceding trial, perceptual choices are *history-congruent*  
1054 (blue line).
- 1055 C. The dynamic probabilities of stimulus- and history-congruence (i.e., computed in sliding  
1056 windows of  $\pm 5$  trials) fluctuate over time.

1057 D. The *mode* of perceptual processing is derived by computing the difference between the  
1058 dynamic probabilities of stimulus- and history-congruence. Values above 0% indicate a  
1059 bias toward external information, whereas values below 0% indicate a bias toward internal  
1060 information.

1061 E. In computational modeling, internal mode is caused by an enhanced impact of perceptual  
1062 history. This causes the posterior (black line) to be close to the prior (blue line). Conversely,  
1063 during external mode, the posterior is close to the sensory information (log likelihood ratio,  
1064 red line).

1065 **8.2 Figure 2**



1066 **Figure 2. Internal and external modes in human perceptual decision-making.**

1067 A. In humans, perception was stimulus-congruent in  $73.46\% \pm 0.15\%$  (in red) and history-congruent in  $52.7\% \pm 0.12\%$  of trials (in blue; upper panel). History-congruent perceptual choices were more frequent when perception was stimulus-incongruent (i.e., on *error* trials; lower panel), indicating that history effects impair performance in randomized psychophysical designs.

1068 B. Relative to randomly permuted data, we found highly significant autocorrelations of stimulus-congruence and history-congruence (dots indicate intercepts  $\neq 0$  in trial-wise linear mixed effects modeling at  $p < 0.05$ ). Across trials, the autocorrelation coefficients were best fit by an exponential function (adjusted  $R^2$  for stimulus-congruence: 0.53; history-congruence: 0.71) as compared to a linear function (adjusted  $R^2$  for stimulus-congruence: 0.52; history-congruence: 0.49).

1079 C. Here, we depict the number of consecutive trials at which autocorrelation coefficients  
1080 exceeded the respective autocorrelation of randomly permuted data within individual partici-  
1081 pants. For stimulus-congruence (upper panel), the lag of positive autocorrelation amounted  
1082 to  $3.24 \pm 2.39 \times 10^{-3}$  on average, showing a peak at trial t+1 after the index trial. For  
1083 history-congruence (lower panel), the lag of positive autocorrelation amounted to  $4.87 \pm$   
1084  $3.36 \times 10^{-3}$  on average, peaking at trial t+2 after the index trial.

1085 D. The smoothed probabilities of stimulus- and history-congruence (sliding windows of  $\pm 5$   
1086 trials) fluctuated as *1/f noise*, i.e., at power densities that were inversely proportional to the  
1087 frequency.

1088 E. The distribution of phase shift between fluctuations in stimulus- and history-congruence  
1089 peaked at half a cycle ( $\pi$  denoted by dotted line).

1090 F. The average squared coherence between fluctuations in stimulus- and history-congruence  
1091 (black dottet line) amounted to  $6.49 \pm 2.07 \times 10^{-3}\%$

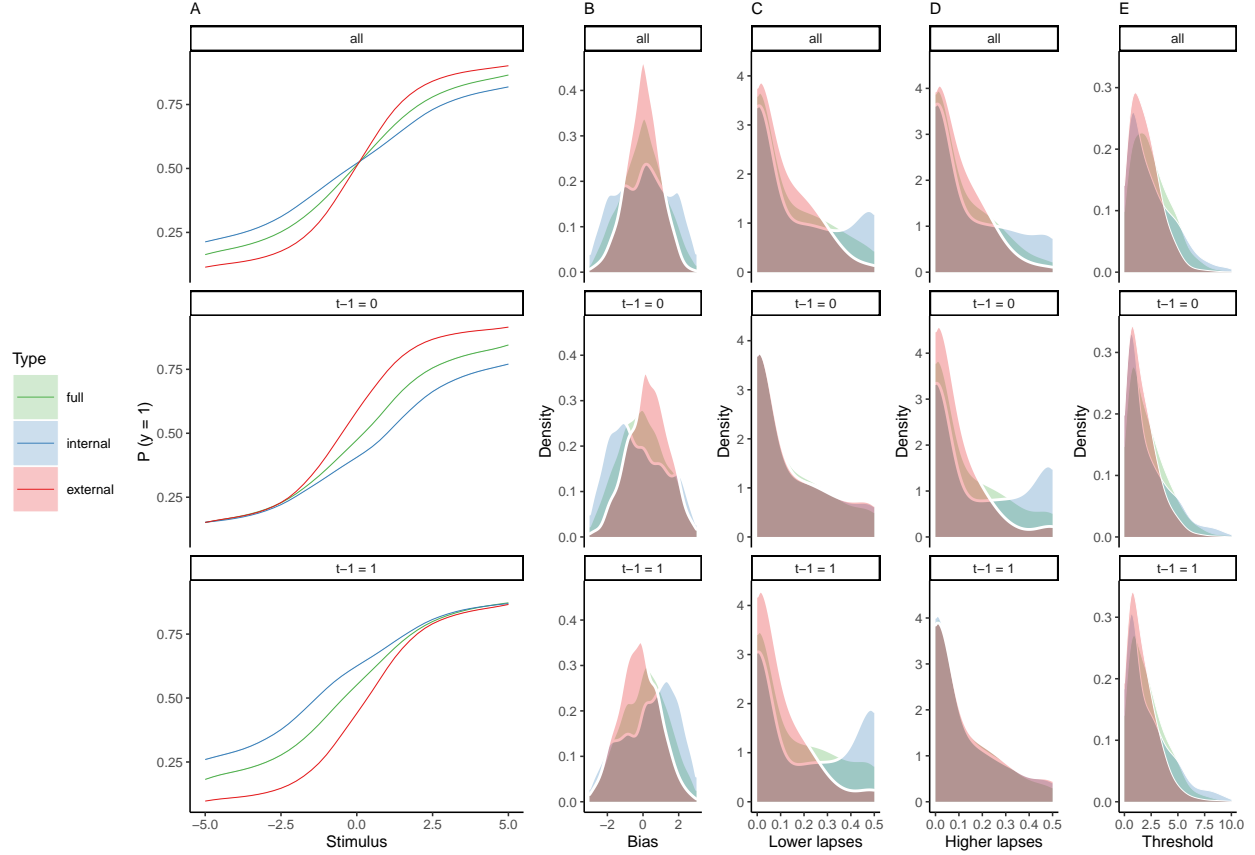
1092 G. We observed faster response times (RTs) for both stimulus-congruence (as opposed to  
1093 stimulus-incongruence,  $\beta = -0.14 \pm 1.61 \times 10^{-3}$ ,  $T(1.99 \times 10^6) = -85.91$ ,  $p < 2.2 \times 10^{-308}$ )  
1094 and history-congruence ( $\beta = -9.73 \times 10^{-3} \pm 1.38 \times 10^{-3}$ ,  $T(1.99 \times 10^6) = -7.06$ ,  $p =$   
1095  $1.66 \times 10^{-12}$ ).

1096 H. The mode of perceptual processing (i.e., the difference between the smoothed probability  
1097 of stimulus- vs. history-congruence) showed a quadratic relationship to RTs, with faster  
1098 response times for stronger biases toward both external sensory information and internal  
1099 predictions provided by perceptual history ( $\beta_2 = -19.86 \pm 0.52$ ,  $T(1.98 \times 10^6) = -38.43$ ,  
1100  $p = 5 \times 10^{-323}$ ). The horizontal and vertical dotted lines indicate maximum RT and the  
1101 associated mode, respectively.

1102 I. Confidence was enhanced for both stimulus-congruence (as opposed to stimulus-  
1103 incongruence,  $\beta = 0.48 \pm 1.38 \times 10^{-3}$ ,  $T(2.06 \times 10^6) = 351.89$ ,  $p < 2.2 \times 10^{-308}$ ) and  
1104 history-congruence ( $\beta = 0.04 \pm 1.18 \times 10^{-3}$ ,  $T(2.06 \times 10^6) = 36.86$ ,  $p = 2.93 \times 10^{-297}$ ).

<sup>1105</sup> J. In analogy to RTs, we found a quadratic relationship between the mode of perceptual  
<sup>1106</sup> processing and confidence, which increased when both externally- and internally-biased modes  
<sup>1107</sup> grew stronger ( $\beta_2 = 39.3 \pm 0.94$ ,  $T(2.06 \times 10^6) = 41.95$ ,  $p < 2.2 \times 10^{-308}$ ). The horizontal  
<sup>1108</sup> and vertical dotted lines indicate minimum confidence and the associated mode, respectively.

1109 **8.3 Figure 3**



1111 **Figure 3. Full and history-conditioned psychometric functions across modes in**  
1112 **humans.**

1113 A. Here, we show average psychometric functions for the full dataset (upper panel) and  
1114 conditioned on perceptual history ( $y_{t-1} = 1$  and  $y_{t-1} = 0$ ; middle and lower panel) across  
1115 modes (green line) and for internal mode (blue line) and external mode (red line) separately.

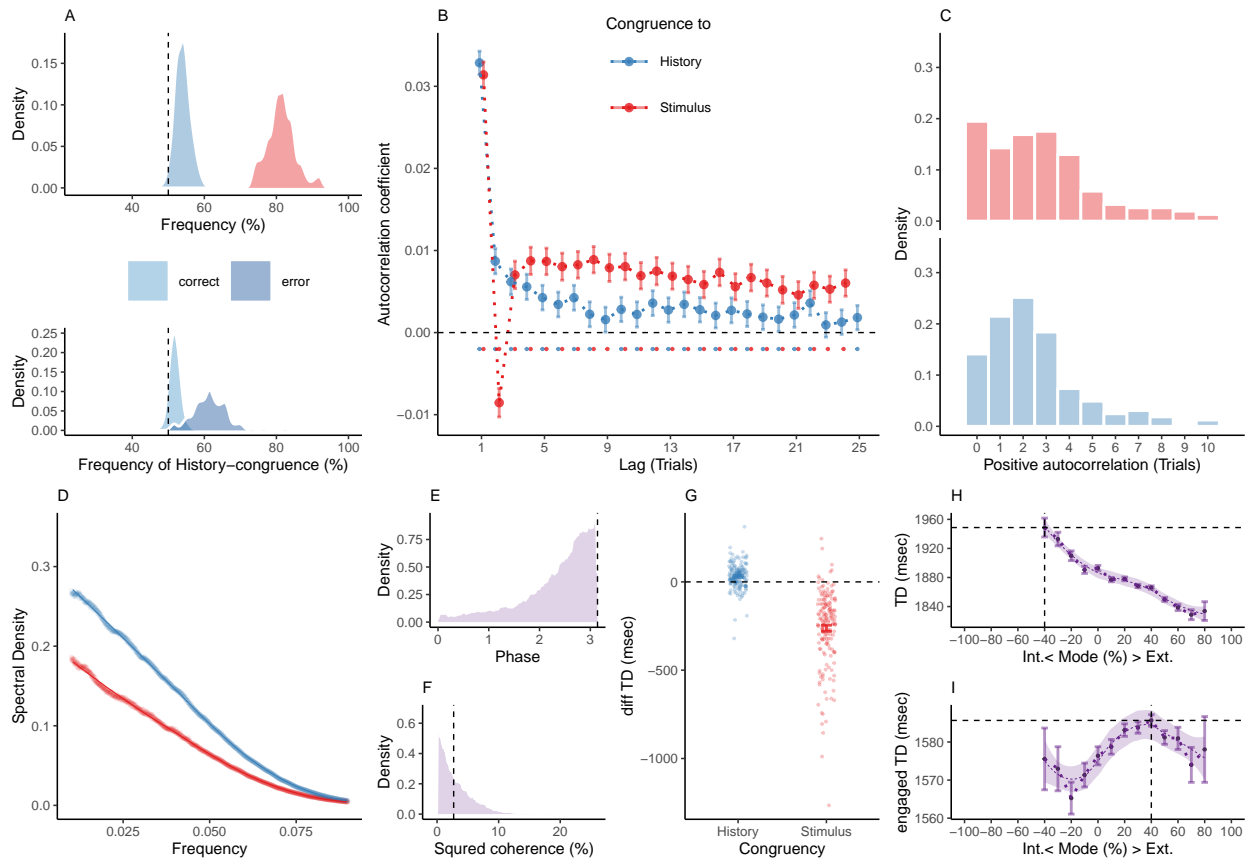
1116 B. Across the full dataset, biases  $\mu$  were distributed around zero ( $\beta_0 = 7.37 \times 10^{-3} \pm 0.09$ ,  
1117  $T(36.8) = 0.08$ ,  $p = 0.94$ ; upper panel), with larger absolute biases  $|\mu|$  for internal as compared  
1118 to external mode ( $\beta_0 = -0.62 \pm 0.07$ ,  $T(45.62) = -8.38$ ,  $p = 8.59 \times 10^{-11}$ ; controlling for  
1119 differences in lapses and thresholds). When conditioned on perceptual history, we observed  
1120 negative biases for  $y_{t-1} = 0$  ( $\beta_0 = 0.56 \pm 0.12$ ,  $T(43.39) = 4.6$ ,  $p = 3.64 \times 10^{-5}$ ; middle  
1121 panel) and positive biases for  $y_{t-1} = 1$  ( $\beta_0 = 0.56 \pm 0.12$ ,  $T(43.39) = 4.6$ ,  $p = 3.64 \times 10^{-5}$ ;  
1122 lower panel).

<sub>1123</sub> C. Lapse rates were higher in internal mode as compared to external mode ( $\beta_0 = -0.05 \pm$   
<sub>1124</sub>  $5.73 \times 10^{-3}$ ,  $T(47.03) = -9.11$ ,  $p = 5.94 \times 10^{-12}$ ; controlling for differences in biases and  
<sub>1125</sub> thresholds; see upper panel and subplot D). Importantly, the between-mode difference in  
<sub>1126</sub> lapses depended on perceptual history: We found no significant difference in lower lapses  
<sub>1127</sub>  $\gamma$  for  $y_{t-1} = 0$  ( $\beta_0 = 0.01 \pm 7.77 \times 10^{-3}$ ,  $T(33.1) = 1.61$ ,  $p = 0.12$ ; middle panel), but a  
<sub>1128</sub> significant difference for  $y_{t-1} = 1$  ( $\beta_0 = -0.11 \pm 0.01$ ,  $T(40.11) = -9.59$ ,  $p = 6.14 \times 10^{-12}$ ;  
<sub>1129</sub> lower panel).

<sub>1130</sub> D. Conversely, higher lapses  $\delta$  were significantly increased for  $y_{t-1} = 0$  ( $\beta_0 = -0.1 \pm$   
<sub>1131</sub>  $9.58 \times 10^{-3}$ ,  $T(36.87) = -10.16$ ,  $p = 3.06 \times 10^{-12}$ ; middle panel), but not for  $y_{t-1} = 1$  ( $\beta_0 =$   
<sub>1132</sub>  $0.01 \pm 7.74 \times 10^{-3}$ ,  $T(33.66) = 1.58$ ,  $p = 0.12$ ; lower panel).

<sub>1133</sub> E. The thresholds  $t$  were larger in internal as compared to external mode ( $\beta_0 = -1.77 \pm 0.25$ ,  
<sub>1134</sub>  $T(50.45) = -7.14$ ,  $p = 3.48 \times 10^{-9}$ ; controlling for differences in biases and lapses) and were  
<sub>1135</sub> not modulated by perceptual history ( $\beta_0 = 0.04 \pm 0.06$ ,  $T(2.97 \times 10^3) = 0.73$ ,  $p = 0.47$ ).

1136 **8.4 Figure 4**



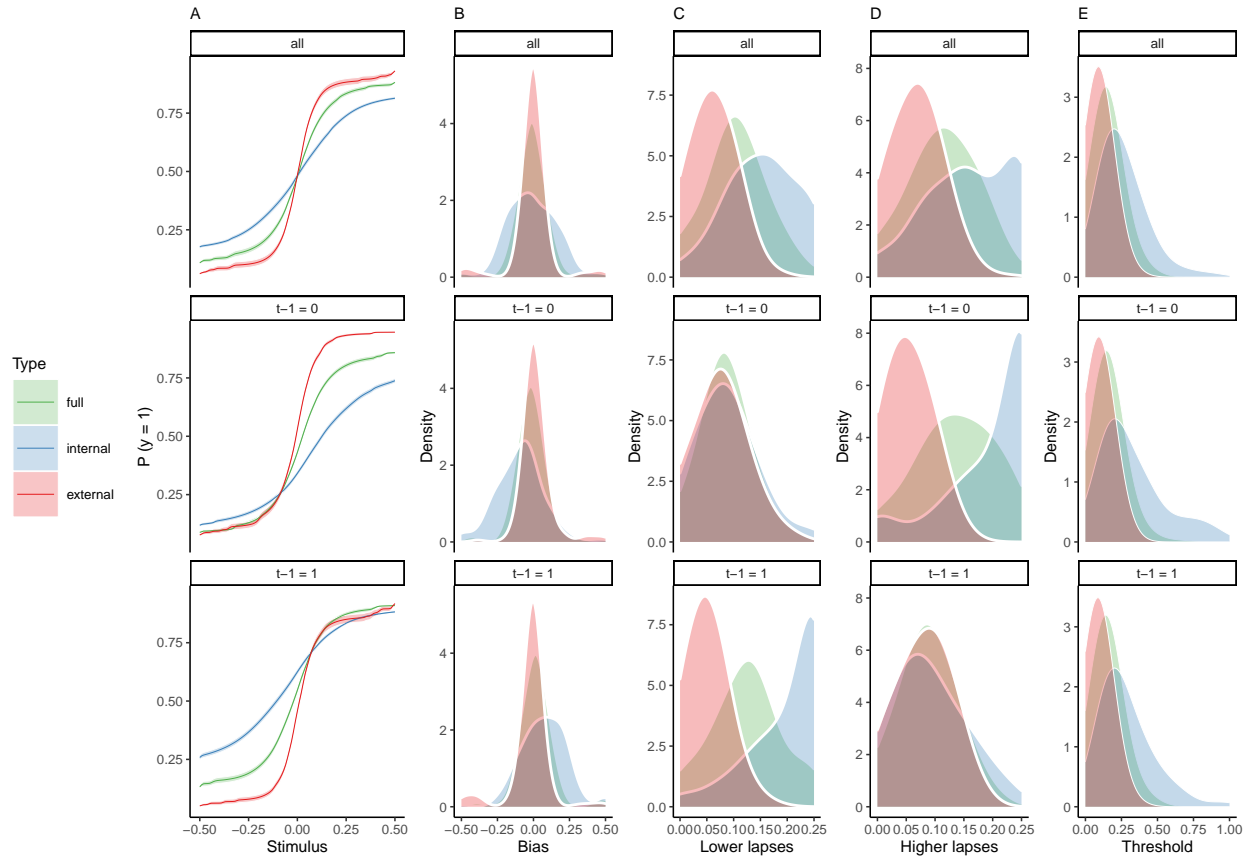
1137 **Figure 4. Internal and external modes in murine perceptual decision-making.**

1138 A. In mice,  $81.37\% \pm 0.3\%$  of trials were stimulus-congruent (in red) and  $54.03\% \pm 0.17\%$  of trials were history-congruent (in blue; upper panel). History-congruent perceptual choices were not a consequence of the experimental design, but a source of error, as they were more frequent on stimulus-incongruent trials (lower panel).

1139 B. Relative to randomly permuted data, we found highly significant autocorrelations of stimulus-congruence and history-congruence (dots indicate intercepts  $\neq 0$  in trial-wise linear mixed effects modeling at  $p < 0.05$ ). Please note that the negative autocorrelation of stimulus-congruence at trial 2 was a consequence of the experimental design (see Supplemental Figure 2D-F). As in humans, autocorrelation coefficients were best fit by an exponential function (adjusted  $R^2$  for stimulus-congruence: 0.44; history-congruence: 0.52) as compared to a linear function (adjusted  $R^2$  for stimulus-congruence:  $3.16 \times 10^{-3}$ ; history-congruence: 0.26).

- 1150 C. For stimulus-congruence (upper panel), the lag of positive autocorrelation was longer in  
1151 comparison to humans ( $4.59 \pm 0.06$  on average). For history-congruence (lower panel), the  
1152 lag of positive autocorrelation was slightly shorter relative to humans ( $2.58 \pm 0.01$  on average,  
1153 peaking at trial t+2 after the index trial).
- 1154 D. In mice, the dynamic probabilities of stimulus- and history-congruence (sliding windows  
1155 of  $\pm 5$  trials) fluctuated as *1/f noise*.
- 1156 E. The distribution of phase shift between fluctuations in stimulus- and history-congruence  
1157 peaked at half a cycle ( $\pi$  denoted by dotted line).
- 1158 F. The average squared coherence between fluctuations in stimulus- and history-congruence  
1159 (black dotted line) amounted to  $3.45 \pm 0.01\%$
- 1160 G. We observed shorter trial durations (TDs) for stimulus-congruence (as opposed to stimulus-  
1161 incongruence,  $\beta = -1.12 \pm 8.53 \times 10^{-3}$ ,  $T(1.34 \times 10^6) = -131.78$ ,  $p < 2.2 \times 10^{-308}$ ), but  
1162 longer TDs for history-congruence ( $\beta = 0.06 \pm 6.76 \times 10^{-3}$ ,  $T(1.34 \times 10^6) = 8.52$ ,  $p =$   
1163  $1.58 \times 10^{-17}$ ).
- 1164 H. TDs decreased monotonically for stronger biases toward external mode ( $\beta_1 = -4.16 \times 10^4$   
1165  $\pm 1.29 \times 10^3$ ,  $T(1.35 \times 10^6) = -32.31$ ,  $p = 6.03 \times 10^{-229}$ ). The horizontal and vertical dotted  
1166 lines indicate maximum TD and the associated mode, respectively.
- 1167 I. For TDs that differed from the median TD by no more than  $1.5 \times \text{MAD}$  (median absolute  
1168 distance<sup>52</sup>), mice exhibited a quadratic component in the relationship between the mode  
1169 of sensory processing and TDs ( $\beta_2 = -1.97 \times 10^3 \pm 843.74$ ,  $T(1.19 \times 10^6) = -2.34$ ,  $p =$   
1170 0.02, Figure 4I). This explorative post-hoc analysis focuses on trials at which mice engage  
1171 more swiftly with the experimental task. The horizontal and vertical dotted lines indicate  
1172 maximum TD and the associated mode, respectively.

1173 **8.5 Figure 5**



1174 **Figure 5. Full and history-conditioned psychometric functions across modes in  
mic.**

1175 A. Here, we show average psychometric functions for the full IBL dataset (upper panel) and  
1176 conditioned on perceptual history ( $y_{t-1} = 1$  and  $y_{t-1} = 0$ ; middle and lower panel) across  
1177 modes (green line) and for internal mode (blue line) and external mode (red line) separately.

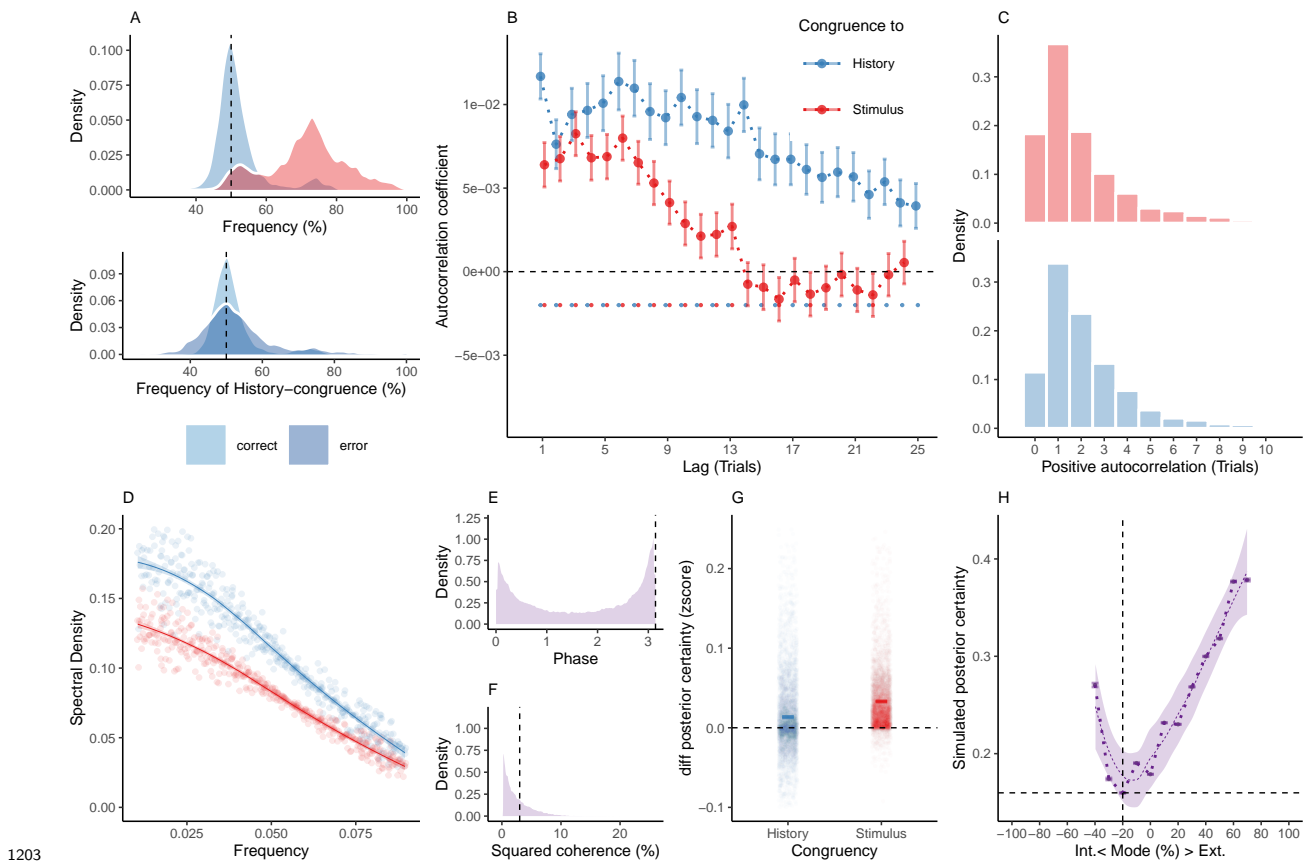
1178 B. Across the full dataset, biases  $\mu$  were distributed around zero ( $T(164) = 0.39$ ,  $p = 0.69$ ;  
1179 upper panel), with larger absolute biases  $|\mu|$  for internal as compared to external mode ( $\beta_0 =$   
1180  $-0.18 \pm 0.03$ ,  $T = -6.38$ ,  $p = 1.77 \times 10^{-9}$ ; controlling for differences in lapses and thresholds).  
1181 When conditioned on perceptual history, we observed negative biases for  $y_{t-1} = 0$  ( $T(164)$   
1182  $= -1.99$ ,  $p = 0.05$ ; middle panel) and positive biases for  $y_{t-1} = 1$  ( $T(164) = 1.91$ ,  $p = 0.06$ ;  
1183 lower panel).

<sub>1186</sub> C. Lapse rates were higher in internal as compared to external mode ( $\beta_0 = -0.11 \pm 4.39 \times 10^{-3}$ ,  
<sub>1187</sub>  $T = -24.8$ ,  $p = 4.91 \times 10^{-57}$ ; controlling for differences in biases and thresholds; upper panel,  
<sub>1188</sub> see also subplot D). For  $y_{t-1} = 1$ , the difference between internal and external mode was  
<sub>1189</sub> more pronounced for lower lapses  $\gamma$  ( $T(164) = -18.24$ ,  $p = 2.68 \times 10^{-41}$ ) as compared to  
<sub>1190</sub> higher lapses  $\delta$  (see subplot D). In mice, lower lapses  $\gamma$  were significantly elevated during  
<sub>1191</sub> internal mode irrespective of the preceding perceptual choice (middle panel: lower lapses  $\gamma$   
<sub>1192</sub> for  $y_{t-1} = 0$ ;  $T(164) = -2.5$ ,  $p = 0.01$ , lower panel: lower lapses  $\gamma$  for  $y_{t-1} = 1$ ;  $T(164) =$   
<sub>1193</sub>  $-32.44$ ,  $p = 2.92 \times 10^{-73}$ ).

<sub>1194</sub> D. For  $y_{t-1} = 0$ , the difference between internal and external mode was more pronounced  
<sub>1195</sub> for higher lapses  $\delta$  ( $T(164) = 21.44$ ,  $p = 1.93 \times 10^{-49}$ , see subplot C). Higher lapses were  
<sub>1196</sub> significantly elevated during internal mode irrespective of the preceding perceptual choice  
<sub>1197</sub> (middle panel: higher lapses  $\delta$  for  $y_{t-1} = 0$ ;  $T(164) = -28.29$ ,  $p = 5.62 \times 10^{-65}$  lower panel:  
<sub>1198</sub> higher lapses  $\delta$  for  $y_{t-1} = 1$ ;  $T(164) = -2.65$ ,  $p = 8.91 \times 10^{-3}$ ; ).

<sub>1199</sub> E. Thresholds  $t$  were higher in internal as compared to external mode ( $\beta_0 = -0.28 \pm 0.04$ ,  
<sub>1200</sub>  $T = -7.26$ ,  $p = 1.53 \times 10^{-11}$ ; controlling for differences in biases and lapses) and were not  
<sub>1201</sub> modulated by perceptual history ( $T(164) = 0.94$ ,  $p = 0.35$ ).

1202 **8.6 Figure 6**



1203 **Figure 6. Internal and external modes in simulated perceptual decision-making.**

1204 A. Simulated perceptual choices were stimulus-congruent in  $71.36\% \pm 0.17\%$  (in red) and  
 1205 history-congruent in  $51.99\% \pm 0.11\%$  of trials (in blue;  $T(4.32 \times 10^3) = 17.42$ ,  $p = 9.89 \times 10^{-66}$ ;  
 1206 upper panel). Due to the competition between stimulus- and history-congruence, history-  
 1207 congruent perceptual choices were more frequent when perception was stimulus-incongruent  
 1208 (i.e., on *error* trials;  $T(4.32 \times 10^3) = 11.19$ ,  $p = 1.17 \times 10^{-28}$ ; lower panel) and thus impaired  
 1209 performance in the randomized psychophysical design simulated here.

1210 B. At the simulated group level, we found significant autocorrelations in both stimulus-  
 1211 congruence (13 consecutive trials) and history-congruence (30 consecutive trials).

1212 C. On the level of individual simulated participants, autocorrelation coefficients exceeded the  
 1213 autocorrelation coefficients of randomly permuted data within a lag of  $2.46 \pm 1.17 \times 10^{-3}$

<sub>1215</sub> trials for stimulus-congruence and  $4.24 \pm 1.85 \times 10^{-3}$  trials for history-congruence.

<sub>1216</sub> D. The smoothed probabilities of stimulus- and history-congruence (sliding windows of  $\pm 5$   
<sub>1217</sub> trials) fluctuated as *1/f noise*, i.e., at power densities that were inversely proportional to the  
<sub>1218</sub> frequency (power  $\sim 1/f^\beta$ ; stimulus-congruence:  $\beta = -0.81 \pm 1.18 \times 10^{-3}$ ,  $T(1.92 \times 10^5) =$   
<sub>1219</sub>  $-687.58$ ,  $p < 2.2 \times 10^{-308}$ ; history-congruence:  $\beta = -0.83 \pm 1.27 \times 10^{-3}$ ,  $T(1.92 \times 10^5) =$   
<sub>1220</sub>  $-652.11$ ,  $p < 2.2 \times 10^{-308}$ ).

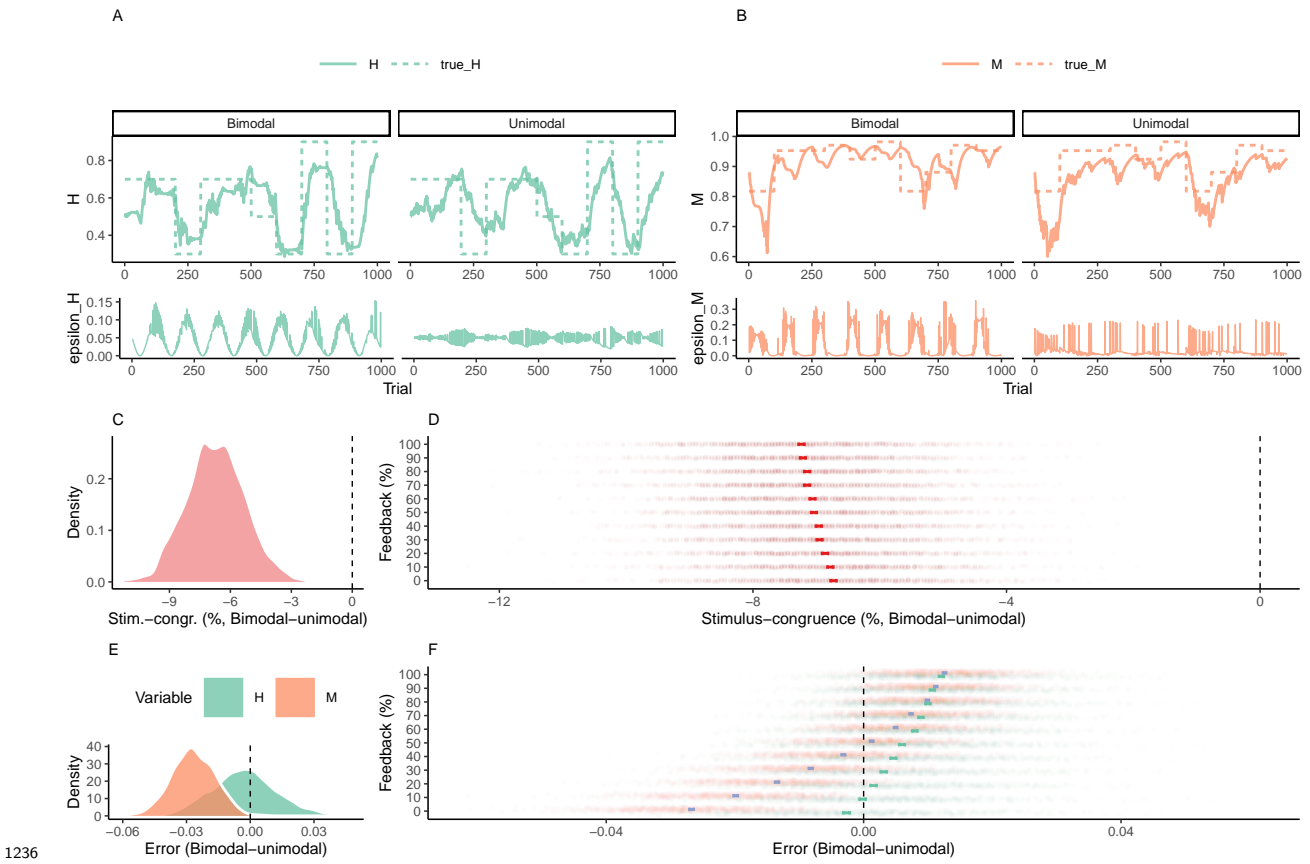
<sub>1221</sub> E. The distribution of phase shift between fluctuations in simulated stimulus- and history-  
<sub>1222</sub> congruence peaked at half a cycle ( $\pi$  denoted by dotted line). The dynamic probabilities of  
<sub>1223</sub> simulated stimulus- and history-congruence were therefore were strongly anti-correlated ( $\beta =$   
<sub>1224</sub>  $-0.03 \pm 8.22 \times 10^{-4}$ ,  $T(2.12 \times 10^6) = -40.52$ ,  $p < 2.2 \times 10^{-308}$ ).

<sub>1225</sub> F. The average squared coherence between fluctuations in simulated stimulus- and history-  
<sub>1226</sub> congruence (black dotted line) amounted to  $6.49 \pm 2.07 \times 10^{-3}\%$ .

<sub>1227</sub> G. Simulated confidence was enhanced for stimulus-congruence ( $\beta = 0.03 \pm 1.71 \times 10^{-4}$ ,  
<sub>1228</sub>  $T(2.03 \times 10^6) = 178.39$ ,  $p < 2.2 \times 10^{-308}$ ) and history-congruence ( $\beta = 0.01 \pm 1.5 \times 10^{-4}$ ,  
<sub>1229</sub>  $T(2.03 \times 10^6) = 74.18$ ,  $p < 2.2 \times 10^{-308}$ ).

<sub>1230</sub> H. In analogy to humans, the simulated data showed a quadratic relationship between the  
<sub>1231</sub> mode of perceptual processing and posterior certainty, which increased for stronger external  
<sub>1232</sub> and internal biases ( $\beta_2 = 31.03 \pm 0.15$ ,  $T(2.04 \times 10^6) = 205.95$ ,  $p < 2.2 \times 10^{-308}$ ). The  
<sub>1233</sub> horizontal and vertical dotted lines indicate minimum posterior certainty and the associated  
<sub>1234</sub> mode, respectively.

1235 **8.7 Figure 7**



1236 **Figure 7. Adaptive benefits of bimodal inference.**

1237 A. When the sensory environment changes unpredictably over time, agents have to update  
 1238 estimates  $H_t$  (solid green line, upper panel) about the true hazard rate  $\hat{H}_t$  from experience  
 1239 (dotted green line, upper panel). Updates to  $H_t$  are driven by an error term  $\epsilon_H$  (solid  
 1240 green line, lower panel) that is defined by the difference between  $H_t$  and the presence of a  
 1241 perceived change in the environment. In contrast to the unimodal model (right panels),  $\epsilon_H$   
 1242 of the bimodal model (left panels) is modulated by a phasic component reflecting ongoing  
 1243 fluctuations between internal and external mode.

1244 B. When the precision of sensory encoding changes unpredictably over time, agents have  
 1245 to update estimates  $M_t$  (solid orange line, upper panel) about the true precision of sensory  
 1246 encoding  $\hat{M}_t$  from experience (dotted orange line, upper panel). Updates to  $M_t$  are driven  
 1247 by an error term  $\epsilon_M$  (red line, lower panel) that is defined by the difference between  $M_t$

<sub>1249</sub> and the posterior decision-certainty. In contrast to the unimodal model (right panels),  $\epsilon_M$   
<sub>1250</sub> of the bimodal model (left panels) is modulated by a phasic component reflecting ongoing  
<sub>1251</sub> fluctuations between internal and external mode.

<sub>1252</sub> C. In the absence of feedback, the bimodal inference model achieved lower stimulus-congruence  
<sub>1253</sub> as compared the unimodal control model ( $\beta_1 = -6.71 \pm 0.03$ ,  $T(8.42 \times 10^3) = -234.31$ ,  $p <$   
<sub>1254</sub>  $2.2 \times 10^{-308}$ ).

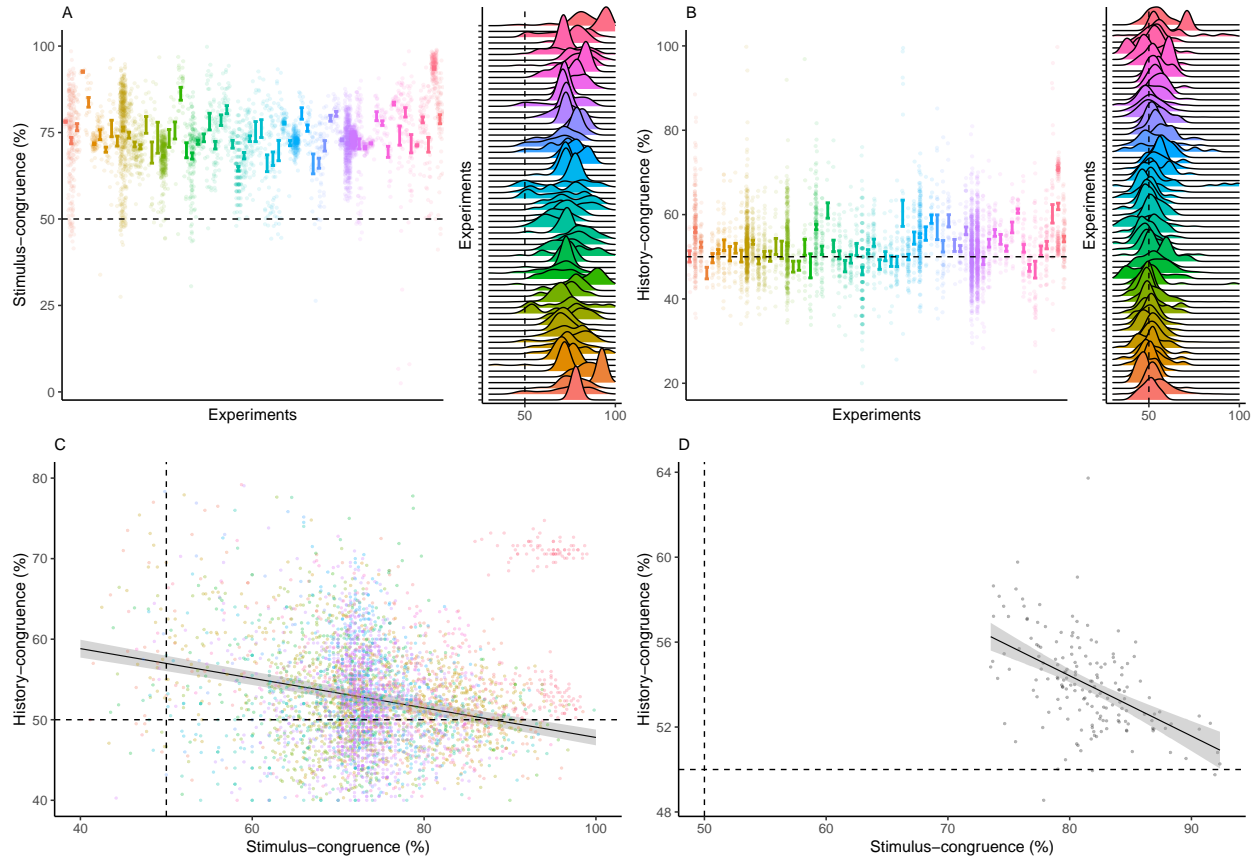
<sub>1255</sub> D. The unimodal control model benefited more strongly from the presence of external feedback,  
<sub>1256</sub> leading to a relative decrease in stimulus-congruence for the bimodal inference model at  
<sub>1257</sub> higher feedback levels ( $\beta_2 = -0.05 \pm 4.13 \times 10^{-3}$ ,  $T(10 \times 10^3) = -12.32$ ,  $p = 1.25 \times 10^{-34}$ ).

<sub>1258</sub> E. In the absence of feedback, the bimodal inference model achieved lower errors in the  
<sub>1259</sub> estimated hazard rate  $H$  ( $\beta_1 = -2.94 \times 10^{-3} \pm 2.89 \times 10^{-4}$ ,  $T(4.96 \times 10^3) = -10.18$ ,  $p =$   
<sub>1260</sub>  $4.11 \times 10^{-24}$ ) as well as lower errors in the estimated probability of stimulus-congruent choices  
<sub>1261</sub>  $M$  ( $\beta_1 = -0.03 \pm 1.86 \times 10^{-4}$ ,  $T(6.07 \times 10^3) = -137.75$ ,  $p < 2.2 \times 10^{-308}$ ).

<sub>1262</sub> F. With an increasing availability of feedback, the advantage of the bimodal inference model  
<sub>1263</sub> was lost with respect to  $H$  ( $\beta_2 = 1.43 \times 10^{-3} \pm 3.71 \times 10^{-5}$ ,  $T(10 \times 10^3) = 38.58$ ,  $p =$   
<sub>1264</sub>  $9.44 \times 10^{-304}$ ) and  $M$  ( $\beta_2 = 3.91 \times 10^{-3} \pm 2.51 \times 10^{-5}$ ,  $T(10 \times 10^3) = 156.18$ ,  $p < 2.2 \times 10^{-308}$ ).

1265 **9 Supplemental Items**

1266 **9.1 Supplemental Figure S1**



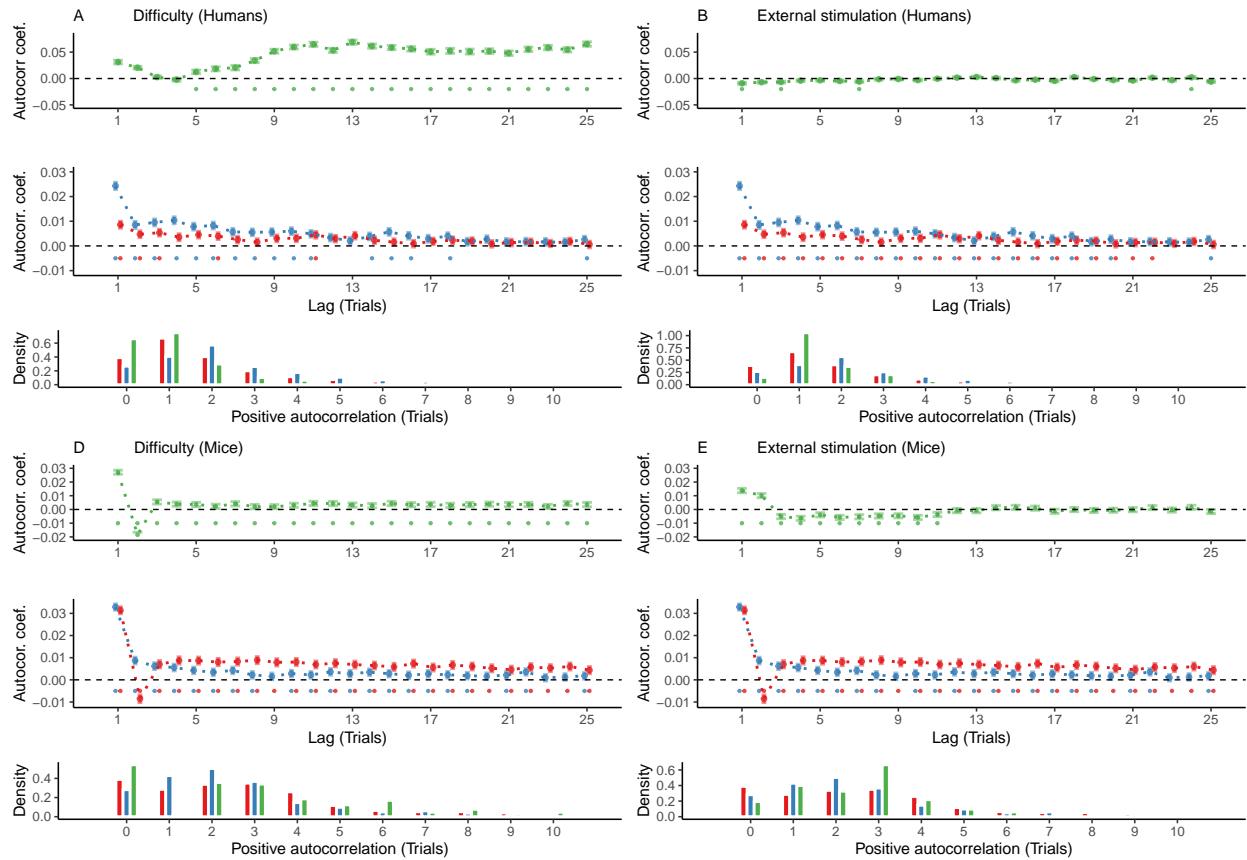
1267 **Supplemental Figure S1. Stimulus- and history-congruence.**

- 1268 A. Stimulus-congruent choices in humans amounted to  $73.46\% \pm 0.15\%$  of trials and were  
1269 highly consistent across the experiments selected from the Confidence Database.  
1270
- 1271 B. History-congruent choices in humans amounted to  $52.7\% \pm 0.12\%$  of trials. In analogy to  
1272 stimulus-congruence, the prevalence of history-congruence was highly consistent across the  
1273 experiments selected from the Confidence Database. 48.48% of experiments showed significant  
1274 ( $p < 0.05$ ) attractive biases toward preceding choices, whereas 3.03% of experiments showed  
1275 significant repulsive biases.
- 1276 C. In humans, we found an enhanced impact of perceptual history in participants who were

<sub>1277</sub> less sensitive to external sensory information ( $T(4.3 \times 10^3) = -14.27$ ,  $p = 3.78 \times 10^{-45}$ ),  
<sub>1278</sub> suggesting that perception results from the competition of external with internal information.

<sub>1279</sub> D. In analogy to humans, mice that were less sensitive to external sensory information  
<sub>1280</sub> showed stronger biases toward perceptual history ( $T(163) = -7.52$ ,  $p = 3.44 \times 10^{-12}$ , Pearson  
<sub>1281</sub> correlation).

1282 **9.2 Supplemental Figure S2**



1283

1284 **Supplemental Figure S2. Controlling for task difficulty and external stimulation.**

1285 In this study, we found highly significant autocorrelations of stimulus- and history-congruence  
 1286 in humans as well as in mice. Here, we show that these autocorrelations are not a trivial  
 1287 consequence of task difficulty or the sequence external stimulation. In addition, we com-  
 1288 puted trial-wise logistic regression coefficients as an alternative approach to assessing serial  
 1289 dependencies in stimulus- and history-congruence.

1290 A. In humans, task difficulty (in green) showed a significant autocorrelated starting at the  
 1291 5th trial (upper panel, dots at the bottom indicate intercepts  $\neq 0$  in trial-wise linear mixed  
 1292 effects modeling at  $p < 0.05$ ). When controlling for task difficulty, linear mixed effects  
 1293 modeling indicated a significant auto-correlation of stimulus-congruence (in red) for the first  
 1294 3 consecutive trials (middle panel). 20% of trials within the displayed time window remained  
 1295 significantly autocorrelated. The autocorrelation of history-congruence (in blue) remained

1296 significant for the first 11 consecutive trials (64% significantly autocorrelated trials within  
1297 the displayed time window). At the level of individual participants, the autocorrelation of  
1298 task difficulty exceeded the respective autocorrelation of randomly permuted within a lag of  
1299  $21.66 \pm 8.37 \times 10^{-3}$  trials (lower panel).

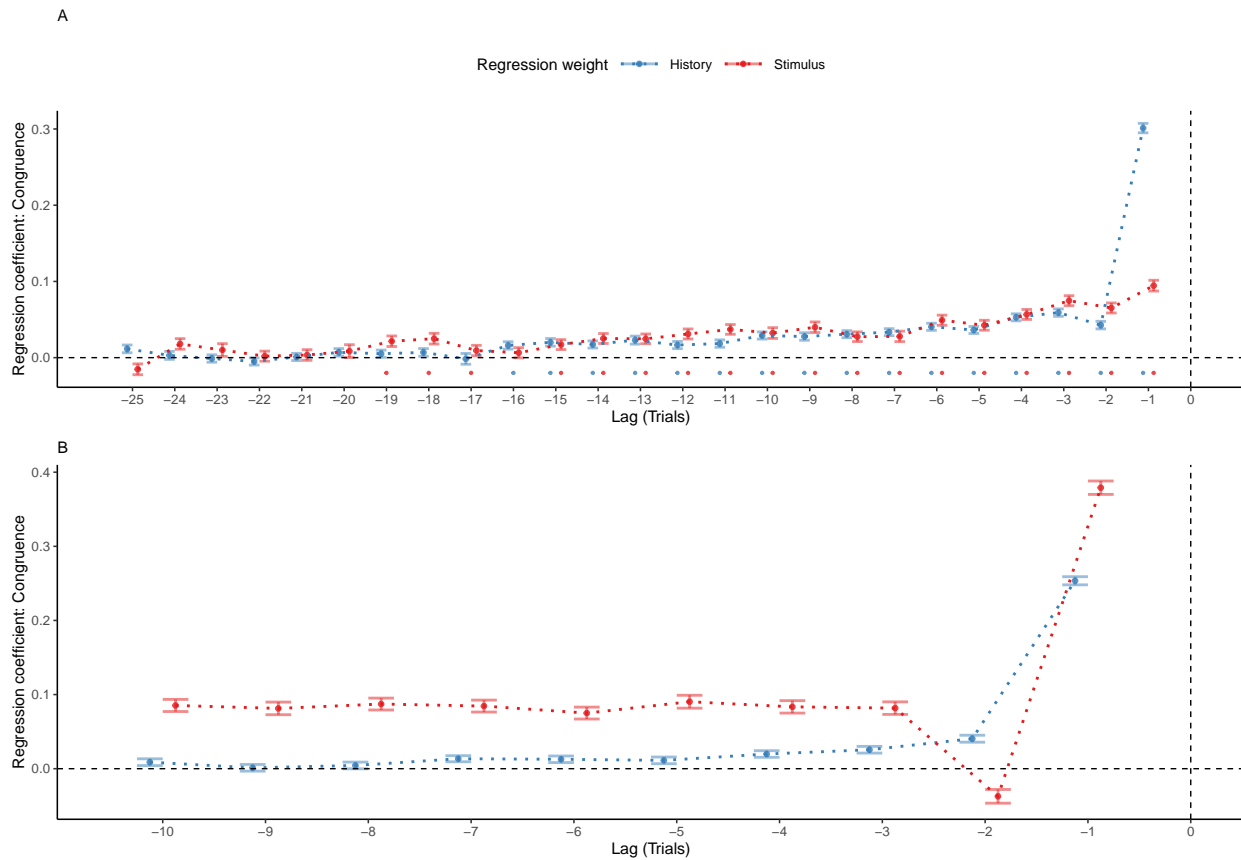
1300 B. The sequence of external stimulation (i.e., which of the two binary outcomes was supported  
1301 by the presented stimuli; depicted in green) was negatively autocorrelated for 1 trial. When  
1302 controlling for the autocorrelation of external stimulation, stimulus-congruence remained  
1303 significantly autocorrelated for 22 consecutive trials (88% of trials within the displayed  
1304 time window; lower panel) and history-congruence remained significantly autocorrelated  
1305 for 20 consecutive trials (84% of trials within the displayed time window). At the level of  
1306 individual participants, the autocorrelation of external stimulation exceeded the respective  
1307 autocorrelation of randomly permuted within a lag of  $2.94 \pm 4.4 \times 10^{-3}$  consecutive trials  
1308 (lower panel).

1309 D. In mice, task difficulty showed an significant autocorrelated for the first 25 consecutive trials  
1310 (upper panel). When controlling for task difficulty, linear mixed effects modeling indicated a  
1311 significant auto-correlation of stimulus-congruence for the first 36 consecutive trials (middle  
1312 panel). In total, 100% of trials within the displayed time window remained significantly  
1313 autocorrelated. The autocorrelation of history-congruence remained significant for the first  
1314 8 consecutive trials, with 84% significantly autocorrelated trials within the displayed time  
1315 window. At the level of individual mice, autocorrelation coefficients for difficulty were elevated  
1316 above randomly permuted data within a lag of  $15.13 \pm 0.19$  consecutive trials (lower panel).

1317 E. In mice, the sequence of external stimulation (i.e., which of the two binary outcomes was  
1318 supported by the presented stimuli) was negatively autocorrelated for 11 consecutive trials  
1319 (upper panel). When controlling for the autocorrelation of external stimulation, stimulus-  
1320 congruence remained significantly autocorrelated for 86 consecutive trials (100% of trials  
1321 within the displayed time window; middle) and history-congruence remained significantly

<sub>1322</sub> autocorrelated for 8 consecutive trials (84% of trials within the displayed time window). At  
<sub>1323</sub> the level of individual mice, autocorrelation coefficients for external stimulation were elevated  
<sub>1324</sub> above randomly permuted data within a lag of  $2.53 \pm 9.8 \times 10^{-3}$  consecutive trials (lower  
<sub>1325</sub> panel).

1326 **9.3 Supplemental Figure S3**



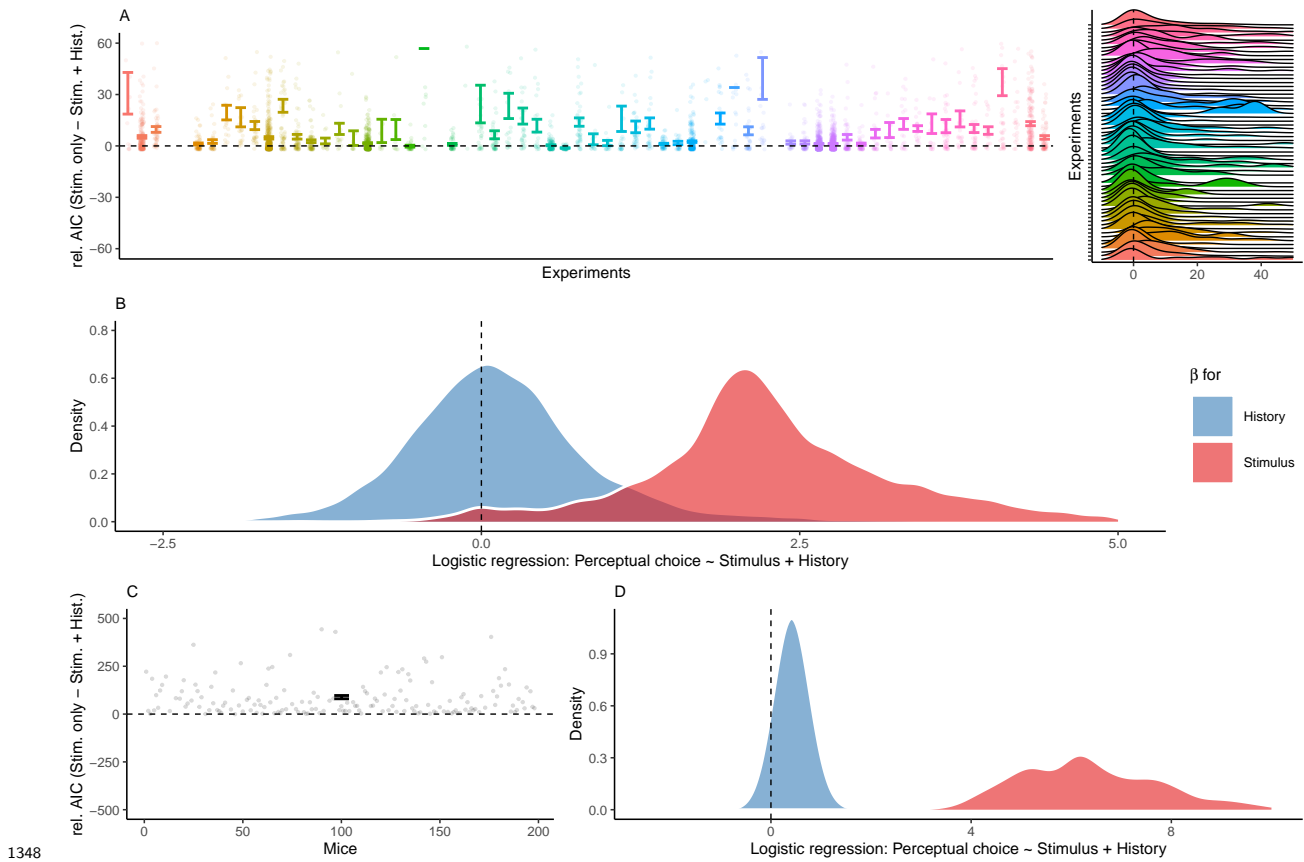
1327 **Supplemental Figure S3. Reproducing group-level autocorrelations using logistic  
1328 regression.**

1329 A. As an alternative to group-level autocorrelation coefficients, we used trial-wise logistic  
1330 regression to quantify serial dependencies in stimulus- and history-congruence. This analysis  
1331 predicted stimulus- and history-congruence at the index trial (trial  $t = 0$ , vertical line) based  
1332 on stimulus- and history-congruence at the 25 preceding trials. Mirroring the shape of the  
1333 group-level autocorrelations, trial-wise regression coefficients (depicted as mean  $\pm$  SEM, dots  
1334 mark trials with regression weights significantly greater than zero at  $p < 0.05$ ) increased  
1335 toward the index trial  $t = 0$  for the human data.

1336 B. Following our results in human data, regression coefficients that predicted history-  
1337 congruence at the index trial (trial  $t = 0$ , vertical line) increased exponentially for trials  
1338 closer to the index trial in mice. In contrast to history-congruence, stimulus-congruence  
1339

<sub>1340</sub> showed a negative regression weight (or autocorrelation coefficient, see Figure 4B) at trial  
<sub>1341</sub> -2. This was due to the experimental design (see also the autocorrelations of difficulty and  
<sub>1342</sub> external stimulation in Supplemental Figure S2C and D): When mice made errors at easy  
<sub>1343</sub> trials (contrast  $\geq 50\%$ ), the upcoming stimulus was shown at the same spatial location and at  
<sub>1344</sub> high contrast. This increased the probability of stimulus-congruent perceptual choices after  
<sub>1345</sub> stimulus-incongruent perceptual choices at easy trials, thereby creating a negative regression  
<sub>1346</sub> weight (or autocorrelation coefficient) of stimulus-congruence at trial -2.

1347 **9.4 Supplemental Figure S4**



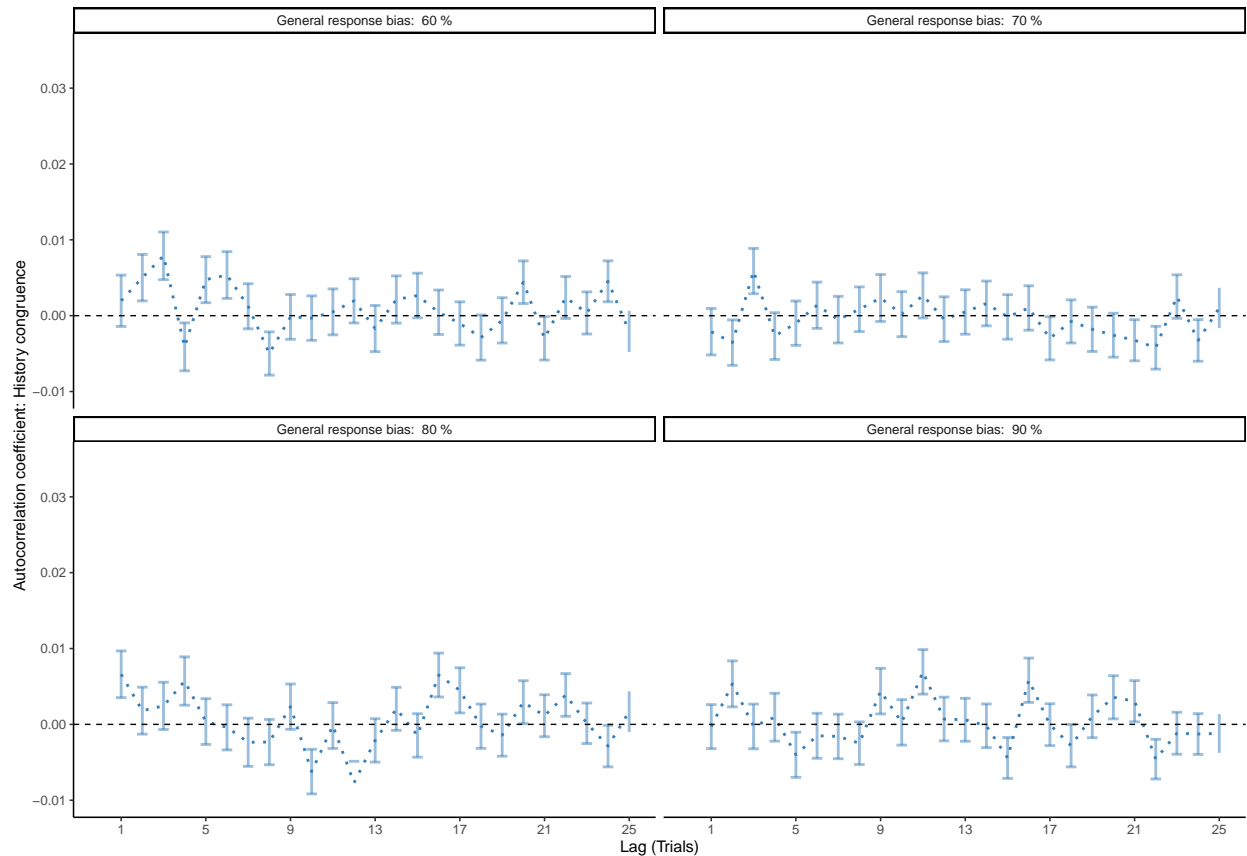
1348 **1349 Supplemental Figure S4. History-congruence in logistic regression.**

1350 A. To ensure that perceptual history played a significant role in perception despite the ongoing  
 1351 stream of external information, we tested whether human perceptual decision-making was  
 1352 better explained by the combination of external and internal information or, alternatively, by  
 1353 external information alone. To this end, we compared Akaike information criteria between  
 1354 logistic regression models that predicted trial-wise perceptual responses either by both current  
 1355 external sensory information and the preceding percept, or by external sensory information  
 1356 alone (values above zero indicate a superiority of the full model). With high consistency across  
 1357 the experiments selected from the Confidence Database, this model-comparison confirmed  
 1358 that perceptual history contributed significantly to perception (difference in AIC =  $8.07 \pm$   
 1359  $0.53$ ,  $T(57.22) = 4.1$ ,  $p = 1.31 \times 10^{-4}$ ).

1360 B. Participant-wise regression coefficients amount to  $0.18 \pm 0.02$  for the effect of perceptual

- <sub>1361</sub> history and  $2.51 \pm 0.03$  for external sensory stimulation.
- <sub>1362</sub> C. In mice, an AIC-based model comparison indicated that perception was better explained  
<sub>1363</sub> by logistic regression models that predicted trial-wise perceptual responses based on both  
<sub>1364</sub> current external sensory information and the preceding percept (difference in AIC =  $88.62 \pm$   
<sub>1365</sub>  $8.57$ ,  $T(164) = -10.34$ ,  $p = 1.29 \times 10^{-19}$ ).
- <sub>1366</sub> D. In mice, individual regression coefficients amounted to  $0.42 \pm 0.02$  for the effect of  
<sub>1367</sub> perceptual history and  $6.91 \pm 0.21$  for external sensory stimulation.

1368 **9.5 Supplemental Figure S5**



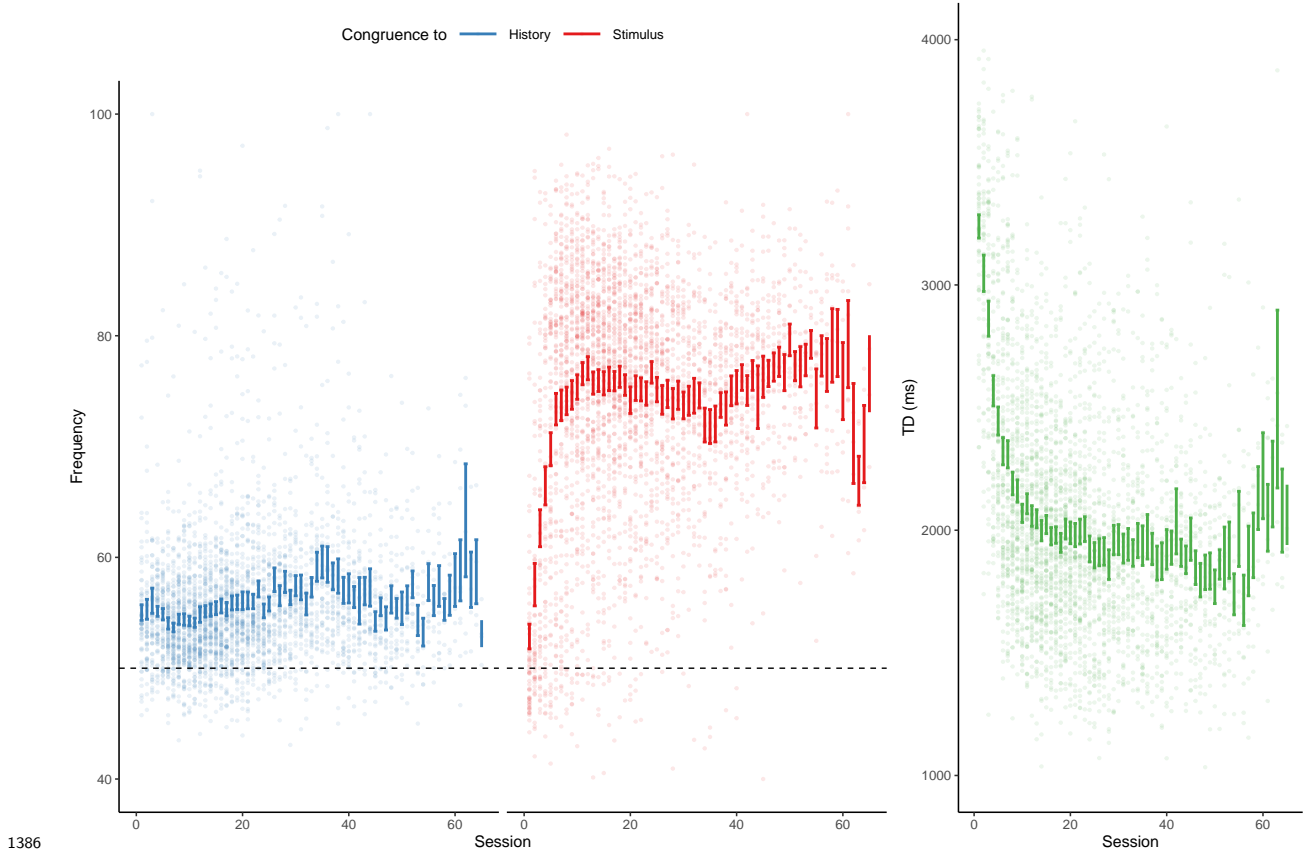
1369

1370 **Supplemental Figure S5. Correcting for general response biases.**

1371 Here, we ask whether the autocorrelation of history-congruence (as shown in Figure 2-3C)  
1372 may be driven by general response biases (i.e., a general propensity to choose one of the  
1373 two possible outcomes more frequently than the alternative). To this end, we generated  
1374 sequences of 100 perceptual choices with general response biases ranging from 60 to 90%  
1375 for 1000 simulated participants each. We then computed the autocorrelation of history-  
1376 congruence for these simulated data. Crucially, we used the correction procedure that is  
1377 applied to all autocorrelation curves shown in this manuscript: All reported autocorrelation  
1378 coefficients are computed relative to the average autocorrelation coefficients obtained for  
1379 100 iterations of randomly permuted trial sequences. The above simulation show that this  
1380 correction procedure removes any potential contribution of general response biases to the  
1381 auto-correlation of history-congruence. This indicates that the autocorrelation of history-

<sup>1382</sup> congruence (as shown in Figure 2-3C) is not driven by general response biases that were  
<sup>1383</sup> present in the empirical data at a level of  $58.71\% \pm 0.22\%$  in humans and  $54.6\% \pm 0.3\%$  in  
<sup>1384</sup> mice.

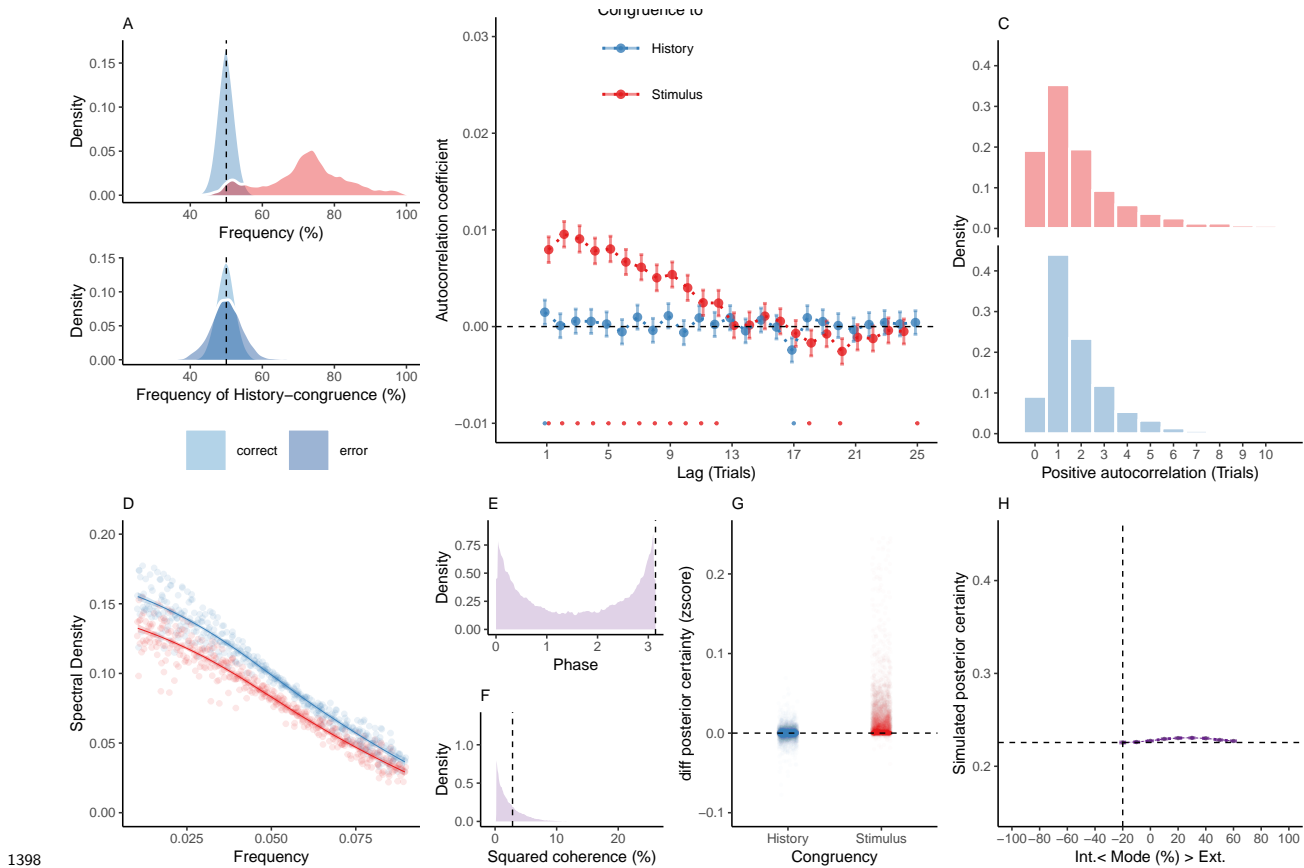
1385 **9.6 Supplemental Figure S6**



1387 **Supplemental Figure S6. History-/stimulus-congruence and TDs during training  
1388 of the basic task.**

1389 Here, we depict the progression of history- and stimulus-congruence (depicted in blue and  
1390 red, respectively; left panel) as well as TDs (in green; right panel) across training sessions in  
1391 mice that achieved proficiency (i.e., stimulus-congruence  $\geq 80\%$ ) in the *basic* task of the IBL  
1392 dataset. We found that both history-congruent perceptual choices ( $\beta = 0.13 \pm 4.67 \times 10^{-3}$ ,  
1393  $T(8.4 \times 10^3) = 27.04$ ,  $p = 1.96 \times 10^{-154}$ ) and stimulus-congruent perceptual choices ( $\beta =$   
1394  $0.34 \pm 7.13 \times 10^{-3}$ ,  $T(8.51 \times 10^3) = 47.66$ ,  $p < 2.2 \times 10^{-308}$ ) became more frequent with  
1395 training. As in humans, mice showed shorter TDs with increase exposure to the task ( $\beta =$   
1396  $-22.14 \pm 17.06$ ,  $T(1.14 \times 10^3) = -1.3$ ,  $p < 2.2 \times 10^{-308}$ ).

1397 **9.7 Supplemental Figure S7**



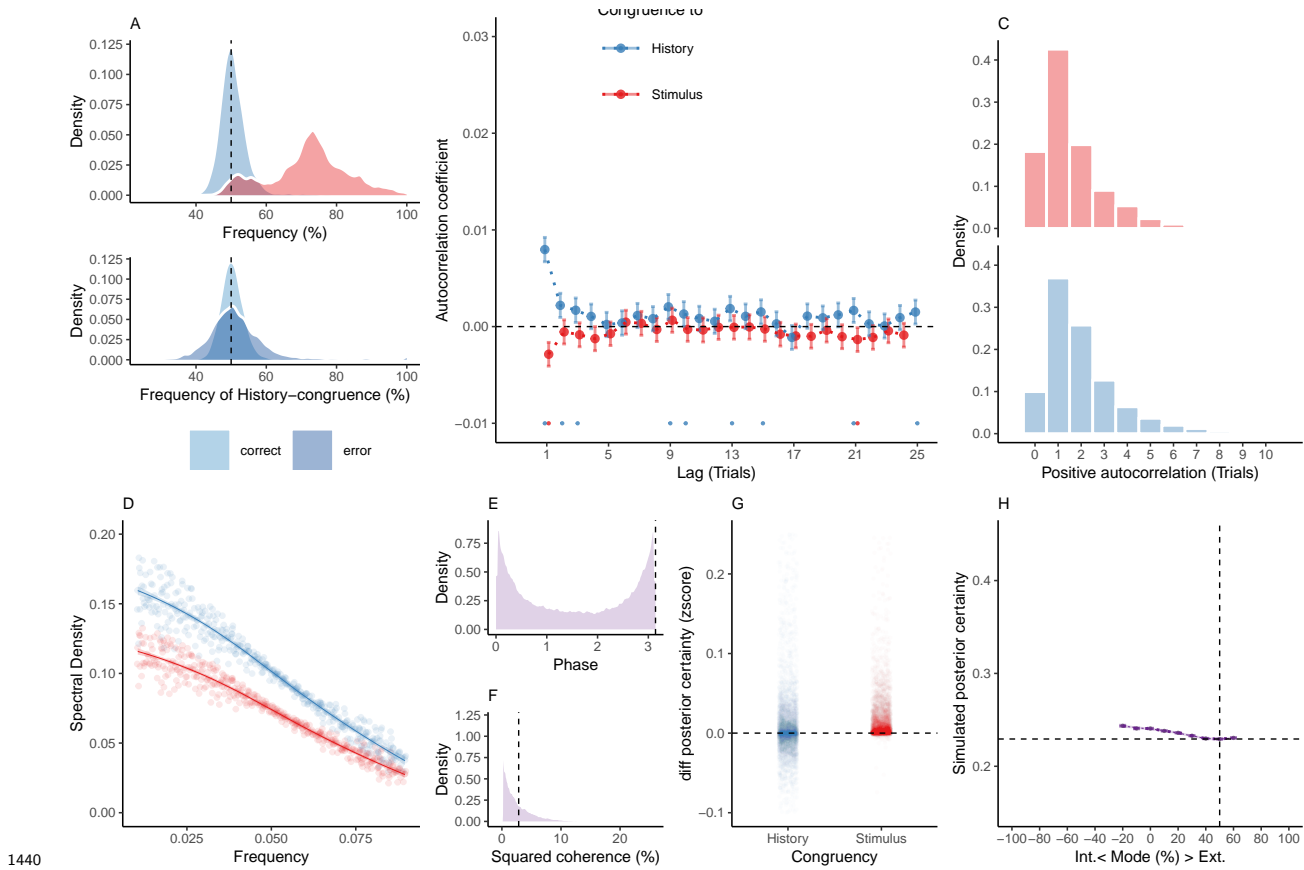
1399 **Supplemental Figure S7. Reduced Control Model 1: No accumulation of information across trials.** When simulating data for the *no-accumulation model*, we removed the  
 1400 accumulation of information across trials by setting the Hazard rate  $H$  to 0.5. Simulated data  
 1401 thus depended only on the participant-wise estimates for the amplitudes  $a_{LLR/\psi}$ , frequency  
 1402  $f$ , phase  $p$  and inverse decision temperature  $\zeta$ .

1404 A. Similar to the full model (Figure 6), simulated perceptual choices were stimulus-congruent  
 1405 in  $72.14\% \pm 0.17\%$  of trials (in red). History-congruent amounted to  $49.89\% \pm 0.03\%$  of  
 1406 trials (in blue). In contrast to the full model, the no-accumulation model showed a significant  
 1407 bias against perceptual history  $T(4.32 \times 10^3) = -3.28$ ,  $p = 1.06 \times 10^{-3}$ ; upper panel). In  
 1408 contrast to the full model, there was no difference in the frequency of history-congruent  
 1409 choices between correct and error trials ( $T(4.31 \times 10^3) = 0.76$ ,  $p = 0.44$ ; lower panel).

- 1410 B. In the no-accumulation model, we found no significant autocorrelation of history-congruence  
1411 beyond the first trial, whereas the autocorrelation of stimulus-congruence was preserved.
- 1412 C. In the no-accumulation model, the number of consecutive trials at which true autocor-  
1413 relation coefficients exceeded the autocorrelation coefficients for randomly permuted data  
1414 increased with respect to stimulus-congruence ( $2.83 \pm 1.49 \times 10^{-3}$  trials;  $T(4.31 \times 10^3) =$   
1415  $3.45$ ,  $p = 5.73 \times 10^{-4}$ ) and decreased with respect to history-congruence ( $1.85 \pm 3.49 \times 10^{-4}$   
1416 trials;  $T(4.32 \times 10^3) = -19.37$ ,  $p = 3.49 \times 10^{-80}$ ) relative to the full model.
- 1417 D. In the no-accumulation model, the smoothed probabilities of stimulus- and history-  
1418 congruence (sliding windows of  $\pm 5$  trials) fluctuated as *1/f noise*, i.e., at power densities that  
1419 were inversely proportional to the frequency (power  $\sim 1/f^\beta$ ; stimulus-congruence:  $\beta = -0.82$   
1420  $\pm 1.2 \times 10^{-3}$ ,  $T(1.92 \times 10^5) = -681.98$ ,  $p < 2.2 \times 10^{-308}$ ; history-congruence:  $\beta = -0.78 \pm$   
1421  $1.11 \times 10^{-3}$ ,  $T(1.92 \times 10^5) = -706.57$ ,  $p < 2.2 \times 10^{-308}$ ).
- 1422 E. In the no-accumulation model, the distribution of phase shift between fluctuations in  
1423 simulated stimulus- and history-congruence peaked at half a cycle ( $\pi$  denoted by dotted  
1424 line). In contrast to the full model, the dynamic probabilities of simulated stimulus- and  
1425 history-congruence were not significantly anti-correlated ( $\beta = 6.39 \times 10^{-4} \pm 7.22 \times 10^{-4}$ ,  
1426  $T(8.89 \times 10^5) = 0.89$ ,  $p = 0.38$ ).
- 1427 F. In the no-accumulation model, the average squared coherence between fluctuations in  
1428 simulated stimulus- and history-congruence (black dotted line) was reduced in comparison to  
1429 the full model ( $T(3.56 \times 10^3) = -9.96$ ,  $p = 4.63 \times 10^{-23}$ ) and amounted to  $2.8 \pm 7.29 \times 10^{-4}\%$ .
- 1430 G. Similar to the full model, confidence simulated from the no-accumulation model was  
1431 enhanced for stimulus-congruent choices ( $\beta = 0.01 \pm 9.4 \times 10^{-5}$ ,  $T(2.11 \times 10^6) = 158.1$ ,  $p <$   
1432  $2.2 \times 10^{-308}$ ). In contrast to the full model (Figure 6), history-congruent choices were not  
1433 characterized by enhanced confidence ( $\beta = 8.78 \times 10^{-5} \pm 8.21 \times 10^{-5}$ ,  $T(2.11 \times 10^6) = 1.07$ ,  
1434  $p = 0.29$ ).
- 1435 H. In the no-accumulation model, the positive quadratic relationship between the mode of

<sup>1436</sup> perceptual processing and confidence was markedly reduced in comparison to the full model  
<sup>1437</sup> ( $\beta_2 = 0.19 \pm 0.06$ ,  $T(2.11 \times 10^6) = 3$ ,  $p = 2.69 \times 10^{-3}$ ). The horizontal and vertical dotted  
<sup>1438</sup> lines indicate minimum posterior certainty and the associated mode, respectively.

1439 **9.8 Supplemental Figure S8**



1440 **Supplemental Figure S8. Reduced Control Model 2: No oscillations.** When  
 1441 simulating data for the *no-oscillation model*, we removed the oscillation from the likelihood  
 1442 and prior terms by setting the amplitudes  $a_{LLR}$  and  $a_\psi$  to zero. Simulated data thus depended  
 1443 only on the participant-wise estimates for hazard rate  $H$  and inverse decision temperature  $\zeta$ .  
 1444

1445 A. Similar to the full model (Figure 6), simulated perceptual choices were stimulus-congruent  
 1446 in  $71.97\% \pm 0.17\%$  of trials (in red). History-congruent amounted to  $50.73\% \pm 0.07\%$  of  
 1447 trials (in blue). As in the full model, the no-oscillation model showed a significant bias  
 1448 toward perceptual history  $T(4.32 \times 10^3) = 9.94$ ,  $p = 4.88 \times 10^{-23}$ ; upper panel). Similarly,  
 1449 history-congruent choices were more frequent at error trials ( $T(4.31 \times 10^3) = 10.59$ ,  $p =$   
 1450  $7.02 \times 10^{-26}$ ; lower panel).

1451 B. In the no-oscillation model, we did not find significant autocorrelations for stimulus-

<sup>1452</sup> congruence. Likewise, we did not observe any autocorrelation of history-congruence beyond  
<sup>1453</sup> the first three consecutive trials.

<sup>1454</sup> C. In the no-oscillation model, the number of consecutive trials at which true autocorrelation  
<sup>1455</sup> coefficients exceeded the autocorrelation coefficients for randomly permuted data decreased  
<sup>1456</sup> with respect to both stimulus-congruence ( $1.8 \pm 1.59 \times 10^{-3}$  trials;  $T(4.31 \times 10^3) = -5.21$ ,  $p$   
<sup>1457</sup>  $= 2 \times 10^{-7}$ ) and history-congruence ( $2.18 \pm 5.48 \times 10^{-4}$  trials;  $T(4.32 \times 10^3) = -17.1$ ,  $p =$   
<sup>1458</sup>  $1.75 \times 10^{-63}$ ) relative to the full model.

<sup>1459</sup> D. In the no-oscillation model, the smoothed probabilities of stimulus- and history-congruence  
<sup>1460</sup> (sliding windows of  $\pm 5$  trials) fluctuated as *1/f noise*, i.e., at power densities that were  
<sup>1461</sup> inversely proportional to the frequency (power  $\sim 1/f^\beta$ ; stimulus-congruence:  $\beta = -0.78 \pm$   
<sup>1462</sup>  $1.1 \times 10^{-3}$ ,  $T(1.92 \times 10^5) = -706.93$ ,  $p < 2.2 \times 10^{-308}$ ; history-congruence:  $\beta = -0.79 \pm$   
<sup>1463</sup>  $1.12 \times 10^{-3}$ ,  $T(1.92 \times 10^5) = -702.46$ ,  $p < 2.2 \times 10^{-308}$ ).

<sup>1464</sup> E. In the no-oscillation model, the distribution of phase shift between fluctuations in simulated  
<sup>1465</sup> stimulus- and history-congruence peaked at half a cycle ( $\pi$  denoted by dotted line). In contrast  
<sup>1466</sup> to the full model, the dynamic probabilities of simulated stimulus- and history-congruence  
<sup>1467</sup> were positively correlated ( $\beta = 4.3 \times 10^{-3} \pm 7.97 \times 10^{-4}$ ,  $T(1.98 \times 10^6) = 5.4$ ,  $p = 6.59 \times 10^{-8}$ ).

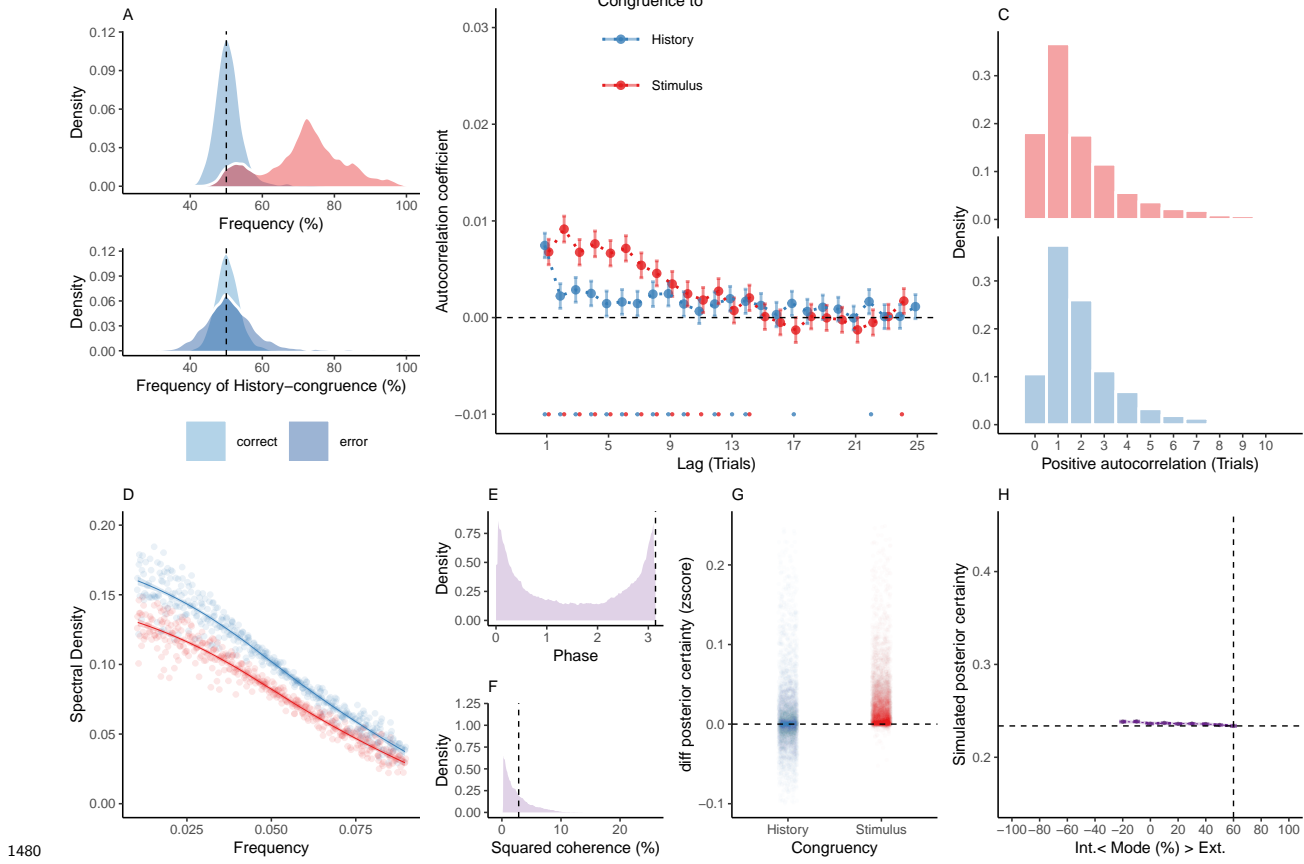
<sup>1468</sup> F. In the no-oscillation model, the average squared coherence between fluctuations in simulated  
<sup>1469</sup> stimulus- and history-congruence (black dotted line) was reduced in comparison to the full  
<sup>1470</sup> model ( $T(3.52 \times 10^3) = -6.27$ ,  $p = 3.97 \times 10^{-10}$ ) and amounted to  $3.26 \pm 8.88 \times 10^{-4}\%$ .

<sup>1471</sup> G. Similar to the full model, confidence simulated from the no-oscillation model was enhanced  
<sup>1472</sup> for stimulus-congruent choices ( $\beta = 0.01 \pm 1.05 \times 10^{-4}$ ,  $T(2.1 \times 10^6) = 139.17$ ,  $p < 2.2 \times 10^{-308}$ )  
<sup>1473</sup> and history-congruent choices ( $\beta = 8.05 \times 10^{-3} \pm 9.2 \times 10^{-5}$ ,  $T(2.1 \times 10^6) = 87.54$ ,  $p <$   
<sup>1474</sup>  $2.2 \times 10^{-308}$ ).

<sup>1475</sup> H. In the no-oscillation model, the positive quadratic relationship between the mode of  
<sup>1476</sup> perceptual processing and confidence was markedly reduced in comparison to the full model  
<sup>1477</sup> ( $\beta_2 = 0.14 \pm 0.07$ ,  $T(2.1 \times 10^6) = 1.95$ ,  $p = 0.05$ ). The horizontal and vertical dotted lines

<sub>1478</sub> indicate minimum posterior certainty and the associated mode, respectively.

1479 **9.9 Supplemental Figure S9**



1480 **Supplemental Figure S9. Reduced Control Model 3: Only oscillation of the likelihood.** When simulating data for the *likelihood-oscillation-only model*, we removed the oscillation from the prior term by setting the amplitude  $a_\psi$  to zero. Simulated data thus depended only on the participant-wise estimates for hazard rate  $H$ , amplitude  $a_{LLR}$ , frequency  $f$ , phase  $p$  and inverse decision temperature  $\zeta$ .

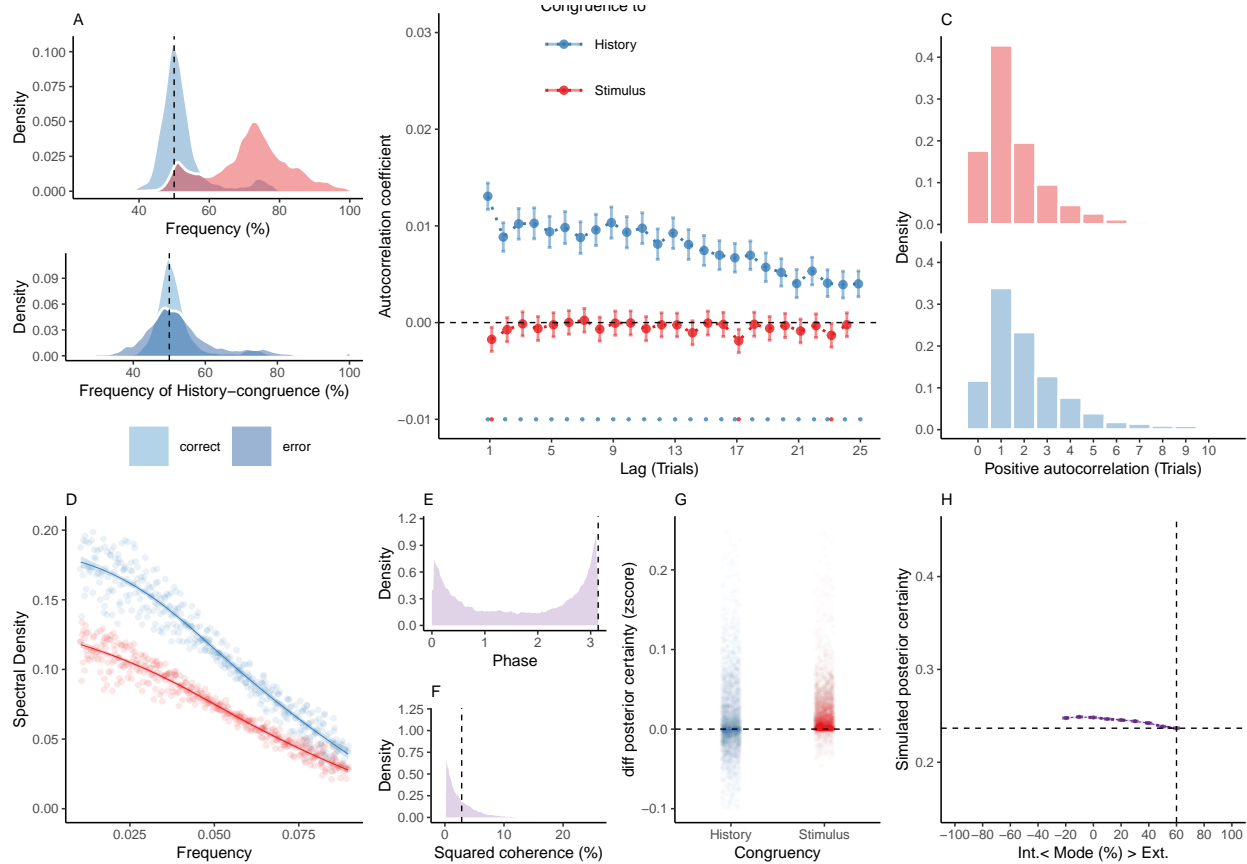
1481 A. Similar to the full model (Figure 6), simulated perceptual choices were stimulus-congruent  
 1482 in  $71.97\% \pm 0.17\%$  of trials (in red). History-congruent amounted to  $50.76\% \pm 0.07\%$  of trials  
 1483 (in blue). As in the full model, the likelihood-oscillation-only model showed a significant bias  
 1484 toward perceptual history  $T(4.32 \times 10^3) = 10.29, p = 1.54 \times 10^{-24}$ ; upper panel). Similarly,  
 1485 history-congruent choices were more frequent at error trials ( $T(4.32 \times 10^3) = 9.71, p =$   
 1490  $4.6 \times 10^{-22}$ ; lower panel).

- 1492 B. In the likelihood-oscillation-only model, we observed that the autocorrelation coefficients for  
1493 history-congruence were reduced below the autocorrelation coefficients of stimulus-congruence.  
1494 This is an approximately five-fold reduction relative to the empirical results observed in humans  
1495 (Figure 2B), where the autocorrelation of history-congruence was above the autocorrelation of  
1496 stimulus-congruence. Moreover, in the reduced model shown here, the number of consecutive  
1497 trials that showed significant autocorrelation of history-congruence was reduced to 11.
- 1498 C. In the likelihood-oscillation-only model, the number of consecutive trials at which true  
1499 autocorrelation coefficients exceeded the autocorrelation coefficients for randomly permuted  
1500 data did not differ with respect to stimulus-congruence ( $2.62 \pm 1.39 \times 10^{-3}$  trials;  $T(4.32 \times 10^3)$   
1501 = 1.85,  $p = 0.06$ ), but decreased with respect to history-congruence ( $2.4 \pm 8.45 \times 10^{-4}$  trials;  
1502  $T(4.32 \times 10^3) = -15.26$ ,  $p = 3.11 \times 10^{-51}$ ) relative to the full model.
- 1503 D. In the likelihood-oscillation-only model, the smoothed probabilities of stimulus- and history-  
1504 congruence (sliding windows of  $\pm 5$  trials) fluctuated as *1/f noise*, i.e., at power densities that  
1505 were inversely proportional to the frequency (power  $\sim 1/f^\beta$ ; stimulus-congruence:  $\beta = -0.81$   
1506  $\pm 1.17 \times 10^{-3}$ ,  $T(1.92 \times 10^5) = -688.65$ ,  $p < 2.2 \times 10^{-308}$ ; history-congruence:  $\beta = -0.79 \pm$   
1507  $1.14 \times 10^{-3}$ ,  $T(1.92 \times 10^5) = -698.13$ ,  $p < 2.2 \times 10^{-308}$ ).
- 1508 E. In the likelihood-oscillation-only model, the distribution of phase shift between fluctuations  
1509 in simulated stimulus- and history-congruence peaked at half a cycle ( $\pi$  denoted by dotted  
1510 line). In contrast to the full model, the dynamic probabilities of simulated stimulus- and  
1511 history-congruence were positively correlated ( $\beta = 2.7 \times 10^{-3} \pm 7.6 \times 10^{-4}$ ,  $T(2.02 \times 10^6) =$   
1512  $3.55$ ,  $p = 3.8 \times 10^{-4}$ ).
- 1513 F. In the likelihood-oscillation-only model, the average squared coherence between fluctuations  
1514 in simulated stimulus- and history-congruence (black dottet line) was reduced in comparison to  
1515 the full model ( $T(3.51 \times 10^3) = -4.56$ ,  $p = 5.27 \times 10^{-6}$ ) and amounted to  $3.43 \pm 1.02 \times 10^{-3}\%$ .
- 1516 G. Similar to the full model, confidence simulated from the likelihood-oscillation-only model  
1517 was enhanced for stimulus-congruent choices ( $\beta = 0.03 \pm 1.42 \times 10^{-4}$ ,  $T(2.1 \times 10^6) = 191.78$ ,

<sub>1518</sub>  $p < 2.2 \times 10^{-308}$ ) and history-congruent choices ( $\beta = 9.1 \times 10^{-3} \pm 1.25 \times 10^{-4}$ ,  $T(2.1 \times 10^6)$   
<sub>1519</sub>  $= 72.51$ ,  $p < 2.2 \times 10^{-308}$ ).

<sub>1520</sub> H. In the likelihood-oscillation-only model, the positive quadratic relationship between the  
<sub>1521</sub> mode of perceptual processing and confidence was markedly reduced in comparison to the full  
<sub>1522</sub> model ( $\beta_2 = 0.34 \pm 0.1$ ,  $T(2.1 \times 10^6) = 3.49$ ,  $p = 4.78 \times 10^{-4}$ ). The horizontal and vertical  
<sub>1523</sub> dotted lines indicate minimum posterior certainty and the associated mode, respectively.

1524 **9.10 Supplemental Figure S10**



1525 **Supplemental Figure S10. Reduced Control Model 4: Only oscillation of the prior.** When simulating data for the *prior-oscillation-only model*, we removed the oscillation from the prior term by setting the amplitude  $a_{LLR}$  to zero. Simulated data thus depended only on the participant-wise estimates for hazard rate  $H$ , amplitude  $a_\psi$ , frequency  $f$ , phase  $p$  and inverse decision temperature  $\zeta$ .

1531 A. Similar to the full model (Figure 6), simulated perceptual choices were stimulus-congruent  
 1532 in  $71.97\% \pm 0.17\%$  of trials (in red). History-congruent amounted to  $52.1\% \pm 0.11\%$  of  
 1533 trials (in blue). As in the full model, the prior-oscillation-only showed a significant bias  
 1534 toward perceptual history  $T(4.32 \times 10^3) = 18.34, p = 1.98 \times 10^{-72}$ ; upper panel). Similarly,  
 1535 history-congruent choices were more frequent at error trials ( $T(4.31 \times 10^3) = 12.35, p =$   
 1536  $1.88 \times 10^{-34}$ ; lower panel).

1537 B. In the prior-oscillation-only model, we did not observe any significant positive autocor-  
1538 relation of stimulus-congruence , whereas the autocorrelation of history-congruence was  
1539 preserved.

1540 C. In the prior-oscillation-only model, the number of consecutive trials at which true au-  
1541 tocorrelation coefficients exceeded the autocorrelation coefficients for randomly permuted  
1542 data did was decreased with respect to stimulus-congruence relative to the full model ( $1.8 \pm$   
1543  $1.01 \times 10^{-3}$  trials;  $T(4.31 \times 10^3) = -6.48$ ,  $p = 1.03 \times 10^{-10}$ ), but did not differ from the full  
1544 model with respect to history-congruence ( $4.25 \pm 1.84 \times 10^{-3}$  trials;  $T(4.32 \times 10^3) = 0.07$ ,  $p$   
1545 = 0.95).

1546 D. In the prior-oscillation-only model, the smoothed probabilities of stimulus- and history-  
1547 congruence (sliding windows of  $\pm 5$  trials) fluctuated as *1/f noise*, i.e., at power densities that  
1548 were inversely proportional to the frequency (power  $\sim 1/f^\beta$ ; stimulus-congruence:  $\beta = -0.78$   
1549  $\pm 1.11 \times 10^{-3}$ ,  $T(1.92 \times 10^5) = -706.62$ ,  $p < 2.2 \times 10^{-308}$ ; history-congruence:  $\beta = -0.83 \pm$   
1550  $1.27 \times 10^{-3}$ ,  $T(1.92 \times 10^5) = -651.6$ ,  $p < 2.2 \times 10^{-308}$ ).

1551 E. In the prior-oscillation-only model, the distribution of phase shift between fluctuations  
1552 in simulated stimulus- and history-congruence peaked at half a cycle ( $\pi$  denoted by dotted  
1553 line). Similar to the full model, the dynamic probabilities of simulated stimulus- and history-  
1554 congruence were anti-correlated ( $\beta = -0.03 \pm 8.61 \times 10^{-4}$ ,  $T(2.12 \times 10^6) = -34.03$ ,  $p =$   
1555  $8.17 \times 10^{-254}$ ).

1556 F. In the prior-oscillation-only model, the average squared coherence between fluctuations in  
1557 simulated stimulus- and history-congruence (black dottet line) was reduced in comparison to  
1558 the full model ( $T(3.54 \times 10^3) = -3.22$ ,  $p = 1.28 \times 10^{-3}$ ) and amounted to  $3.52 \pm 1.04 \times 10^{-3}\%$ .

1559 G. Similar to the full model, confidence simulated from the prior-oscillation-only model was  
1560 enhanced for stimulus-congruent choices ( $\beta = 0.02 \pm 1.44 \times 10^{-4}$ ,  $T(2.03 \times 10^6) = 128.53$ ,  
1561  $p < 2.2 \times 10^{-308}$ ) and history-congruent choices ( $\beta = 0.01 \pm 1.26 \times 10^{-4}$ ,  $T(2.03 \times 10^6) =$   
1562  $88.24$ ,  $p < 2.2 \times 10^{-308}$ ).

<sub>1563</sub> H. In contrast to the full model, the prior-oscillation-only model did not yield a positive  
<sub>1564</sub> quadratic relationship between the mode of perceptual processing and confidence ( $\beta_2 = -0.17$   
<sub>1565</sub>  $\pm 0.1$ ,  $T(2.04 \times 10^6) = -1.66$ ,  $p = 0.1$ ). The horizontal and vertical dotted lines indicate  
<sub>1566</sub> minimum posterior certainty and the associated mode, respectively.

1567 **9.11 Supplemental Table T1**

Authors	Journal	Year
Bang, Shekhar, Rahnev	JEP:General	2019
Bang, Shekhar, Rahnev	JEP:General	2019
Calder-Travis, Charles, Bogacz, Yeung	Unpublished	NA
Clark & Merfeld	Journal of Neurophysiology	2018
Clark	Unpublished	NA
Faivre, Filevich, Solovey, Kuhn, Blanke	Journal of Neuroscience	2018
Faivre, Vuillaume, Blanke, Cleeremans	bioRxiv	2018
Filevich & Fandakova	Unplublished	NA
Gajdos, Fleming, Saez Garcia, Weindel, Davranche	Neuroscience of Consciousness	2019
Gherman & Philiastides	eLife	2018
Haddara & Rahnev	PsyArXiv	2020
Haddara & Rahnev	PsyArXiv	2020
Hainguerlot, Vergnaud, & de Gardelle	Scientific Reports	2018
Hainguerlot, Gajdos, Vergnaud, & de Gardelle	Unpublished	NA
Jachs, Blanco, Grantham-Hill, Soto	JEP:HPP	2015
Jachs, Blanco, Grantham-Hill, Soto	JEP:HPP	2015
Jachs, Blanco, Grantham-Hill, Soto	JEP:HPP	2015
Jaquiere, Yeung	Unpublished	NA
Kvam, Pleskac, Yu, Busemeyer	PNAS	2015
Kvam, Pleskac, Yu, Busemeyer	PNAS	2015
Kvam and Pleskac	Cognition	2016
Law, Lee	Unpublished	NA
Lebreton, et al.	Sci. Advances	2018
Lempert, Chen, & Fleming	PlosOne	2015
Locke*, Gaffin-Cahn*, Hosseiniavah, Mamassian, & Landy	Attention, Perception, & Psychophysics	2020
Maniscalco, McCurdy,Odegaard, & Lau	J Neurosci	2017
Maniscalco, McCurdy,Odegaard, & Lau	J Neurosci	2017
Maniscalco, McCurdy,Odegaard, & Lau	J Neurosci	2017
Maniscalco, McCurdy,Odegaard, & Lau	J Neurosci	2017
Martin, Hsu	Unpublished	NA
Massoni & Roux	Journal of Mathematical Psychology	2017
Massoni	Unpublished	NA
Mazor, Friston & Fleming	eLife	2020
Mei, Rankine,Olafsson, Soto	bioRxiv	2019
Mei, Rankine,Olafsson, Soto	bioRxiv	2019
O'Hora, Zgonnikov, Kenny, Wong-Lin	Fechner Day proceedings	2017
O'Hora, Zgonnikov, CiChocki	Unpublished	NA

(continued)

Authors	Journal	Year
O'Hora, Zgonnikov, Neverauskaite	Unpublished	NA
Palser et al	Consciousness & Cognition	2018
Pereira, Faivre, Iturrate et al.	bioRxiv	2018
Prieto et al.	Submitted	NA
Rahnev et al	J Neurophysiol	2013
Rausch & Zehetleitner	Front Psychol	2016
Rausch et al	Attention, Perception, & Psychophysics	2018
Rausch et al	Attention, Perception, & Psychophysics	2018
Rausch, Zehetleitner, Steinhauser, & Maier	NeuroImage	2020
Recht, de Gardelle & Mamassian	Unpublished	NA
Reyes et al.	PlosOne	2015
Reyes et al.	Submitted	NA
Rouault, Seow, Gillan, Fleming	Biol. Psychiatry	2018
Rouault, Seow, Gillan, Fleming	Biol. Psychiatry	2018
Rouault, Dayan, Fleming	Nat Commun	2019
Sadeghi et al	Scientific Reports	2017
Schmidt et al.	Consc Cog	2019
Shekhar & Rahnev	J Neuroscience	2018
Shekhar & Rahnev	PsyArXiv	2020
Sherman et al	Journal of Neuroscience	2016
Sherman et al	Journal of Cognitive Neuroscience	2016
Sherman et al	Unpublished	NA
Sherman et al	Unpublished	NA
Siedlecka, Wereszczyski, Paulewicz, Wierzchon	bioRxiv	2019
Song et al	Consciousness & Cognition	2011
van Boxtel, Orchard, Tsuchiya	bioRxiv	2019
van Boxtel, Orchard, Tsuchiya	bioRxiv	2019
Wierzchon, Paulewicz, Asanowicz, Timmermans & Cleeremans	Consciousness and Cognition	2014
Wierzchon, Anzulewicz, Hobot, Paulewicz & Sackur	Consciousness and Cognition	2019

1568 **References**

- 1569 1. Schrödinger, E. *What is Life? The Physical Aspect of the Living Cell.* (Cambridge  
1570 University Press, 1944).
- 1571 2. Ashby, W. R. Principles of the self-organizing dynamic system. *Journal of General  
1572 Psychology* **37**, 125–128 (1947).
- 1573 3. Friston, K. Life as we know it. *Journal of The Royal Society Interface* **10**, 20130475  
1574 (2013).
- 1575 4. Palva, J. M. *et al.* Roles of multiscale brain activity fluctuations in shaping the  
variability and dynamics of psychophysical performance. in *Progress in brain research*  
1576 vol. 193 335–350 (Elsevier B.V., 2011).
- 1577 5. VanRullen, R. Perceptual Cycles. *Trends in Cognitive Sciences* **20**, 723–735 (2016).  
1578
- 1579 6. Verplanck, W. S. *et al.* Nonindependence of successive responses in measurements of  
1580 the visual threshold. *Journal of Experimental Psychology* **44**, 273–282 (1952).
- 1581 7. Atkinson, R. C. A variable sensitivity theory of signal detection. *Psychological Review*  
1582 **70**, 91–106 (1963).
- 1583 8. Dehaene, S. Temporal Oscillations in Human Perception. *Psychological Science* **4**,  
1584 264–270 (1993).
- 1585 9. Gilden, D. L. *et al.* On the Nature of Streaks in Signal Detection. *Cognitive Psychology*  
1586 **28**, 17–64 (1995).
- 1587 10. Gilden, D. L. *et al.* 1/f noise in human cognition. *Science* **67**, 1837–1839 (1995).  
1588
- 1589 11. Monto, S. *et al.* Very slow EEG fluctuations predict the dynamics of stimulus detection  
1590 and oscillation amplitudes in humans. *Journal of Neuroscience* **28**, 8268–8272 (2008).

- 1591 12. Ashwood, Z. C. *et al.* Mice alternate between discrete strategies during perceptual  
1592 decision-making. *Nature Neuroscience* **25**, 201–212 (2022).
- 1593 13. Gilden, D. L. Cognitive emissions of 1/f noise. *Psychological Review* **108**, 33–56 (2001).
- 1594
- 1595 14. Duncan, K. *et al.* Memory’s Penumbra: Episodic memory decisions induce lingering  
1596 mnemonic biases. *Science* **337**, 485–487 (2012).
- 1597 15. Clare Kelly, A. M. *et al.* Competition between functional brain networks mediates  
1598 behavioral variability. *NeuroImage* **39**, 527–537 (2008).
- 1599 16. Hesselmann, G. *et al.* Spontaneous local variations in ongoing neural activity bias  
1600 perceptual decisions. *Proceedings of the National Academy of Sciences of the United  
States of America* **105**, 10984–10989 (2008).
- 1601 17. Schroeder, C. E. *et al.* Dynamics of Active Sensing and perceptual selection. *Current  
1602 Opinion in Neurobiology* **20**, 172–176 (2010).
- 1603 18. Honey, C. J. *et al.* Switching between internal and external modes: A multiscale  
1604 learning principle. *Network Neuroscience* **1**, 339–356 (2017).
- 1605 19. Weilnhammer, V. *et al.* Bistable perception alternates between internal and external  
1606 modes of sensory processing. *iScience* **24**, (2021).
- 1607 20. Rahnev, D. *et al.* The Confidence Database. *Nature Human Behaviour* **4**, 317–325  
1608 (2020).
- 1609 21. The International Brain Laboratory. Standardized and reproducible mea-  
1610 surement of decision-making in mice. *bioRxiv* 2020.01.17.909838 (2020)  
doi:10.1101/2020.01.17.909838.
- 1611 22. Fischer, J. *et al.* Serial dependence in visual perception. *Nat. Neurosci.* **17**, 738–743  
1612 (2014).

- 1613 23. Liberman, A. *et al.* Serial dependence in the perception of faces. *Current Biology* **24**,  
1614 2569–2574 (2014).
- 1615 24. Abrahamyan, A. *et al.* Adaptable history biases in human perceptual decisions. *Proceedings of the National Academy of Sciences of the United States of America* **113**,  
1616 E3548–E3557 (2016).
- 1617 25. Cicchini, G. M. *et al.* Compressive mapping of number to space reflects dynamic  
1618 encoding mechanisms, not static logarithmic transform. *Proceedings of the National  
Academy of Sciences of the United States of America* **111**, 7867–7872 (2014).
- 1619 26. Cicchini, G. M. *et al.* Serial dependencies act directly on perception. *Journal of Vision*  
1620 **17**, (2017).
- 1621 27. Fritzsche, M. *et al.* A bayesian and efficient observer model explains concurrent attractive  
1622 and repulsive history biases in visual perception. *eLife* **9**, 1–32 (2020).
- 1623 28. Urai, A. E. *et al.* Pupil-linked arousal is driven by decision uncertainty and alters serial  
1624 choice bias. *Nature Communications* **8**, (2017).
- 1625 29. Akrami, A. *et al.* Posterior parietal cortex represents sensory history and mediates its  
1626 effects on behaviour. *Nature* **554**, 368–372 (2018).
- 1627 30. Braun, A. *et al.* Adaptive history biases result from confidence-weighted accumulation  
1628 of past choices. *Journal of Neuroscience* **38**, 2418–2429 (2018).
- 1629 31. Bergen, R. S. V. *et al.* Probabilistic representation in human visual cortex reflects  
1630 uncertainty in serial decisions. *Journal of Neuroscience* **39**, 8164–8176 (2019).
- 1631 32. Urai, A. E. *et al.* Choice history biases subsequent evidence accumulation. *eLife* **8**,  
1632 (2019).
- 1633 33. Hsu, S. M. *et al.* The roles of preceding stimuli and preceding responses on assimilative  
1634 and contrastive sequential effects during facial expression perception. *Cognition and  
Emotion* **34**, 890–905 (2020).

- 1635 34. Dong, D. W. *et al.* Statistics of natural time-varying images. *Network: Computation*  
1636      *in Neural Systems* **6**, 345–358 (1995).
- 1637 35. Burr, D. *et al.* Vision: Efficient adaptive coding. *Current Biology* **24**, R1096–R1098  
1638      (2014).
- 1639 36. Montroll, E. W. *et al.* On 1/f noise and other distributions with long tails. *Proceedings*  
1640      *of the National Academy of Sciences* **79**, 3380–3383 (1982).
- 1641 37. Bak, P. *et al.* Self-organized criticality: An explanation of the 1/f noise. *Physical*  
1642      *Review Letters* **59**, 381–384 (1987).
- 1643 38. Chialvo, D. R. Emergent complex neural dynamics. *Nature Physics* **6**, 744–750 (2010).
- 1644
- 1645 39. Wagenmakers, E. J. *et al.* Estimation and interpretation of 1/f $\alpha$  noise in human  
1646 cognition. *Psychonomic Bulletin and Review* **11**, 579–615 (2004).
- 1647 40. Van Orden, G. C. *et al.* Human cognition and 1/f scaling. *Journal of Experimental*  
1648      *Psychology: General* **134**, 117–123 (2005).
- 1649 41. Chopin, A. *et al.* Predictive properties of visual adaptation. *Current Biology* **22**,  
1650      622–626 (2012).
- 1651 42. Cicchini, G. M. *et al.* The functional role of serial dependence. *Proceedings of the Royal*  
1652      *Society B: Biological Sciences* **285**, (2018).
- 1653 43. Kiyonaga, A. *et al.* Serial Dependence across Perception, Attention, and Memory.  
1654      *Trends in Cognitive Sciences* **21**, 493–497 (2017).
- 1655 44. McGinley, M. J. *et al.* Waking State: Rapid Variations Modulate Neural and Behavioral  
1656 Responses. *Neuron* **87**, 1143–1161 (2015).
- 1657 45. Rosenberg, M. *et al.* Sustaining visual attention in the face of distraction: A novel  
1658 gradual-onset continuous performance task. *Attention, Perception, and Psychophysics*  
    **75**, 426–439 (2013).

- 1659 46. Zalta, A. *et al.* Natural rhythms of periodic temporal attention. *Nature Communications*  
1660 **11**, 1–12 (2020).
- 1661 47. Prado, J. *et al.* Variations of response time in a selective attention task are linked  
1662 to variations of functional connectivity in the attentional network. *NeuroImage* **54**,  
541–549 (2011).
- 1663 48. St. John-Saaltink, E. *et al.* Serial Dependence in Perceptual Decisions Is Reflected in  
1664 Activity Patterns in Primary Visual Cortex. *Journal of Neuroscience* **36**, 6186–6192  
(2016).
- 1665 49. Cicchini, G. M. *et al.* Perceptual history propagates down to early levels of sensory  
1666 analysis. *Current Biology* **31**, 1245–1250.e2 (2021).
- 1667 50. Kepcs, A. *et al.* Neural correlates, computation and behavioural impact of decision  
1668 confidence. *Nature* **455**, 227–231 (2008).
- 1669 51. Fleming, S. M. *et al.* How to measure metacognition. *Frontiers in Human Neuroscience*  
1670 **8**, 443 (2014).
- 1671 52. Leys, C. *et al.* Detecting outliers: Do not use standard deviation around the mean, use  
1672 absolute deviation around the median. *Journal of Experimental Social Psychology* **49**,  
764–766 (2013).
- 1673 53. Maloney, L. T. *et al.* Past trials influence perception of ambiguous motion quartets  
1674 through pattern completion. *Proceedings of the National Academy of Sciences of the  
United States of America* **102**, 3164–3169 (2005).
- 1675 54. Glaze, C. M. *et al.* Normative evidence accumulation in unpredictable environments.  
1676 *eLife* **4**, (2015).
- 1677 55. Wexler, M. *et al.* Persistent states in vision break universality and time invariance.  
1678 *Proceedings of the National Academy of Sciences of the United States of America* **112**,  
14990–14995 (2015).

- 1679 56. Rao, R. P. *et al.* Predictive coding in the visual cortex: a functional interpretation of  
1680 some extra-classical receptive-field effects. *Nature neuroscience* **2**, 79–87 (1999).
- 1681 57. Jardri, R. *et al.* Experimental evidence for circular inference in schizophrenia. *Nature  
1682 Communications* **8**, 14218 (2017).
- 1683 58. Guggenmos, M. *et al.* Mesolimbic confidence signals guide perceptual learning in the  
1684 absence of external feedback. *eLife* **5**, (2016).
- 1685 59. Mathys, C. D. *et al.* Uncertainty in perception and the Hierarchical Gaussian Filter.  
1686 *Frontiers in human neuroscience* **8**, 825 (2014).
- 1687 60. Sterzer, P. *et al.* The Predictive Coding Account of Psychosis. *Biological Psychiatry*  
1688 **84**, 634–643 (2018).
- 1689 61. Bengio, Y. *et al.* Towards Biologically Plausible Deep Learning. *bioRxiv* (2015).
- 1690
- 1691 62. Dijkstra, N. *et al.* Perceptual reality monitoring: Neural mechanisms dissociating  
1692 imagination from reality. *PsyArXiv* (2021) doi:10.31234/OSF.IO/ZNGEQ.
- 1693 63. Andrillon, T. *et al.* Predicting lapses of attention with sleep-like slow waves. *Nature  
1694 Communications* **12**, 3657 (2021).
- 1695 64. Passingham, R. E. *Understanding the prefrontal cortex : selective advantage, connectiv-  
1696 ity, and neural operations.* (Oxford University Press).
- 1697 65. Ashwood, Z. C. *et al.* Mice alternate between discrete strategies during perceptual  
1698 decision-making. *bioRxiv* 2020.10.19.346353 (2021) doi:10.1101/2020.10.19.346353.
- 1699 66. Bak, P. Complexity and Criticality. in *How nature works* 1–32 (Springer New York,  
1700 1996). doi:10.1007/978-1-4757-5426-1\_1.
- 1701 67. Denève, S. *et al.* Efficient codes and balanced networks. *Nature Neuroscience* **19**,  
1702 375–382 (2016).

- 1703 68. Beggs, J. M. *et al.* Neuronal Avalanches in Neocortical Circuits. *Journal of Neuroscience*  
1704 **23**, 11167–11177 (2003).
- 1705 69. Wang, X. J. Synaptic basis of cortical persistent activity: The importance of NMDA  
1706 receptors to working memory. *Journal of Neuroscience* **19**, 9587–9603 (1999).
- 1707 70. Wang, X. J. Synaptic reverberation underlying mnemonic persistent activity. *Trends*  
1708 *in Neurosciences* **24**, 455–463 (2001).
- 1709 71. Wang, M. *et al.* NMDA Receptors Subserve Persistent Neuronal Firing during Working  
1710 Memory in Dorsolateral Prefrontal Cortex. *Neuron* **77**, 736–749 (2013).
- 1711 72. Bliss, D. P. *et al.* Synaptic augmentation in a cortical circuit model reproduces serial  
1712 dependence in visual working memory. *PLOS ONE* **12**, e0188927 (2017).
- 1713 73. Stein, H. *et al.* Reduced serial dependence suggests deficits in synaptic potentiation in  
1714 anti-NMDAR encephalitis and schizophrenia. *Nature Communications* **11**, 1–11 (2020).
- 1715 74. Durstewitz, D. *et al.* Neurocomputational Models of Working Memory. *Nature*  
1716 *Neuroscience* **3**, 1184–1191 (2000).
- 1717 75. Seamans, J. K. *et al.* Dopamine D1/D5 receptor modulation of excitatory synaptic  
1718 inputs to layer V prefrontal cortex neurons. *Proceedings of the National Academy of*  
*Sciences of the United States of America* **98**, 301–306 (2001).
- 1719 76. Kobayashi, T. *et al.* Reproducing Infra-Slow Oscillations with Dopaminergic Modulation.  
1720 *Scientific Reports* **7**, 1–9 (2017).
- 1721 77. Chew, B. *et al.* Endogenous fluctuations in the dopaminergic midbrain drive behavioral  
1722 choice variability. *Proceedings of the National Academy of Sciences of the United States*  
*of America* **116**, 18732–18737 (2019).
- 1723 78. Fritzsche, M. *et al.* Opposite Effects of Recent History on Perception and Decision.  
1724 *Current Biology* **27**, 590–595 (2017).

- 1725 79. Gekas, N. *et al.* Disambiguating serial effects of multiple timescales. *Journal of Vision*  
1726 **19**, 1–14 (2019).
- 1727 80. Weilnhammer, V. *et al.* Psychotic Experiences in Schizophrenia and Sensitivity to  
1728 Sensory Evidence. *Schizophrenia bulletin* **46**, 927–936 (2020).
- 1729 81. Fletcher, P. C. *et al.* Perceiving is believing: a Bayesian approach to explaining the  
1730 positive symptoms of schizophrenia. *Nature reviews. Neuroscience* **10**, 48–58 (2009).
- 1731 82. Corlett, P. R. *et al.* Hallucinations and Strong Priors. *Tics* **23**, 114–127 (2019).

1732